KOÇ
ÜNİVERSİTESİ
GRADUATE SCHOOL
OF HEALTH SCIENCES

DNA Damage-Induced and TAp63-Mediated Oocyte Apoptosis Is Not Associated with c-Abl Activation in Human Ovary

by

Gamze BİLDİK ELCİK

A Doctoral Dissertation
Submitted to the Graduate School of Health Sciences
in Partial Fulfillment of the Requirements for the Degree of

Doctor of Philosophy

in

Cellular and Molecular Medicine

Advisor: Prof. Dr. Özgür ÖKTEM

May 28, 2019

This is to certify that I have examined this copy of a doctoral dissertation named "DNA Damage-Induced and TAp63-Mediated Oocyte Apoptosis Is Not Associated with c-Abl Activation in Human Ovary"

by Gamze BİLDİK ELCİK

and have found that it is complete and satisfactory in all respects and that any and all revisions required by the final examining committee have been made.

Committee Members: **Signatures:**

Özgür Öktem, MD (Advisor)   _____

Serçin Karahüseyinoğlu, MD   _____

Kayhan Yakın, MD   _____

Nezih Hekim, MD, PhD   _____

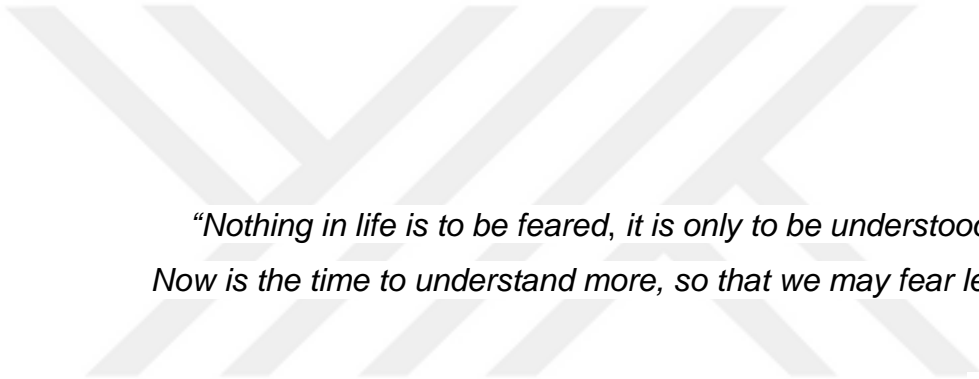Bilal E. Kerman, PhD   _____

DECLARATION

I declare that this thesis and the work presented in it are my own and has been generated by me as the result of my own original research. I confirm that; there is no unethical behavior in any stages from the planning of the thesis to the writing, I have obtained all the information in this thesis within academic and ethical rules, I have quoted all the information and comments that are not obtained by this thesis in the references list. There is no violation of patent and copyright rights during the study and writing of this thesis.

_____

Gamze Bildik Elcik

"Nothing in life is to be feared, it is only to be understood.
Now is the time to understand more, so that we may fear less."

- Marie Curie

Dedicated to my lovely grandmother,

the smartest woman I have known.

I would not be who I am today if it was not for your faith in me.

ACKNOWLEDGEMENTS

Even though only my name is seen on the cover of this dissertation, many wonderful people have contributed to this moment of accomplishment. I owe my gratitude to all those people who have made this possible.

My deepest gratitude is to my advisor, Dr. Özgür Öktem, for his expectations that I perform to the best of my ability. I have been fortunate to have an advisor who gave me freedom and guidance at the same time. I am grateful to Dr. Kayhan Yakın for his everlasting encouragements and advice. I am thankful to Dr. Serçin Karahüseyinoğlu for her cooperation and practical contributions. I would like to thank Dr. Nezih Hekim and Dr. Bilal E. Kerman for being in my thesis committee and sparing their precious time for me.

No research is possible without infrastructure and resource. For this, I extend thanks to Koç University School of Medicine, Koç University Graduate School of Health Sciences and TÜBİTAK BİDEB 2211 Doctoral Scholarship Program for their fundings during my doctoral studies. I am grateful to my previous lab mates, Nazlı Akın, Gupse Özcan and Esra Bilir for the stimulating discussions, for the sleepless nights we were working together before deadlines, and for all the fun we have had. In addition, I owe special thanks to the graduate students and staff at KUTTAM, American Hospital and Koç University Hospital IVF laboratory, for their various forms of support during my graduate study. My dear friends, Dolay Damla Çelik, Seda Ateş and Tuğçe Ayık, helped me stay sane through difficult times and made it easier whenever I stumbled.

Most importantly, my special thanks to my husband Burak Elcik, for being my greatest support, my biggest comfort and my strongest motivation. I deeply appreciate his belief in me.

Last but not least, my family whom this thesis is dedicated to, has been a constant source of love, concern, support and strength all these years. None of this would have been possible without their love and patience.

TABLE OF CONTENTS

LIST OF TABLES

LIST OF FIGURES

imatinib or GNF-2, as a validation experiment showing in-vitro biological activity of these drugs.

Figure 38: Real-time growth curves of the cells treated with imatinib, GNF-2, anti-CD117 and cisplatin in vitro.

Figure 39: Cell death was confirmed with intravital YO-PRO1 staining in immunofluorescence microscopy.

NOMENCLATURE

TAp63	Isoform of tumor protein p63
c-Abl	Abelson tyrosine kinase
DNA	Deoxyribonucleic acid
POF	Premature ovarian failure
HSCT	Hematopoietic stem cell transplantation
ATM	Ataxia-telangiectasia mutated kinase
5-FU	5-Fluorouracil
AMH	Anti-mullerian hormone
FSH	Follicle stimulating hormone
E_2	Estradiol
AFC	Antral follicle count
COV434	Human ovarian granulosa tumor cell line
HGrC1	Human non-luteinized granulosa cell line
SIGC	Rat spontaneously immortalized granulosa cell line
HLGCs	Human luteal granulosa cells
IVF	In vitro fertilization
COS	Controlled ovarian stimulation
IRB	Institutional review board
p53	Tumor protein p53
TP53	Gene encoding p53 protein
p63	Tumor protein p63
p73	Tumor protein p33
TA isoform	Transactivation domain
ΔN isoform	N-terminal truncated isoform
DBD	The DNA binding domain
p53RE	p53 response elements
PFs	Primordial follicles
IR	Ionizing radiation
Chk-2	Checkpoint kinase 2
Cdk2	Cyclin-dependent kinase 2
p70s6K	Ribosomal protein S6 kinase beta 1

p38 MAPK	p38 mitogen-activated protein kinase
Iκβ	Inhibitor kB
Plk	Polo-like kinase 1
GAPDH	Glyceraldehyde 3-phosphate dehydrogenase
PUMA	p53 upregulated modulator of apoptosis
NOXA	Immediate-early-response protein APR
CASP3	Cleaved caspase 3
BCL-2	B-cell lymphoma 2
ABL1	Gene encoding abelson murine leukemia viral oncogene homolog 1
Bcr/Abl	Bcr and Abl fusion protein
UV	Ultraviolet
ATP	Adenosine triphosphate
TK	Tyrosine kinase
PDGFR	Platelet-derived growth factor receptor
Ph+	Philadelphia-positive
CML	Chronic myeloid leukemia
ALL	Acute lymphocytic leukemia
GIST	Gastrointestinal stromal tumor
Chk-1	Checkpoint kinase 1
Chk-2	Checkpoint kinase 2
CK1	Casein kinase 1
GV	Germinal vesicle
DMEM/F12	Dulbecco's modified eagle medium/Nutrient mixture F-12
FBS	Fetal bovine serum
4-OOH CY	4-hydroperoxy cyclophosphamide
Anti-CD117	Neutralizing c-kit antibody
GNF-2	Bcr-Abl inhibitor
SAPK	Stress-activated protein kinase
JNK	c-Jun N-terminal kinase
ɣ-H2A.X	Gamma H2A histone family member X
PARP	Poly (ADP-ribose) polymerase

CTG	Cell Titer-GLO
DMSO	Dimethyl sulfoxide
PBS	Phosphate buffered saline
LH	Luteinizing hormone
H&E	Hematoxylin-eosin
RIPA	Radio-immunoprecipitation assay
SDS	Sodium dodecyl sulfate
PVDF	Polyvinylidene difluoride
TBS	Tris-buffered saline
TBS-T	0.1% Tween-20 in Tris-buffered saline
Tris-HCl	Tris-hydrochloride
NaCl	Sodium chloride
HRP	Horseradish peroxidase
ECL	Enhanced luminol-based chemiluminescent
PFA	Paraformaldehyde
DPBS-T	0.1% Tween-20 in Dulbecco's PBS
IF	Immunofluorescence
CI	Cell index
RTCA	Real time cell analysis
E-Plate	Electronic microtiter plate
qRT-PCR	Quantitative real-time PCR
MIS/AMH	Mullerian inhibiting substance/Anti-mullerian hormone
ELISA	Enzyme-linked Immunosorbent assay
ECLIA	Electrochemiluminescence immunoassay

ABSTRACT

Rates of young cancer survivors have improved in recent years owing to novel treatments. This success, however, creates an increasing problem: long-term side effects of chemotherapy such as infertility. It is controversial whether c-Abl is essential for oocyte apoptosis and its inhibition with imatinib prevents chemotherapy-induced oocyte damage in mice. As no human data is available, this thesis aimed to explore the mechanism triggered by chemotherapy and the role of c-Abl in TAp63-mediated DNA damage-induced oocytes apoptosis.

Ovarian damage was induced with cisplatin in human ovaries which were either xenografted to mice or in vitro cultured. Human immature oocytes, primary granulosa cells, and two different granulosa cell lines were also included. Cisplatin caused DNA damage as evidenced by γ-H2AX, activated checkpoint sensors Chk-1 and Chk-2 and SAPK/JNK pathway, induced TAp63 phosphorylation and triggered apoptosis in human oocytes and granulosa cells whereas it did not associate with c-Abl upregulation. Moreover, imatinib exposure resulted in the formation of bizarrely shaped follicles lacking oocytes and increased follicular atresia. To better understand the actions of imatinib, ovarian tissues were incubated with anti-CD117, a c-kit antagonist drug, but not with another c-Abl inhibitor GNF-2, which lacks an inhibitory action on c-kit and similar toxic effects were observed. Intraperitoneal administration of imatinib to the xenografted animals produced similar histomorphological abnormalities in the ovarian grafts and did not prevent cisplatin-induced follicle loss.

In conclusion, phosphorylation of TAp63 at Ser395 has not yet been associated with any function before, so here we define Ser395 for the first time as a site for TAp63 activation in response to DNA damage. Moreover, we provide the first molecular evidence for ovarian toxicity of imatinib in human and heighten the concerns about its gonadotoxicity on the human ovary and urge caution in its use in young female patients.

Keywords: ovary, apoptosis, cisplatin, DNA damage, imatinib, p63

ÖZET

Kanser tedavisinde geliştirilen son yaklaşımlar, kanser sonrası sağkalım oranlarını arttırmış olup, bu nedenle kanser tedavilerinin uzun vadeli yan etkilerini en aza indirgemek son derece önemli bir hale gelmiştir. Literatürde TAp63-bağımlı apoptozisin indüksiyonu için c-Abl isimli tirozin kinazın zorunlu olup olmadığı ve c-Abl'in, inhibitörü olan imatinib ile inhibe edilmesinin farede kemoterapiye bağlı oosit apoptozisini önleyebileceği tartışmalı bir konudur. Bu konuda insan üzerinde yapılmış herhangi bir moleküler çalışma bulunmamaktadır. Bu tez çalışmasında sisplatin kaynaklı DNA hasarının, TAp63 yolağının yanı sıra c-Abl aktivasyonu üzerine etkileri ve c-Abl inhibisyonunun insan oosit ölümünü önleyip önlemediğinin araştırılması amaçlamıştır.

Elde edilen sonuçlara göre; sisplatine bağlı DNA hasarı, TAp63 ve SAPK/JNK yolaklarını aktive ederek insan oositlerinde ve granüloza hücrelerinde apoptozisi indüklemiştir. Ancak TAp63 aktivasyonundaki artışın, c-Abl'in ifadesinde herhangi bir artışla ilişkili olmadığı gözlenmiştir. Imatinib, granüloza hücrelerinin veya oositlerin sisplatin kaynaklı apoptozisini önlememiştir. Ayrıca, imatinib maruziyeti, anormal morfoloji gösteren foliküllerin oluşmasına ve artmış foliküler atreziye neden olmuştur. Over dokuları, bir c-kit antagonisti olan anti-CD117 ile inkübe edildiğinde benzer toksik etkiler gözlenmiş, ancak c-kit inhibitör bir etkiye sahip olmayan başka bir c-Abl tirozin kinaz inhibitörü olan GNF-2'da bu etki gözlenmemiştir. İmatinib'in insan over ksenograftı yapılan hayvanlara intraperitoneal uygulaması, greftlerde benzer histomorfolojik anormalliklere sebep olmuş ve sisplatin ile birlikte verildiğinde sisplatine bağlı folikül kaybını önlememiştir.

Bulgularımız, insanda imatinibin over toksisitesi için ilk moleküler kanıtları sunmaktadır. Ayrıca bu çalışma, imatinib tedavisi gören iki farklı kadın hastada yetersiz over yanıtı ve prematür overyan yetmezlik bildiren önceki iki vaka çalışması ile düşünüldüğünde, özellikle üreme çağındaki genç kadınlarda gonadotoksisitesi sebebiyle kullanımı konusunda endişeleri arttırmaktadır.

Anahtar kelimeler: over, apoptozis, sisplatin, DNA hasarı, imatinib, p63

CHAPTER 1
REVIEW OF LITERATURE

1. Anticancer Treatments and Female Fertility

Cancer is one of the most important global public health problems all around the world. Building on many years of progress in cancer detection and treatment, overall survival rates after cancer have risen to almost 80% [1-4]. Over the last 30 years, the overall 5-year relative survival rate for all childhood cancers (children between the age of 0-14) has radically improved from 58% to 83%, because of new and better treatments [5]. This success, however, creates a new and increasing problem: long-term side effects of cancer treatments.

Over 6.6 million women are diagnosed with cancer [6] every year worldwide, and about 10% of them are diagnosed during their reproductive age (age < 40) [7]. They usually receive aggressive chemotherapy and radiotherapy that may cause gonadotoxicity, premature ovarian failure (POF) and subsequent fertility loss in more than 80% of cases [8]. Anticancer treatments such as chemotherapy and radiotherapy have detrimental side effects on the ovary and are considered the most common causes of pathological fertility loss in women [9]. Regrettably, a wide range of adverse health conditions emerges in these survivors, varying from metabolic and endocrine problems to cognitive defects, as a result of previous exposure to cytotoxic chemotherapy regimens and radiation [10].

Infertility and premature ovarian failure are reproductive consequences of exposure to cytotoxic chemotherapy regimens in young females with cancer. Chemotherapy agents exert their cytotoxic effects systemically and therefore induce damage in the ovaries, leading to infertility, premature ovarian failure, and early menopause [11]. They initiate follicle death by inducing genomic damage in the oocyte and somatic cells of dormant primordials and growing follicles [12-14]. Cancer survivors are more prone to developing poor reproductive and obstetrical outcomes than the general population as a result of previous exposure to chemotherapy and radiation [15]. Ovarian insufficiency and other poor reproductive and obstetrical outcomes are other long-term

effects of cancer treatment in survivors. Premature ovarian failure is also accompanying other adverse health-related consequences, including osteoporosis, hot flashes, sleep disturbance, and sexual dysfunction, which can negatively impact on short- and long-term quality of life [16-18]. Radiation therapies are detrimental to both the ovaries and the uterus, in this manner causing a greater magnitude of adverse effects on the female reproductive function [19, 20]. Infertility, premature ovarian failure, fetal growth restrictions, miscarriage, fetal growth restrictions, perinatal deaths, preterm births, delivery of small-for-gestational-age infants, preeclampsia, and abnormal placentation can be listed as adverse effects of radiation therapies.

Cytotoxic chemotherapy regimens and radiotherapy induce apoptotic death of the oocytes and surrounding granulosa cells in the ovary leading to early exhaustion of the follicle stockpile, infertility and premature ovarian failure [1, 12]. Young females diagnosed with breast cancer, lymphomas/leukemias as well as non-malignant diseases (Table 1) requiring the use of cytotoxic chemotherapy regimens are at the greatest risk of premature ovarian failure and infertility following adjuvant chemotherapy [9, 21]. Premature menopause not only results in reduced quality of life but also has associated risks including hot flashes and night sweats; mood swings and disrupted sleep; genitourinary disorders; skeletal abnormalities like osteoporosis with resultant fractures; cardiovascular diseases; and infertility [22]. The impact of anticancer treatments on female fertility depends on the woman's age at the time of treatment, the chemotherapy protocol, the duration and dosage [23].

Table 1. Diseases requiring counseling for fertility preservation [15]. (Abbreviation: HSCT, hematopoietic stem cell transplantation)

Disease	Indication for fertility preservation
Breast	Chemotherapy
Leukemia/lymphoma	Chemotherapy/HSCT
Gynecological malignancies	Chemotherapy/radiotherapy
Myelodysplasia	HSCT
Thalassemia major	HSCT
Aplastic anemia	HSCT
Other hematological diseases	Chemotherapy/HSCT
Autoimmune diseases	Chemotherapy/HSCT
Wegener disease	Chemotherapy/HSCT
Systemic lupus erythematosus	Chemotherapy/HSCT
Wilms tumor	Chemotherapy
Neuroblastoma	Chemotherapy/radiotherapy
Osteosarcoma	Chemotherapy
Ewing sarcoma	Chemotherapy
Tumors of the pelvis and spine	Chemotherapy/radiotherapy
Retroperitoneal tumors	Chemotherapy/radiotherapy
Rhabdomyosarcoma	Radiotherapy
Turner syndrome	Premature ovarian failure
Galactosemia	Premature ovarian failure
Fragile X syndrome	Premature ovarian failure
Y-chromosome mosaicism	Gonadectomy
Teratoma	Gonadectomy

The most common indications for fertility preservation in children, adolescents, and young adult patients are listed in Table 1 above. Over and above malignancies; some precancerous, autoimmune, and benign diseases are also treated with cytotoxic chemotherapy drugs and/or radiation, either to induce disease remission or to suppress the immune system as myeloablative preconditioning treatment before hematopoietic stem cell transplantation [15].

2. Gonadotoxicity of Different Types of Chemotherapy Agents

Chemotherapy-induced ovarian toxicity was first defined in a woman treated with busulfan for chronic myelogenous leukemia in 1956 by Louis et al. [24]. Even though it is foreseen that chemotherapy and radiotherapy have a detrimental influence on oocytes and in the surrounding granulosa cells in the ovary, molecular events at leading to early exhaustion of the follicle stockpile and premature ovarian failure are still not clear.

2.1. Alkylating Agents

Chemotherapy agents belong to alkylating category, such as nitrogen mustards (cyclophosphamide, busulfan) and hydrazines (procarbazine) are recognized to be the most harmful to the ovary than the drugs of all other categories [23, 25]. These agents are not cell cycle specific, thereby do not require cell proliferation to perform their cytotoxic actions (Figure 1) [26]. Consequently, they may affect cells that are not actively dividing, such as oocytes or primordial follicles in the dormant stage. They induce DNA damage and organelle impairment in the cells regardless of the stage of cell cycle ensuring more widespread apoptosis and organ damage [1].

Cyclophosphamide is an alkylating agent that is considered as a standard for gonadotoxic chemotherapy and serves as a backbone in many chemotherapeutic regimens. Destruction of both primordial and growing follicles has been reported in many pre-clinical studies and in vitro studies conducted on human ovarian tissues exposed to cyclophosphamide in a dose-dependent manner. It increases the risk of POF rates above the age of 35 years and this improved risk reach >80% for women over 40 years old [27].

Cyclophosphamide-induced toxicity was well-documented in many other studies as well [28, 29].

DNA

```
      5'           3'
      |            |
      A            T
      |            |
      G            C
       \           |
        \ (1)      G
      C /          |
      |            G
      C            |
      |            A
      T            |
      |            C
      G            |
       \ (2)       G
      C /          |
      |            T
      A            |
      |            T
      G  (3)   C   |
       \      /    C
      C /      \   |
      |            G
      T            |
      |            A
 (4)  |            |
   \  G            C
      |            |
      A            T
      |            |
      3'           5'
```

1 = G-X-C / C-X-G
  Interstrand crosslink caused by
  nitrogen mustards.
  e.g., cyclophosphamide

2 = G-C / C-G
  Interstrand crosslink caused by
  azridines and epoxides, e.g.
  mitomycin C

3 = G / C
  Interstrand crosslink caused by
  nitrosoureas, e.g. BCNU

4 = O^6-Alkylation or Methylation
  caused by hydrazine and triazine
  derivatives, e.g., Procarbazine

Figure 1: Schematic representation of the alkylation of DNA by alkylating agents [26].

2.2. Platinum-Based Regimens

Cisplatin, oxaliplatin, and carboplatin are frequently used agents in the treatments of many types of cancers belong to platinum-based antineoplastics. Cisplatin, which is the most investigated member of this class, acts by specifically provoking crosslinking of DNA as monoadduct, interstrand crosslinks, intrastrand crosslinks or DNA protein crosslinks (Figure 2). platinum-based regimens mostly act on the adjacent N-7 position of guanine, forming a 1, 2 intrastrand crosslink [30, 31]. The consequential crosslinking inhibits DNA repair and DNA synthesis in cancer cells [32]. Cisplatin-induced ovarian toxicity

relates its "off-target" effects on normal cells such as oocytes, granulosa and theca cells in addition to rapidly growing cancer cells [33].
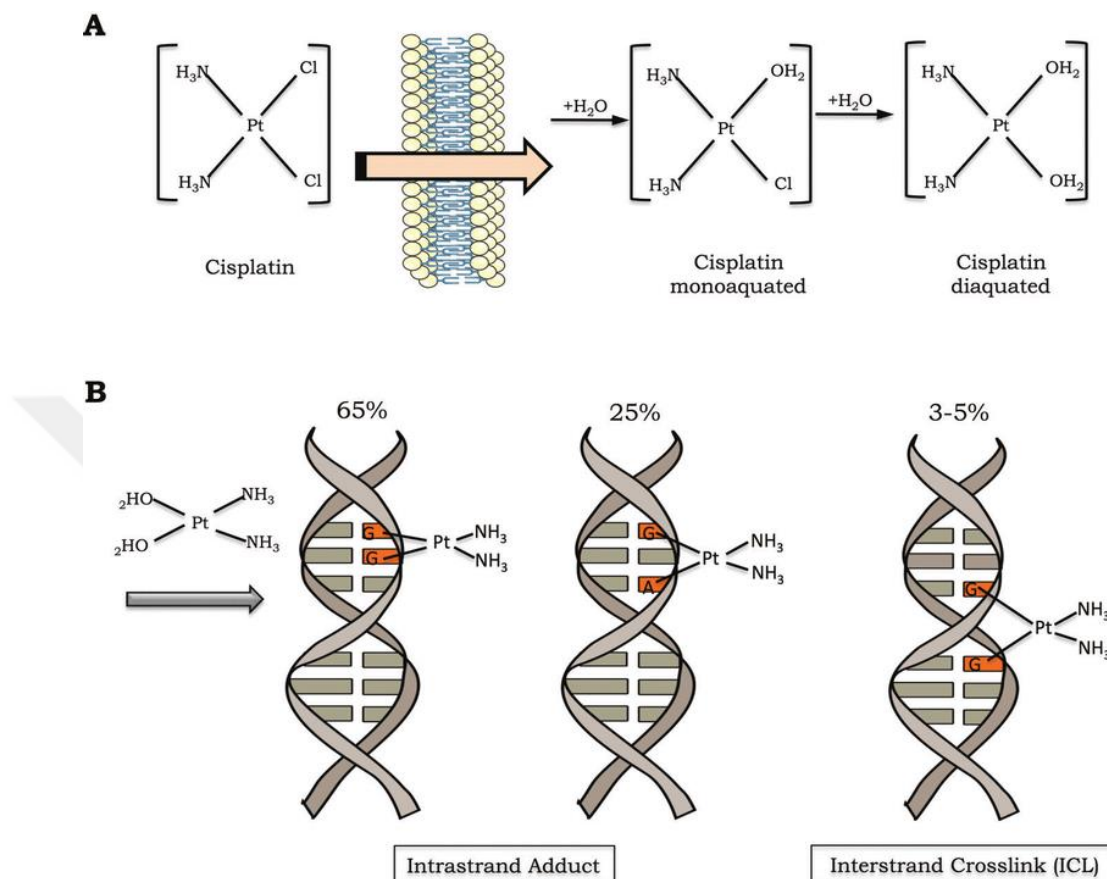
Figure 2: Activation and DNA damage induction of cisplatin. **(A)** Activation of cisplatin requires an exchange of one or two of its chlorides for water molecules (monoaquated and diaquated, respectively). **(B)** Cisplatin forms covalent bonds with DNA and creates crosslinks. The majority of DNA lesions are intrastrand DNA adducts and interstrand crosslinks. The percentages demonstrate the frequency of each type of DNA damage induced by cisplatin [34].

2.3. Anthracyclines

Doxorubicin is a frequently used anthracycline in the treatments of lymphomas, leukemia, breast cancer, and sarcomas. It intercalates with DNA and prevents its replication and transcription partially by inhibiting topoisomerase II. Another mechanism of action is that it causes DNA double-

strand breaks leading to activation of ataxia telangiectasia mutated protein kinase (ATM), a DNA repair protein which may initiate apoptosis in the incidence of high levels of DNA damage [35, 36]. Doxorubicin was formerly considered as a weak gonadotoxic agent, recent findings reveal that this may not be true and doxorubicin could affect the ovary by any, or in fact all, of the above mechanisms [37]. According to recent findings, doxorubicin reveals its gonadotoxicity in a dose-dependent manner on ovarian folliculogenesis, sex steroid production, and oocyte maturation, which are three main factors to support the female reproductive and endocrine functions [38].

2.4. Antimetabolites

Anti-metabolite cancer drugs mainly target the cells actively dividing, and therefore are generally associated with milder ovarian toxicity than cyclophosphamide and cisplatin. This type of regimens such as gemcitabine, methotrexate, and 5-fluorouracil are found to be less gonadotoxic than cyclophosphamide and cisplatin-based on the results of clinical reports indicating lower rates of amenorrhea in women receiving antimetabolite-based treatments compared with those treated with the protocols containing an alkylating drug or a platinum-based compound [1, 10].

Fluoropyrimidine is a subgroup of antimetabolites and acts primarily on cells that are actively synthesizing DNA. Apecitabine, floxuridine, and fluorouracil (5-FU) belong to this group are considered as the backbone of adjuvant treatment for colorectal cancer. The widely used member of this class is 5-fluorouracil. Standard antimetabolite-based chemotherapy protocols are considered to have minimal effects on female fertility. The clinical data regarding the impact of fluoropyrimidines on fertility are limited mainly due to the older age of patients and paucity of the premenopausal population in the trials [23].

2.5. Taxanes

Taxanes are complex anticancer agents including paclitaxel and docetaxel with a unique mechanism of action. The main mechanism of action of taxanes is based on their ability to target microtubules; however, their action is

associated with microtubule stabilization rather than microtubule disruption. They are widely used in various malignancies and have become a pivotal cornerstone in the adjuvant treatment of breast cancer. Paclitaxel and docetaxel act on the cytoskeleton: they stabilize microtubules and disrupt normal polymerization/depolymerization, leading to an arrest of the cells at the G2–M phase of the cell cycle. Molecular and clinical evidence in literature is limited and inconsistent regarding their potential gonadotoxicity. Few clinical studies have observed no additional increase in amenorrhea rates in women treated by taxane-containing regimens, or a mild increase in reversible amenorrhea [39-41]. Nevertheless, several prospective studies have indicated a higher rate of amenorrhea in taxane-based chemotherapy regimens compared to anthracycline-based chemotherapy regimens [42, 43].

3. Assessment of Ovarian Reserve

Ovarian reserve testing is a keystone in patients who underwent gonadotoxic therapies. At the present time, there are several methods used universally to assess the ovarian reserve in women. These include the levels of follicle-stimulating hormone (FSH) and estradiol (E_2) at day 3 of the menstrual cycle, level of anti-mullerian hormone (AMH) and antral follicle count (AFC) [44]. AMH measurement and AFC evaluation have been shown to have a higher predictive value. To enhance its sensitivity, it could be combined with E_2 levels measurement [45].

4. Potential Mechanisms of Chemotherapy-Induced DNA Damage

At any given time, follicles at different stages of maturation reside within the ovary. It is likely that specific stages are more vulnerable to chemotherapy-induced damage than others. A study conducted by Oktem and Oktay discovered that ovarian tissues obtained from patients underwent chemotherapy harbored significantly lower primordial follicle counts than untreated controls [13]. More mature follicles are also susceptible to damage by chemotherapy agents. Diminution of growing follicles also accelerates the depletion of primordial follicle reserve due to the decreased level of inhibitory

substances produced by growing follicles [46, 47]. Consequently, more primordials undergo growth initiation to replace damaged growing follicles and eventually ovarian reserve burn out (Figure 3). Another study performed by Yuksel and Bildik demonstrated that mitotic and non-mitotic granulosa cells are affected by the cytotoxic effects of chemotherapy agents at different levels. They have shown that mitotic human granulosa cells have a higher sensitivity to gemcitabine, an antimetabolite agent, than non-mitotic luteal granulosa cells. They validated that gemcitabine triggered a dose-dependent growth arrest and induced apoptosis of proliferating human (COV434 and HGrC1) and rat (SIGC) granulosa cells in vitro, whereas it did not alter the survival of non-mitotic human luteal granulosa cells (HLGCs) in the same doses of gemcitabine [25]. It is to be expected that the non-mitotic nature of these cells confers them resistance to this mitosis-specific anti-neoplastic actions of this drug.
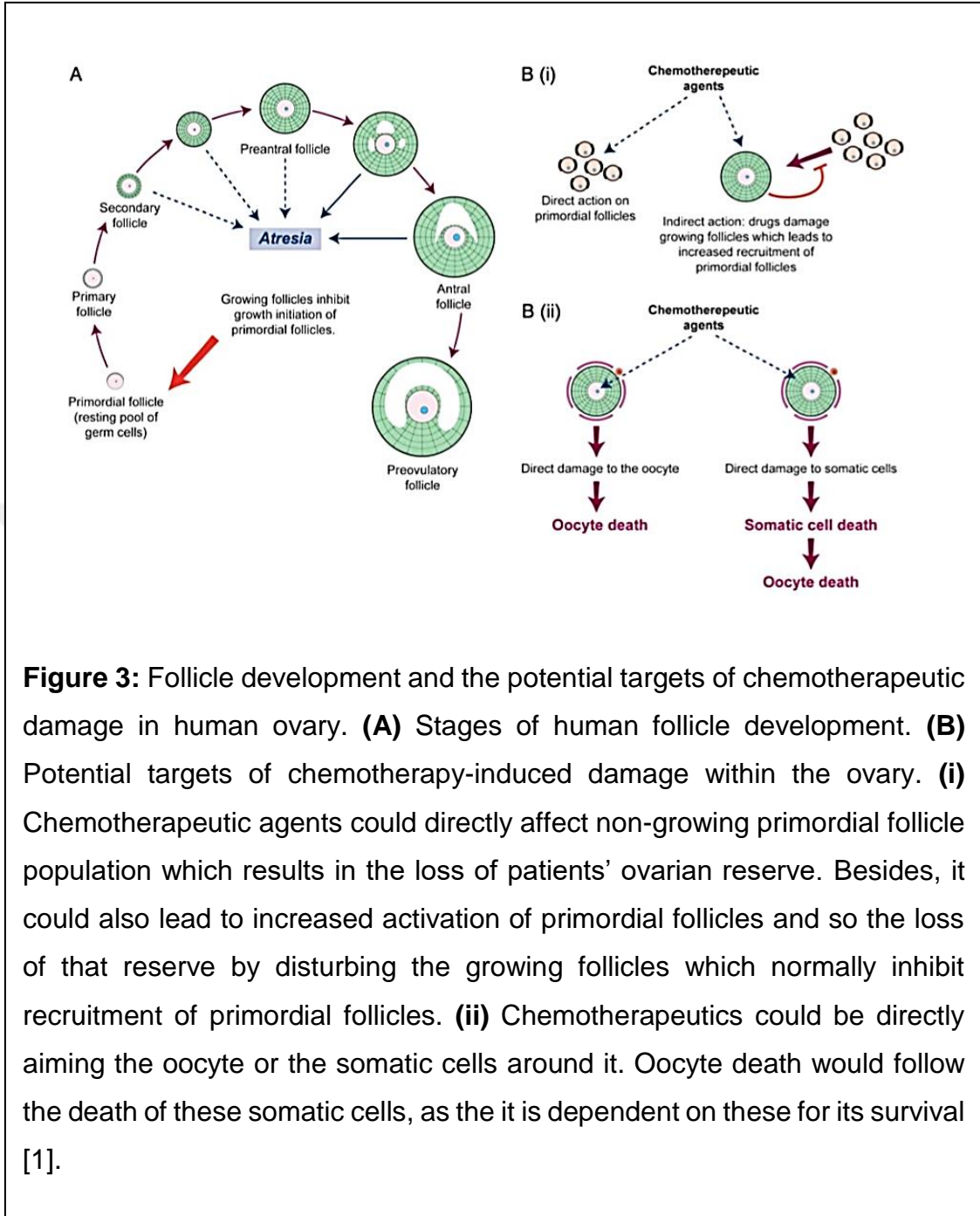
Figure 3: Follicle development and the potential targets of chemotherapeutic damage in human ovary. **(A)** Stages of human follicle development. **(B)** Potential targets of chemotherapy-induced damage within the ovary. **(i)** Chemotherapeutic agents could directly affect non-growing primordial follicle population which results in the loss of patients' ovarian reserve. Besides, it could also lead to increased activation of primordial follicles and so the loss of that reserve by disturbing the growing follicles which normally inhibit recruitment of primordial follicles. **(ii)** Chemotherapeutics could be directly aiming the oocyte or the somatic cells around it. Oocyte death would follow the death of these somatic cells, as the it is dependent on these for its survival [1].

5. Protecting the Ovary from Chemotherapy-Induced Damage

There are three fertility preservation strategies currently available for women who are diagnosed with cancer and will undergo chemotherapy/radiation for treatment of cancer: cryopreservation of patient's oocyte, embryo, and ovarian tissue [48, 49].

5.1. Cryopreservation of Oocyte

Oocyte vitrification applied to oncological patients aims to provide healthy oocytes for a further IVF (in vitro fertilization) cycle once the patient is cured. Oocyte cryopreservation can bedone by using two methods; conventional slow freezing or vitrification [50, 51]. Vitrification is now the most widely used method attributable to the improved survival and fertilization rates, compared to the slow freezing. One of the limitations of this technique is that prognosis depends on the number of available mature oocytes, with a limited number of IVF attempts [52]. Usually, there is the possibility of only one ovarian stimulation attempt as the time before chemotherapy starts. Age is another factor that contributes to the procedure's success, as survival rates after thawing diminish when age increases. Survival of oocytes is related to oocyte quality, an age-dependent factor which, despite possibly serving as a selection filter, may overshadow the procedure's benefits [53, 54]. Another shortness of this method is that it cannot be used in pediatric patients.

5.2. Cryopreservation of Embryo

Embryo cryopreservation is a well-established and beneficial method that offers a high success rate depending on the number and quality of stored embryos. However, there are some disadvantages of this technique. As a sperm sample is needed for fertilization process, the patient should have a partner before starting the treatment. Anyways, similar to oocyte cryopreservation, embryo cryopreservation can only be performed in prepubertal girls [49]. Even though both oocyte or embryo cryopreservation prior to chemotherapy can benefit women achieve pregnancy and live birth, none of these strategies can reverse menopause in the native ovaries. Other drawbacks (mostly related to controlled ovarian stimulation, COS) of embryo and oocyte cryopreservation are:

  i. risk of thromboembolic phenomena
  ii. the potential negative effect of COS on hormone-sensitive tumors
  iii. retrieval of a limited number of oocytes/embryos
  iv. a limited number of future IVF attempts [44].

5.3. Cryopreservation of Ovarian Tissue

To date, there are 60 live births reported after transplantation of frozen-thawed ovarian cortical pieces [55]. However, ovarian tissue cryopreservation is considered still experimental in guidelines and therefore should be performed under an institutional review board (IRB) approval [56]. In this technique, one of the ovaries is generally removed laparoscopically for freezing [15]. Pathological examination of removed ovaries is a prerequisite to rule out any tumor invasion in the ovaries, especially in cancers with a high risk of ovarian metastasis, such as leukemia, neuroblastoma, and genital rhabdomyosarcoma [57]. Slow freezing is the conventional method for cryopreservation of the ovarian tissue [58]. Almost all of the ongoing pregnancies and live births reported to date were achieved from transplantation of slowly frozen ovaries. There is also a report of two pregnancies after engraftment of vitrified and warmed ovaries [55]. Even so, ovarian tissue transplantation carries the risk of re-introducing cancer cells, especially in hematological malignancies. Therefore, any drug that preserves ovarian function during anticancer treatment can potentially maintain normal reproductive life span and eliminate the need for gamete freezing prior to chemotherapy.

Encouraged by the initial reports of animal studies showing a beneficial effect of c-Abl inhibitor imatinib mesylate co-administration with chemotherapy has been proposed as a potential fertility preservation strategy. But studies on this subject launched so far to assess the effectiveness of this method has shown contradictory results. Few studies conducted on mice have demonstrated a protective effect of c-Abl/TAp63 inhibition in preserving ovarian function during chemotherapy, whereas others could not. This fact, together with the lack of a proven molecular mechanism of action for ovarian protection with TAp63 inhibition places this approach under assessment as a potential fertility preservation strategy.

6. TAp63 Pathway and Chemotherapy-Induced Female Infertility

6.1. Structure and Function of TAp63

Tumor-suppressor protein p53, encoded by TP53 gene is the most well-known member of the p53 protein family. It modulates cell reaction in response to various conditions emerging from stress and cellular environments by incorporating endogenous and exogenous signals [59]. Recently, additional regulatory mechanisms have emerged through the identification of p63 isoforms (Figure 4). These are physiological proteins expressed in normal cells from the TP63 gene owing to the use of alternative promoters, splicing sites and/or translational initiation sites [60].

p63 belong to and is the most ancient member of the to p53 gene family, in which is included also p73 [61]. p63, similar to p53 and p73, uses an alternative promoter at the 5′ end of its gene to allow the expression of two different N-terminal isoforms, one containing the N-terminal transactivation domain (TA isoform) and an N-terminal truncated isoform (ΔN isoform) that lacks this domain [62]. Moreover, the C-terminal sequence goes through alternative splicing that leads to a broad range of TA and ΔN isoforms with different C-terminal organization [63, 64]. p53 family proteins share strong structural, biochemical and functional homologies. In particular, the DNA binding domain (DBD) is the highly conserved region among different protein members. All members of this family act via binding to p53 response elements (p53RE) in promoter DNA, a highly conserved region. Nevertheless, there may be the same understated variances in the particular nucleotide sequence in the RE recognized by different family members.
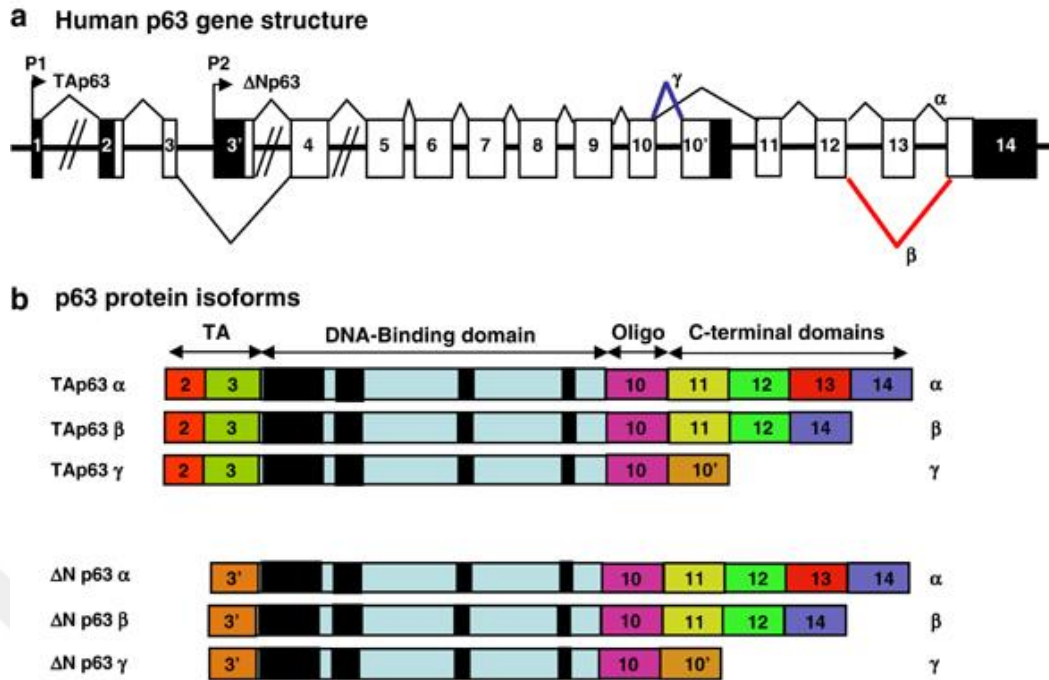
Figure 4: Gene structure and protein isoforms of human p63. **(A)** Diagram of the human p63 gene structure: alternative splicing and alternative promoters (P1 and P2) are indicated. **(B)** p63 protein isoforms: TAp63 proteins encoded from promoter P1 contain the conserved N-terminal domain of transactivation (TA). Np63 proteins encoded from promoter P2 are amino-truncated proteins containing an N-terminal domain different from TAp63 proteins. Numbers indicate the exons encoding p63 protein isoforms [63].

6.2. TAp63 Pathway and DNA Damage Response of Oocytes

Studies conducted on p63 knockout mouse have established an essential role for p63 in DNA damage-induced apoptosis in primordial follicles (PFs) received ionizing radiation (IR) [65] and cisplatin [66] treatments. The oocytes contained by PFs are exceedingly sensitive to genotoxic insults attributable to the constitutive expression of TAp63, an isoform of p63. Deutsch et. al reported that TAp63 isoform in healthy oocytes of PFs forms inactive dimers in normal conditions [67]. When DNA damage occurs, however, its transactivation inhibitory domain at S621 is phosphorylated by checkpoint

kinase 2 (Chk-2). This phosphorylation, in turn, promotes a conformational change and finally formation of active tetramers in TAp63 [67]. Recently, Coutandin et al. have shown that the inactive conformation adopted by TAp63 in resting mouse oocytes arranges a kinetically trapped high-energy state that can be converted into the more thermodynamically stable tetramer by phosphorylation [67, 68]. This activation mechanism implies that modulation of DNA damage response at the transition from inactive dimer to active tetramer could be a strategy to prevent oocyte death during cancer treatments [67, 69]. Therefore, characterization of phosphorylation sites and responsible kinases and revelation of activation mechanisms are of key importance.

In mouse oocytes, phosphorylation of TAp63 seems to be a key step to the introduction of DNA damage response. According to a study conducted by Gonfloni et al., c-Abl TK has been identified to be one of the upstream factors responsible to initiate this process by its kinase activity [70]. This finding highlighted the role of c-Abl in the regulation of primordial oocytes cell death and to some extent elucidated the molecular pathway involved in TAp63 recruitment during oocyte DNA damage response. However, it is still debatable how critical is the role of c-Abl for TAp63 phosphorylation for DNA damage-induced oocytes apoptosis. So far, several kinases have been shown to phosphorylate p63, including ATM, Cdk2, p70s6K, p38 MAPK, Iκβ and Plk (Figure 5) [61]. However, there is no data showing any of them at least partially overcome c-Abl inhibition.
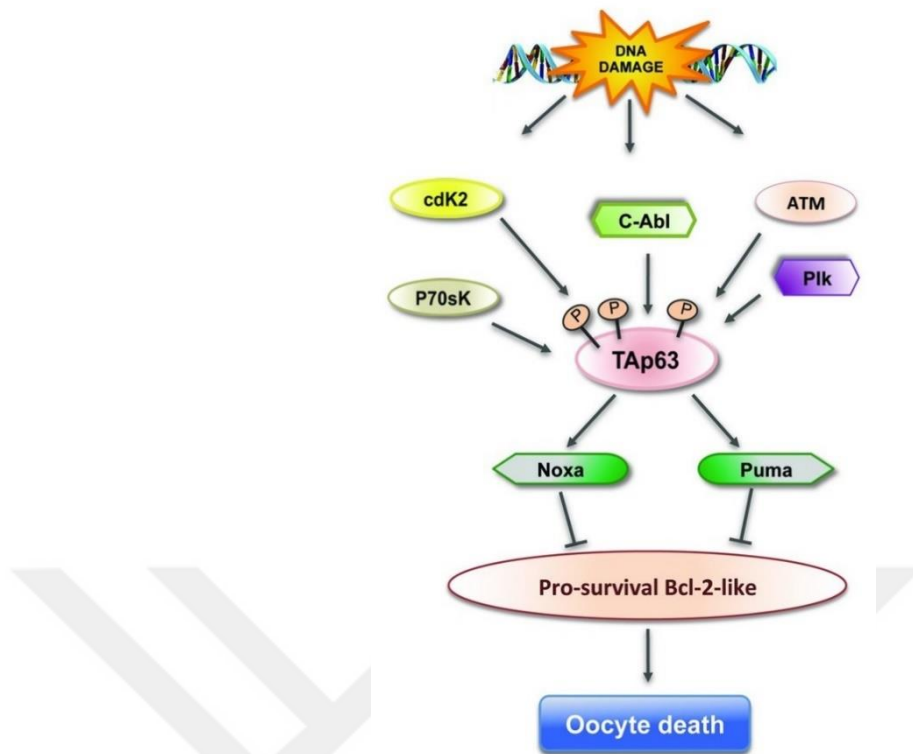
Figure 5: DNA damage-induced oocyte death is triggered with TAp63 phosphorylation which leads to activation of TAp63. Activated TAp63 then induces transcription of BH3-only proapoptotic family members, PUMA, and NOXA which can inhibit pro-survival BCL-2 proteins [61].

6.3. Structure and Function of c-Abl

c-Abl, a protein tyrosine kinase which has been linked to many cellular processes including differentiation, division, adhesion, death, and the stress response is encoded by ABL1 gene. [71]. It is a proto-oncoprotein that belongs to Src family of non-receptor tyrosine kinases which becomes activated in response to various extra or intracellular stimuli (Figure 6). c-Abl is recognized as the cellular homolog of the Abelson murine leukemia virus and its variants have been implicated in tumorigenesis and in many important cellular processes. In chronic myeloid leukemia patients, the first exon of the c-Abl tyrosine kinase gene is replaced by the BCR gene promoter resulting in a constitutively active c-Abl kinase. Bcr/Abl expression give rise to enhanced proliferation, morphological transformation, and anti-apoptotic effects.

Even though many interactions between c-Abl and two or more protein molecules have been resolved, the observable outcomes of these interactions still need to be ascertained. A promising way to study c-Abl function is to identify its direct downstream effectors [71]. Using this approach, identification of a number of candidates which predominantly belong to the DNA repair machinery became possible [72]. Numerous DNA damaging agents are identified to activate c-Abl such as ionizing radiation. Contrarywise to IR, ultraviolet (UV) radiation is reported not to trigger c-Abl activation attributing certain specificity to the c-Abl response [73]. The first pro-apoptotic function of c-Abl is defined by Kharbanda et al by describing c-Abl knockout cells are compromised in the apoptotic response to IR attributing a pro-apoptotic role to c-Abl [74]. These contradictory functions of c-Abl set the stage for more comprehensive molecular and functional analysis of this tyrosine kinase.
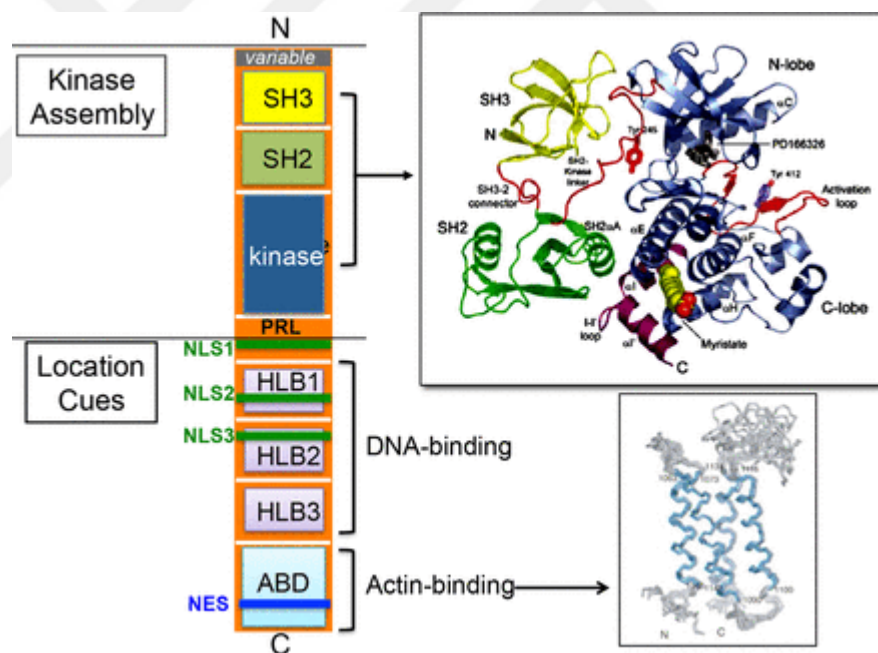
Figure 6: Schematic diagram of ABL domains and structures.

N: N terminal; variable: alternative promoter and 5′ exon encode two ABL variants, type Ia/b (human) and type I/IV (mouse); SH3: Src homology 3 domain (yellow); SH2: Src homology 2 domain (green); kinase: kinase domain (blue) [75].

6.4. Imatinib Mesylate

Imatinib mesylate, the mesylate salt of imatinib, is a targeted therapy and classified as a signal transduction inhibitor with antineoplastic activity (Figure 7). It binds close to the adenosine triphosphate (ATP) binding site of specific tyrosine kinases (TK), thereby inhibiting ATP binding and preventing phosphorylation results in prevention of subsequent activation of growth receptors and their downstream signal transduction pathways. Imatinib is targeted to inhibit Bcr-Abl mutant oncogenic tyrosine kinase as well as by the c-kit and platelet-derived growth factor receptor (PDGFR) oncogenes to a lesser extent. Inhibition of the Bcr-Abl TK results in reduced proliferation rate and heightened apoptotic death in malignant cells of Philadelphia-positive (Ph+) hematological malignancies such as chronic myeloid leukemia (CML) and acute lymphocytic leukemia (ALL). Its activity on c-kit TK results in inhibition of mast-cell and cellular proliferation in those diseases overexpressing c-kit, such as mastocytosis and gastrointestinal stromal tumor (GIST) [76, 77].
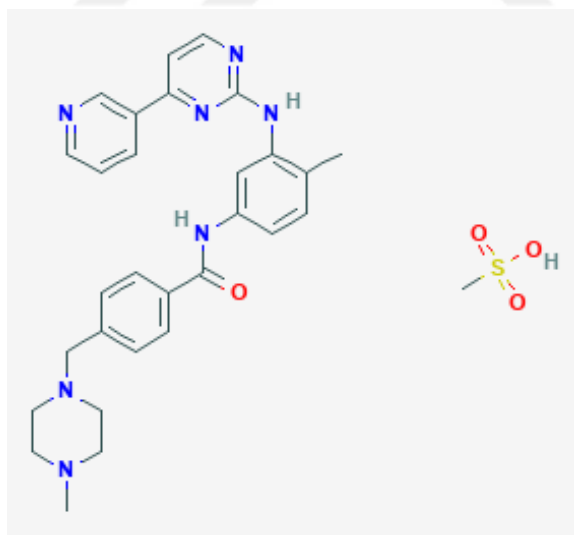
Figure 7: Chemical structure depiction of imatinib mesylate. (PubChem)

6.5. Inhibition of c-Abl/TAp63 as a Fertility Preservation Strategy

As mentioned earlier in this section, phosphorylation of TAp63 is seen to be the most important step for activation of DNA damage response in oocytes. c-Abl tyrosine kinase has been described by Gonfloni et al. to be at least one of the upstream factors responsible for p63 phosphorylation [37]. Moreover, it is suggested that inhibition of c-Abl via its pharmacological inhibitor, imatinib mesylate, may be a promising strategy to prevent oocyte damage induced by chemotherapy.

In 2009, Gonfloni et al. reported that c-Abl is activated along with TAp63 pathway upon exposure to chemotherapy agent cisplatin and that inhibition of this tyrosine kinase with imatinib protects oocytes from cisplatin-induced death in mice [70]. Three years later another group of investigators obtained opposite results by showing that imatinib itself exerts a similar degree of cytotoxicity to cisplatin on the mouse ovaries and does not protect primordial follicles from apoptosis caused by cisplatin or prevent loss of fertility in two independent strains of mice [78]. The authors in the latter study also demonstrated that imatinib-sensitive kinases, such as c-Abl, are not required for the DNA damage-activated oocyte apoptosis that is mediated by TAp63. Furthermore, they raised their concerns about the gonadotoxic potential of this drug because of its inhibitory actions on c-kit, which is a survival factor for ovarian follicles [79]. In 2013, Kim et al showed using in vitro culture and subrenal capsule grafting of mouse ovaries that imatinib inhibits the cisplatin-induced apoptosis of oocytes within primordial follicles. In that study, the investigators demonstrated that cisplatin induces c-Abl and TAp73 expression in the oocyte. While imatinib was unable to block cisplatin-induced DNA damage and damage response, such as the upregulation of p53, it inhibited the cisplatin-induced nuclear accumulation of c-Abl/TAp73 and the subsequent downregulation of TAp63 and upregulation of Bax, thereby abrogating oocyte cell death [66]. The same year Morgan et al reported that imatinib protected follicles against damage induced by cisplatin but not doxorubicin in mouse newborn ovaries under in-vitro conditions [80]. And very recently, Tuppi et al demonstrated that TAp63 activation after exposure to chemotherapy drugs requires phosphorylation by both the priming

kinase checkpoint kinase-2 (CHK-2) and the executioner kinase casein kinase-1 (CK1) in mouse primordial follicles and that c-Abl is not involved in this process. Further, the inhibition of CK1 with a pharmacological inhibitor rescued primary oocytes from doxorubicin and cisplatin-induced apoptosis [81].

To date, no human data is available on this controversial issue. The effects of imatinib on the human ovary are largely unknown except for two separate case reports showing compromised ovarian function [82] and premature ovarian failure in patients while on imatinib treatment [83]. We, therefore, aimed in this translational research study to determine ovarian effects of imatinib and explore whether genomic damage induced by chemotherapy drug cisplatin activates c-Abl along with TAp63 pathway and its inhibition with imatinib prevents apoptosis in human ovarian follicles, isolated oocytes and granulosa cells using in-vitro experiments and in-vivo human ovarian xenograft model.

CHAPTER 2
MATERIALS AND METHODS

1. Study Design, Size, and Duration

This is an in vitro translational research study conducted on human luteal granulosa cells, immature oocytes, ovarian tissues, and granulosa cell lines between the years of 2015-2019 in Koç University Hospital and American Hospital.

2. Patients

Ovarian cortical tissues were obtained from 20 patients (mean age ± SD: 27.2 ± 2.4) undergoing laparoscopic excisions of benign ovarian cysts between the years 2015-2017. All patients underwent operations at the late follicular phase of the cycle (the mean ± SD of the cycle day: 8.2 ± 2.4).

Discarded immature human oocytes at germinal vesicle (GV) (n=40) were obtained during oocyte retrieval procedure from IVF patients (n=10). Human luteal granulosa cells were recovered from follicular fluid during oocyte retrieval procedure in 20 IVF patients (mean age ± SD: 32.6 ± 3.5). The etiologies for infertility were as follows: unexplained (n=12), diminished ovarian reserve (n=8).

Informed consents were obtained from all patients and the study was approved by the institutional review board of Koc University (2015.204.IRB2.074).

3. Animals

All procedures involving mice were authorized by the Institutional Animal Care and Use Committee of Koc University. Athymic nude mice were maintained in accordance with the Guide for the Care and Use of Laboratory Animals in Koc University Animal Research Facility.

4. Culture Medium Formulation

Ovarian tissue samples, HLGCs, HGrC1, and COV434 granulosa cell lines were maintained at 37°C with 5% CO_2, in DMEM/F12 supplemented with 10% (v/v) FBS and 1% (v/v) Penicillin-Streptomycin-Amphotericin B Solution.

5. Chemicals and Reagents

Imatinib mesylate and cisplatin were purchased from Cayman Chemicals (Cas# 220127-57-1, MI, USA) and Eli Lilly and Company (IN, USA), respectively. 4-hydroperoxy cyclophosphamide (4-OOH CY), the active in vitro metabolite of the drug was purchased from Niomech (Bielefeld, Germany) [84]. Anti-CD117 neutralizing c-kit antibody and GNF-2, which is another Bcr-Abl inhibitor without c-kit blocking actions, were obtained from Sigma-Aldrich Company GmbH (Germany).

All cell culture reagents, YO-PRO®-1 Iodide (491/509) and Alexa probes were purchased from Life Technologies (Thermo Fisher Scientific Inc., MA, USA). Anti-cleaved caspase-3 (#9664), Anti-phospho $SAPK/JNK^{Thr183/Tyr185}$ (#9251), Anti-SAPK/JNK (#9252), Anti-phospho $Chk1^{Ser345}$ (#2348), Anti-phospho $Chk2^{Thr68}$ (#2197) antibodies and Hoechst 33342 (#4082) were purchased from Cell Signaling Technology Inc. (MA, USA). Anti-γH2A.X^{Ser139} antibody (clone JBW301) was from Millipore (MA, USA). Anti-TAp63 (EPR5701) and Anti-phospho $TAp63^{Ser395}$ antibodies were purchased from Abcam (USA). Anti-c-Abl (K-12, sc-131) and Anti-PARP (C2-10, 556362) antibodies were obtained from Santa Cruz Biotechnology, Inc (CA, USA) and BD Biosciences (CA, USA), respectively. Anti-Vinculin antibody was from Sigma-Aldrich Chemie GmbH (Germany). xCELLigence system is a product of Roche Diagnostics (Mannheim, Germany). COV434 cell line was purchased from Sigma (St. Louis, MA, USA). HGrC1 was a gift from Dr. Ikara Iwase (Nagoya University, Japan). All western blotting buffers and reagents were purchased from BioRad (USA). Super Block reagent (#AAA125) was purchased from ScyTek Laboratories. Cell Titer-Glo® (CTG) Luminescent Cell Viability Assay was obtained from Promega (WI, USA).

Chemotherapy drugs cisplatin, 4-OOH CY and imatinib mesylate were administered in vitro at their therapeutic blood concentrations. 4-OOH CY, the active metabolite of the drug was used at 50 and 100 µM concentration [84]. 4-OOH CY form was used in vitro experiments because cyclophosphamide needs to be metabolized in by cytochrome p450 in the liver (Figure 8). Cisplatin was used at 5, 20 and 40 µM [85, 86]. Imatinib mesylate was given at three different concentrations, 2.5, 5 and 10 µM. GNF-2 was used at 3, 7 and 14 µM while Anti-CD117 was administered 0.8, 1.6 and 3.2 ng/ml.
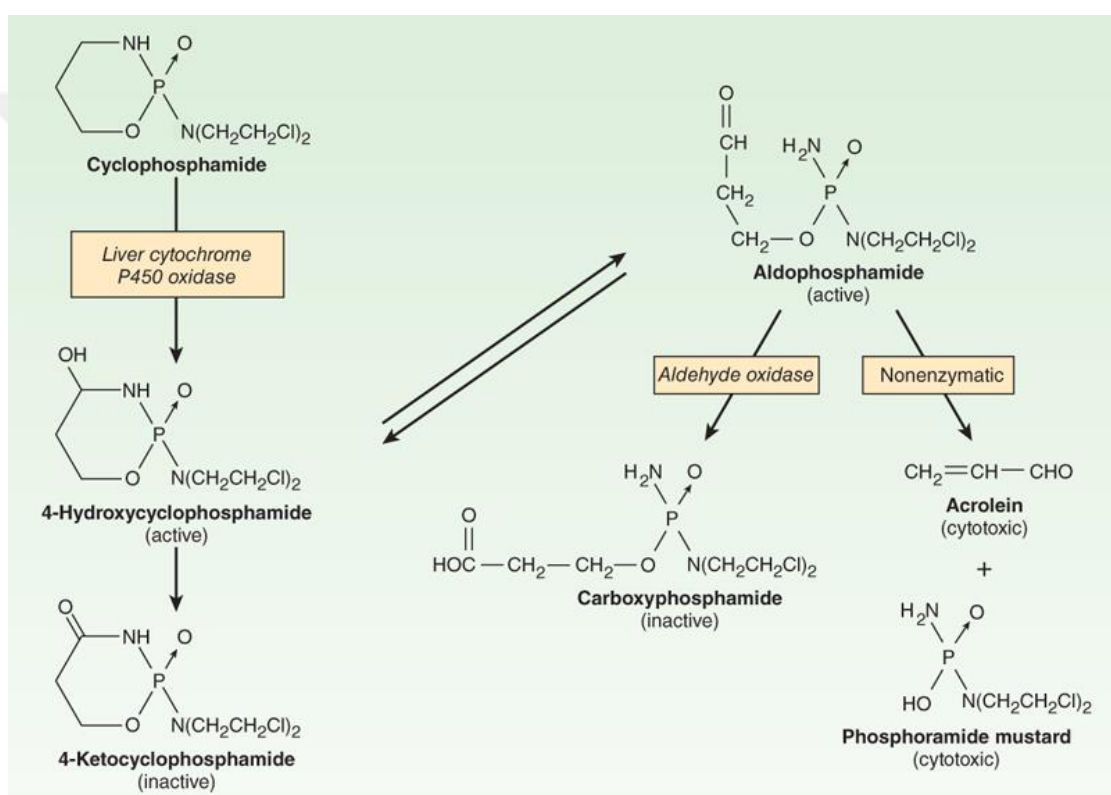
Figure 8: Metabolism of cyclophosphamide [87, 88].

6. Experiments on Human Ovarian Tissue

6.1. Preparation of Human Ovarian Cortical Tissues

Ovarian cortices embedded in the cyst wall were removed during laparoscopic excisions of benign ovarian cysts under sterile conditions, minced into pieces of equal size (0.5 x 0.5 cm) and either xenografted subcutaneously to 8-week-old nude mice or in vitro cultured in 24-well format culture plate (Figure 9) using 2 ml of culture media as we described previously [89].
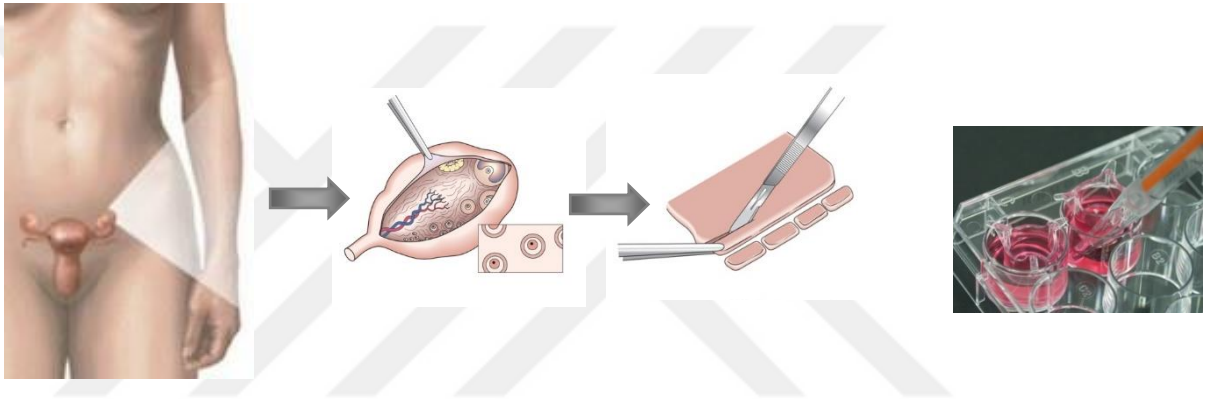
Figure 9: Schematic diagram demonstrating the preparation and culture of human ovarian cortical tissues.

6.2. Human Ovarian Xenograft in Nude Mice

Human ovarian tissues obtained from patients were minced under sterile conditions into small fragments of equal size (0.5 x 0.5 cm) and then xenografted subcutaneously to the right flank region of the 8-week-old nude mice (n=4 per group).

Animals were randomly divided into 4 groups:
  i. Control
  ii. Cisplatin
  iii. Imatinib
  iv. Cisplatin + Imatinib (2 hours before cisplatin)

At 6th weeks post-transplantation, the animals received a single intraperitoneal injection of cisplatin (5 mg per kg body weight), imatinib (7.5 mg per kg body weight) or cisplatin (5 mg per kg body weight) in combination with imatinib (7.5 mg per kg body weight). The drugs were used at the concentrations that were previously used in the papers of Gonfloni and Kerr et al [70, 78]. Control animals received dimethyl sulfoxide (DMSO) only. The animals were euthanized, and the xenografts were removed at 24 hours. Intra-cardiac blood samples were obtained immediately post-mortem for AMH measurement.

6.3. In Vitro Model of Human Ovarian Cortical Samples

Ovarian cortices embedded in the cyst wall were removed under sterile conditions, minced into pieces of equal size (0.5 × 0.5 cm) and cultured for in 24-well format culture plate using 2 ml of culture media. The drugs were added to the culture media at the indicated concentrations. DMSO was used as vehicle drug.

    i.   Control
    ii.   Cisplatin
    iii.   Imatinib
    iv.   Cisplatin + Imatinib
    v.   GNF-2
    vi.   Anti-CD117

7. Human Immature Oocyte Culture

A total of 40 morphologically normal GV stage oocytes were used in this study. They were incubated in the G-IVF culture medium (Vitrolife, Goteborg, Sweden). Imatinib and/or chemotherapy agents were added to the culture medium at the indicated concentrations.

8. Human Granulosa Cells

8.1. Non-Mitotic Luteinized Granulosa Cells

8.1.1. Isolation of Human Luteal Granulosa Cells

In routine IVF protocols, the developed follicles are punctured under transvaginal ultrasound guidance and the contents are aspirated. The cumulus-oocyte complexes are then visualized and manually collected from the aspirated fluids. After the first follicle has been punctured, localized bleeding occurs, so that subsequent follicular aspirates contain some blood. Therefore, once follicular aspirates have been pooled, the majority of cells in these preparations are erythrocytes. These red blood cells have a greater density than granulosa-luteal cells and settle to the bottom of culture dishes faster. If the culture surface is completely covered with these cells, the granulosa-luteal cells will not be able to attach. Therefore, it is necessary to remove these erythrocytes to maximize plating efficiency and obtain enriched cultures.

HLGCs were recovered from follicular fluid during oocyte retrieval procedure in 10 IVF patients. For the isolation of human luteal granulosa cells from follicular fluid, hypo-osmotic lysis technique was used described by Lobb et. al. [90]. The aspirates of follicular fluids were spun down at 500xg for 5 minutes and the supernatant was discarded. 0.5 ml of the cell slurry was pipetted into a 15 ml conical bottomed polystyrene centrifuge tube. 9 ml of sterile distilled water added, and the tube was capped and mixed. After 40 seconds, 1 ml of 10X concentrated phosphate buffered saline (PBS), pH 7.4 was added and the tube was capped and mixed. The tubes were then centrifuged at 500xg for 5 minutes and then decanted by inverting the tubes. The cell pellet was resuspended in culture media. Then recovered cells were plated in 24 well format culture plate in a density of 5000 cells per well (Figure 10).
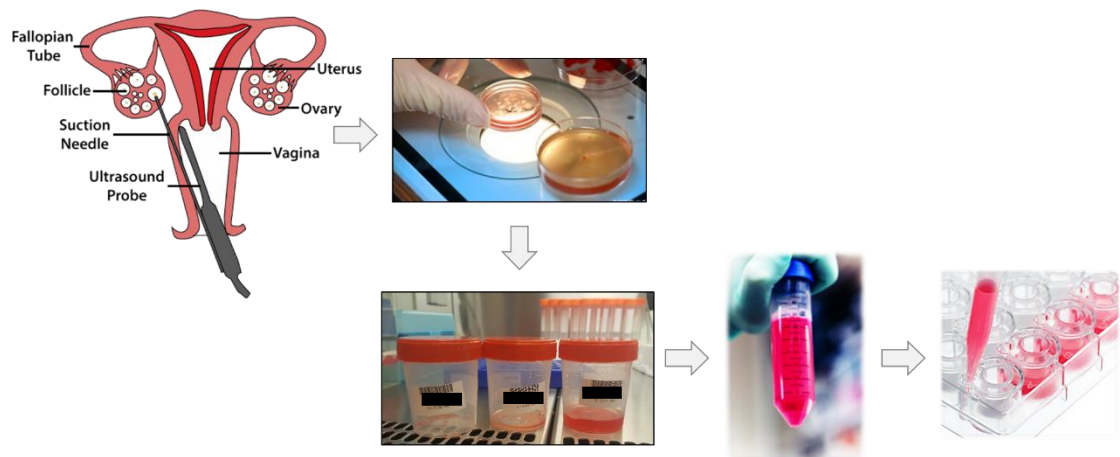
Figure 10: Schematic representation demonstrating the isolation of human granulosa cells.

8.1.2. Culture of Human Luteal Granulosa Cells

HLGCs are highly specialized primary luteinized granulosa cells. They do not proliferate either spontaneously, or after stimulation with a mitogenic agent. They produce large amounts of progesterone and estradiol hormones in vitro [89].They are Oil Red O positive cells, an indicator of their steroid content, one of the distinguishing characteristics of sex steroid-producing cells.
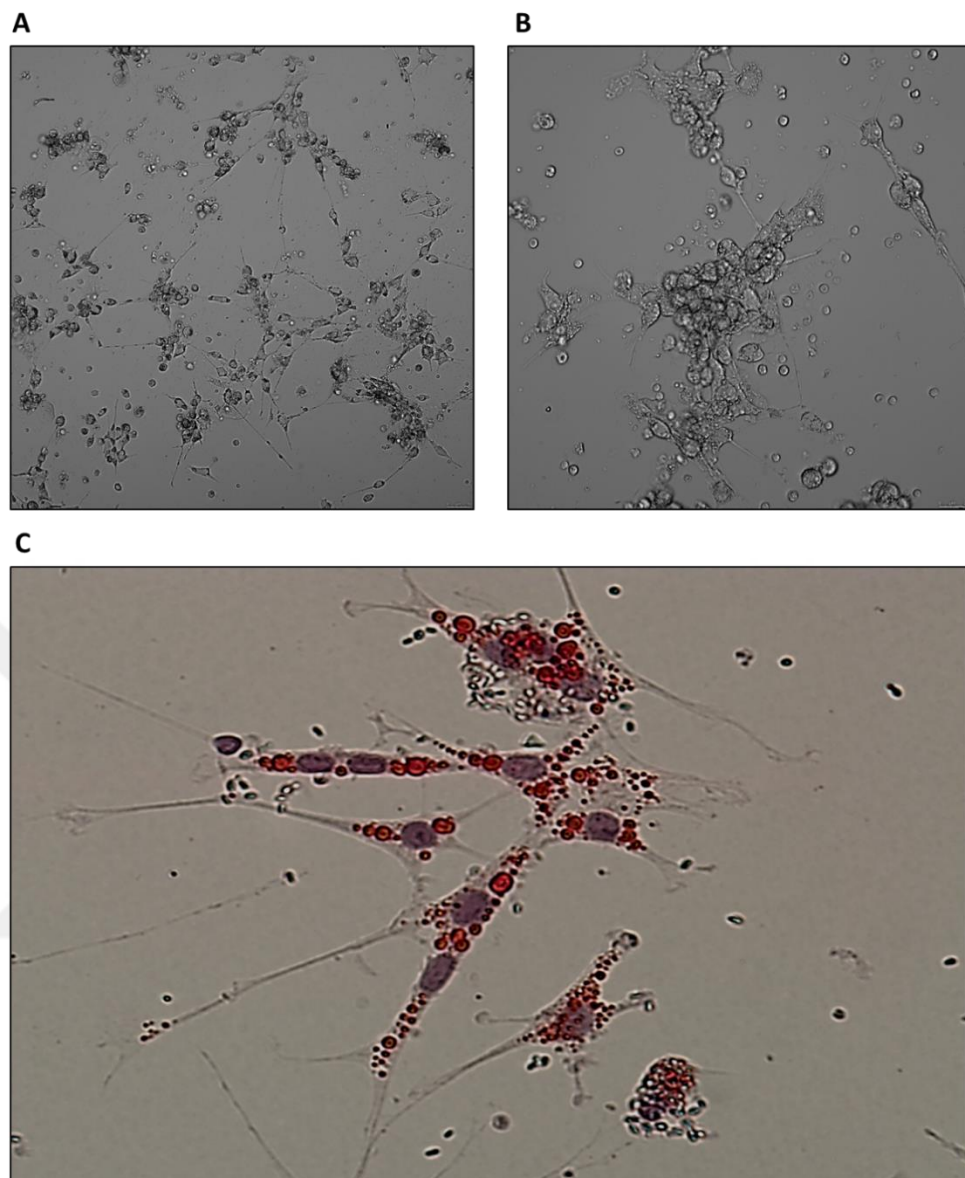
Figure 11: Isolated human luteal granulosa cells under the light microscope at **(A)** 10X and **(B)** 20X magnifications. **(C)** HLGCs stained with Oil Red O to confirm their steroid content, one of the distinguishing characteristics of sex steroid-producing cells at 40X magnification.

8.2. Mitotic Granulosa Cell Lines

8.2.1. HGrC1

HGrC1 is a human non-luteinized granulosa cell line expressing enzymes related to sex steroid syntheses, such as steroidogenic acute regulatory protein, aromatase, and gonadotropin receptors. They were granulosa cells obtained from a 35-yr-old female and immortalized by lentivirus-mediated transfer of several genes so as to establish a human nonluteinized granulosa cell line HGrC1 by Bayasula, et al. [91]. These cells are not capable of undergoing luteinization, resembling the characteristics of granulosa cells belonging to follicles in the early stage. HGrC1 might also be capable of displaying the growth transition from a gonadotropin-independent status to gonadotropin-dependent one [91].
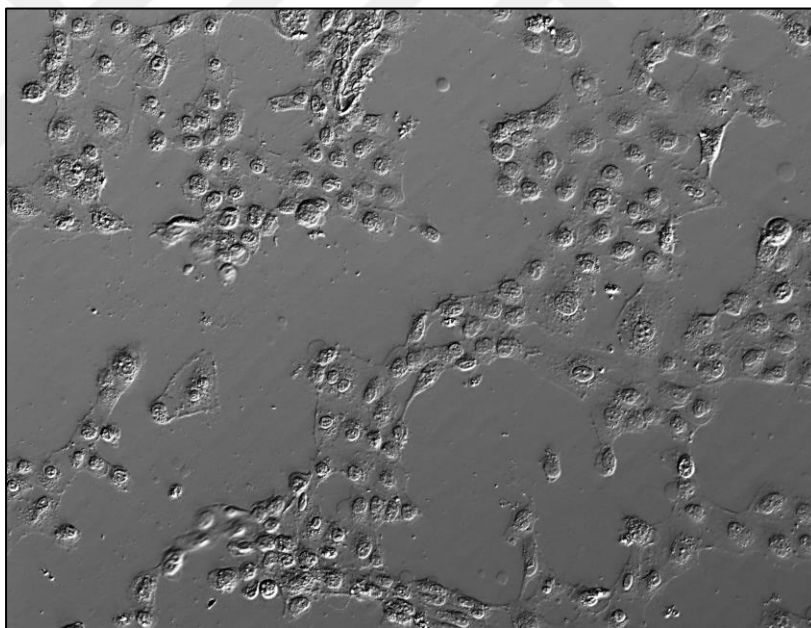
Figure 12: HGrC1 cells under the light microscope at 20X magnification.

8.2.2. COV434

COV434 cell line was purchased from Sigma Co. These cells are originated from the cells obtained from a patient with a granulosa cell tumor. The biological characteristics of this cell line include the production of 17 beta-

estradiol in response to FSH; the absence of luteinizing hormone (LH) receptor; no luteinization capability, and the presence of specific molecular markers of apoptosis enabling the induction of follicular atresia [92].
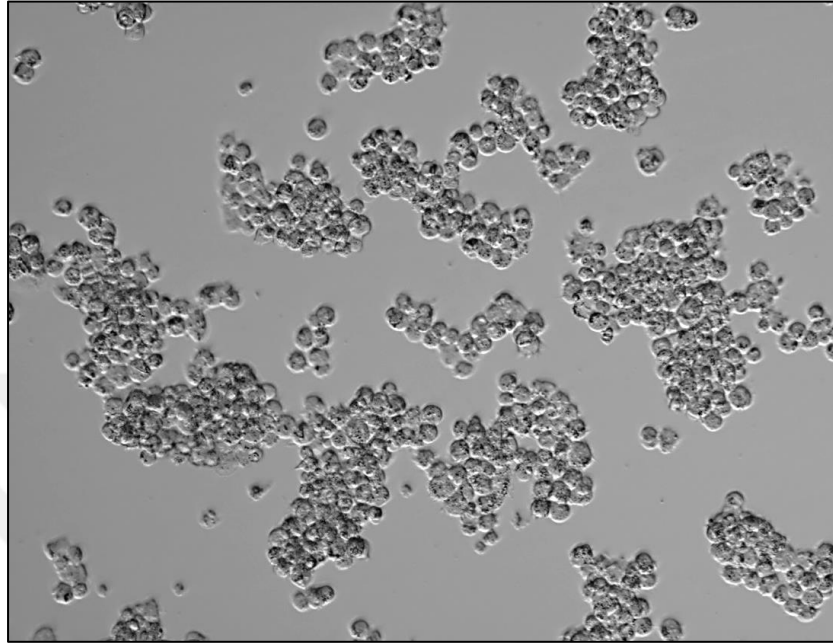
Figure 13: COV434 cells under the light microscope at 20X magnification.

9. Histomorphometric Assessment and Follicle Counts

Paraffin-embedded sections were serially sectioned at the 5-µm thickness and primordial follicle density was determined from serial sections as the mean of follicle counts per square millimeter in every fifth section after staining with hematoxylin-eosin (H&E). Follicle density was expressed as follicle count/mm^2. Light microscopic images were taken under a Zeiss Axioscope or Olympus IX71.

10. Immunoblotting

Treated cells were detached by trypsinization and the cell pellet was obtained with centrifugation at 500xg for 5 minutes. Pellets were then washed with ice-cold PBS and then re-suspended in an appropriate volume of Radio-Immunoprecipitation Assay (RIPA) cell lysis buffer containing, 150 mM NaCl, 1.0% IGEPAL® CA-630, 0.5% sodium deoxycholate, 0.1% sodium dodecyl

sulfate (SDS), and 50 mM Tris, 1X phosphatase inhibitor cocktail and 1X protease inhibitor cocktail (Sigma, MA, USA). Following 20 minutes of incubation on ice, centrifugation at 14,000xg for 20 minutes at 4^0C was performed to obtain supernatants containing total cell extract.

Proteins were separated by SDS-polyacrylamide gel electrophoresis and transferred onto a polyvinylidene difluoride (PVDF) membrane by Trans-Blot® Turbo™ RTA Mini PVDF Transfer Kit (#170-4272, BioRad, USA). The membranes were blocked with 5% nonfat dry milk in Tris-buffered saline-Tween 20 (TBS-T) (20 mM Tris-HCl, pH 7.8, 150 mM NaCl, 0.1%, v/v Tween-20) at room temperature for 1 hour. Then the primary antibodies at indicated dilutions were added and incubated rocking overnight at 4^0C. Anti-γ-H2AX and anti-cleaved caspase-3 antibodies were used at 1:1000 and 1:500 dilutions to assess DNA damage and apoptosis, respectively. Anti-SAPK/JNK and anti-phospho-SAPK/JNK antibodies were both performed at 1:1000 dilutions. Anti-p63, anti-phospho-p63 and anti-c-Abl antibodies were used at 1:500 dilutions. Anti-vinculin at a dilution of 1:10000 is used as a loading control. Secondary antibodies conjugated to horseradish peroxidase (HRP), anti-rabbit and anti-mouse were used in 1:2000. Quantification of protein within membranes was done by using Clarity™ Western Enhanced chemiluminescence (ECL) Substrate. Chemiluminescence detections were performed by ChemiDoc XRS+ Imaging System (BioRad, USA).

11. Immunofluorescent Staining

For immunofluorescence studies, cells grown on coverslips were fixed with 4% paraformaldehyde (PFA) for 20 minutes at room temperature, permeabilized with 0.1% Triton X-100 and then treated with superblock for 10 minutes. After rinsing with DPBS-T (0.1% Tween-20 in Dulbecco's PBS), they were incubated with the cleaved caspase-3 antibody for detection of apoptosis and γ-H2AX antibody for detection of DNA damage in superblock at 1:50 dilutions overnight at 4°C. The cells were washed with DPBS-T and incubated with fluorochrome-conjugated secondary antibody diluted in PBS for 90 minutes at 37°C. This step was followed by rinsing the coverslips and adding Hoechst

33342 (1µg/mL) for DNA staining. The images were taken under appropriate channels using immunofluorescence (IF) microscope (Olympus IX71, Japan).

12. Real-Time and Quantitative Assessment of Cell Proliferation and Viability Using xCELLigence System

xCELLigence is a cell culture system that allows real-time quantitative analysis of cell proliferation, viability, cytotoxicity, adhesion/invasion/receptor activity assays without using any compound and labeling agent. The system uses specially designed microtiter plates containing interdigitated gold microelectrodes to non-invasively monitor the viability of cultured cells using electrical impedance as the readout and generates real-time curves of cell viability and proliferation [93]. We previously used and described this system in our other studies that validated that this platform can be used as a tool to assess cytotoxic and mitogenic agents on human granulosa cells [25, 89]. The electronic readout of cell–sensor impedance is displayed in real-time as a cell index (CI), a value directly influenced by cell attachment, spreading, and/or cell proliferation. The cells were treated with the drugs at log phase. The viability and proliferation of the cells were monitored on the Real-Time Cell Analyzer (RTCA) system at 30-minute time intervals for up to 140 hours. The results were expressed by normalized CI derived from the ratio of CIs before and after the addition of the compounds.

xCELLigence RTCA system is composed of an impedance analyzer, a computer with RTCA software, a 96-well electronic microtiter plate (E-Plate) and the RTCA station, which is placed inside the cell culture incubator (Figure 14-A). The application of a low voltage leads to generate an electric field between the electrodes, which can be impeded by cell presence. The electronic readout of cell–sensor impedance is displayed in real-time as CI, a value directly influenced by cell attachment, spreading, and/or cell proliferation (Figure 14-B).

100 µL of complete media was added to each well of 96-well E-Plate. Following 15-minute incubation at room temperature, the background impedance was measured. Cells were seeded in 96-well E-Plate at the density of 10,000 cells per well in a final volume of 200 µL, then incubated at 37°C with

5% CO_2 and continuously monitored on the RTCA system at 30-minute time intervals. When the cells reached the log growth phase (18-20 hours after plating), they were treated with the chemotherapy drugs ± imatinib at the indicated concentrations. The proliferation and the viability of the cells were monitored in a real-time and quantitative manner every 30 minutes for up to 140 hours. The results were expressed by normalized CI; which are derived from the ratio of CIs before and after the addition of the compounds. The normalization of CI arbitrarily sets CI to 1 at the indicated time points. Recording of CI and normalization CI was performed using the xCELLigence RTCA Software 1.2.
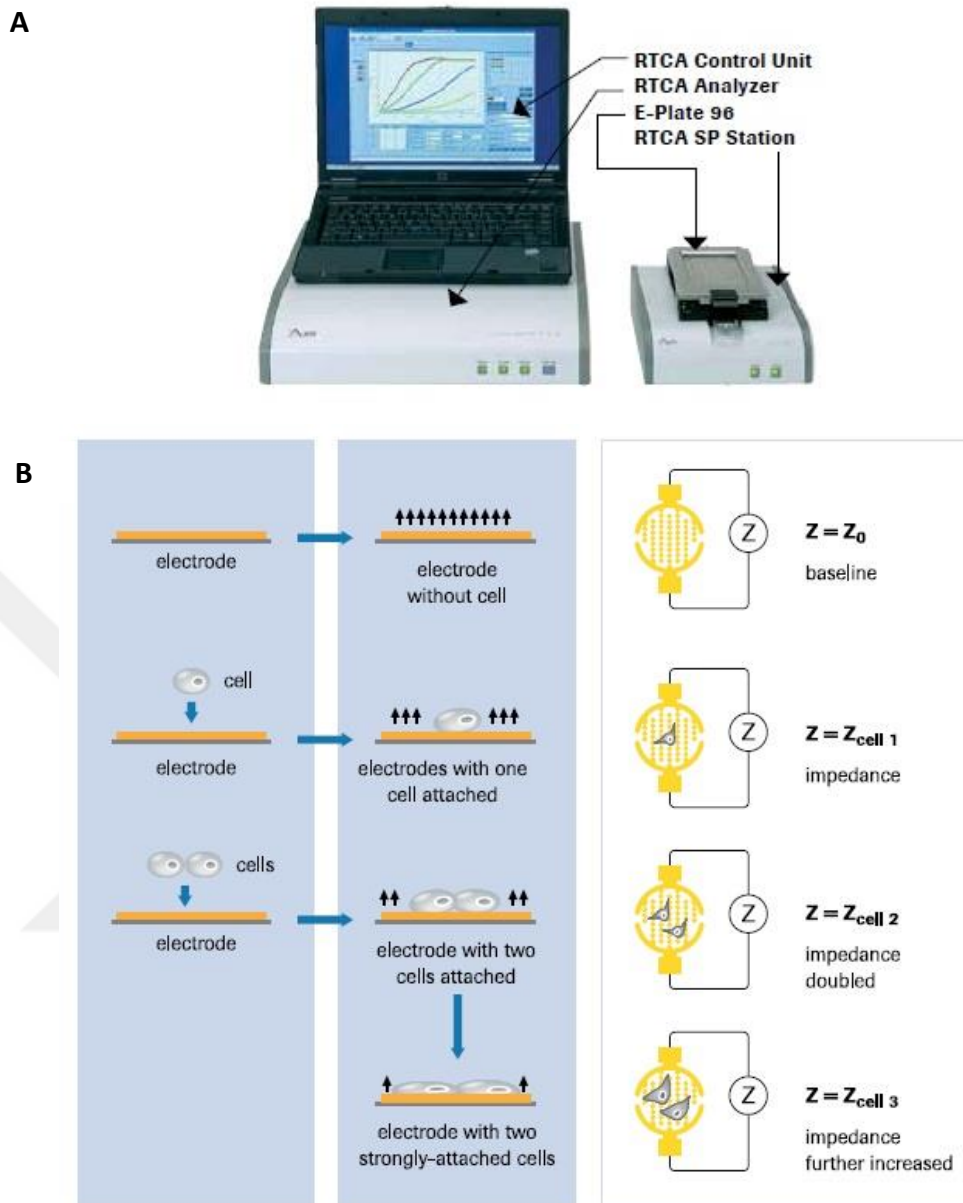
Figure 14: xCELLigence RTCA SP system overview. **(A)** xCELLigence RTCA SP Analyzer. **(B)** The presence of cells on top of the E-Plate electrodes affects the electrode/solution interface, leading to an increase in electrode impedance. The more cells that are attached on the electrodes, the larger the increases in electrode impedance. When cells are not present or are not well-adhered on the electrodes, the CI is zero.

13. Cell Viability Analysis

13.1. Live Cell Imaging with YO-PRO-1 Staining for the Assessment of Cell Viability

Apoptosis-based changes occur in the permeability of cell membranes. Apoptotic cells become permeant to the green-fluorescent carbocyanine nucleic acid stain YO-PRO-1 (1µM) (absorbance 491 nm, emission 509 nm), which selectively passes through the plasma membranes and labels them with moderate green fluorescence. Under fluorescent microscopy, YO-PRO-1 positive cells demonstrate the morphological features of cells undergoing apoptosis such as nuclear shrinkage and fragmentation. An important characteristic of the dye that differs from all other nuclear dyes previously used for the detection of apoptosis is that it does not label living cells.

YO-PRO-1 (0,1 µM) and Hoechst 33342 (1µg/mL) were added to culture media at the indicated concentrations. Live/dead cell imaging of the cells was undertaken under appropriate channels using IF microscope (Olympus IX71, Japan) after 30 minutes of exposure. Five hundred cells were counted at four different high magnification areas and the percentage of the cells expressing YO-PRO-1 was calculated.
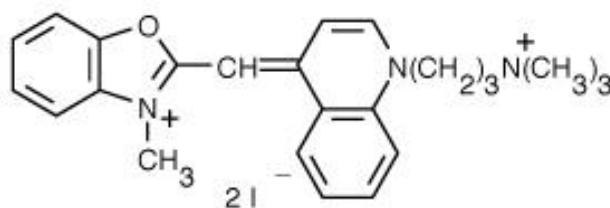
Figure 15: Chemical structure of YO-PRO-1. Its relatively large size (630 Da) prevent it from penetrating the intact plasma membrane of living cells.

13.2. Cell Titer-GLO Luminescent Cell Viability Assay

The cells were plated at a density of 10,000 cells per well in a 96-well white, assay plate and treated with imatinib at the indicated concentrations. Cell Titer-Glo reagent was added at 1:1 volume ratio. The plate was placed on a

rocking platform for 2 minutes and incubated at room temperature for 10 minutes before the luminescence signal was read in a plate reader (Thermo Scientific). Luminescence readings were background subtracted and normalized to control wells.

14. Gene Expression Analysis via Quantitative Real-Time PCR

RNA isolation was performed with Quick-RNA MicroPrep Kit (Zymo Research, Irvine, CA, USA) by following the manufacturer's instructions. RNA was quantified with spectrophotometric read at 260 nm by Nanodrop 2000 (Thermo Fisher Scientific, MA, USA) and 1000 ng cDNA was prepared by using M-MLV Reverse Transcriptase (Invitrogen). Quantitative real-time expressions of mRNAs were detected and compared by using Light Cycler 480 SYBR Green I Master (Roche, Germany). The primers of the genes used in the study are shown in Table 2.

Table 2. List of primers and their sequences used in quantitative real-time PCR (qRT-PCR).
F: forward, R: reverse primer

Gene		Sequence
CASP-3	F	5'-CATGGAAGCGAATCAATGGACT-3'
	R	5'-CTGTACCAGACCGAGATGTCA-3'
GAPDH	F	5'-AGCCACATCGCTCAGACAC-3'
	R	5'-GCCCAATACGACCAAATCC-3'
NOXA	F	5'-ACCAAGCCGGATTTGCGATT-3'
	R	5'-ACTTGCACTTGTTCCTCGTGG-3'
PUMA	F	5'-GACCTCAACGCACAGTACGAG-3'
	R	5'-AGGAGTCCCATGATGAGATTGT-3'

15. Hormone Assays

15.1. AMH

AMH levels in the supernatants were determined using Active Mullerian Inhibiting Substance/Anti-Mullerian Hormone (MIS/AMH) (Diagnostic Systems Laboratories, Inc., USA) enzyme-linked immunosorbent assay (ELISA) kit. The analytical sensitivity of the kit was 0.006 ng/mL. Intra-assay repeatability and the coefficient of variations were given as 4.6% (0.144 ng/mL), 2.4% (0.843 ng/mL), and 3.3% (4.408 ng/mL), respectively.

15.2. Estradiol and Progesterone

The levels of both hormones were determined using the electrochemiluminescence immunoassay (ECLIA), an immunoassay for the in vitro quantitative determination of estradiol and progesterone levels. ECLIA kits specific for progesterone (Elecsys Progesterone II, Cobas) and estradiol (Elecsys Estradiol II, Cobas) were used according to manufacturer's instructions to measure the corresponding hormone levels in the culture media. All analyses were performed on the Cobas® 6000 analyzer series (Roche Diagnostics, USA). Lower detection limits for estradiol and progesterone were 18.4 pmol/L (5.00 pg/mL) and 0.095 nmol/L (0.030 ng/mL), respectively.

16. Statistical Analysis

Follicle counts, hormone levels and cell index readouts of the xCELLigence system were continuous data, therefore expressed as the mean ± [SD]. ANOVA and multiple comparison post-hoc test were used to compare continuous data among the groups if the data is parametric, or Kruskal-Wallis test and Dunn's post-hoc comparison if it is non-parametric. Nominal data were compared between the groups using Fisher' exact or Chi-square tests where appropriate. Statistical analyses were done using SPSS for windows 21 statistical package program. $p < 0.05$ is considered significant.
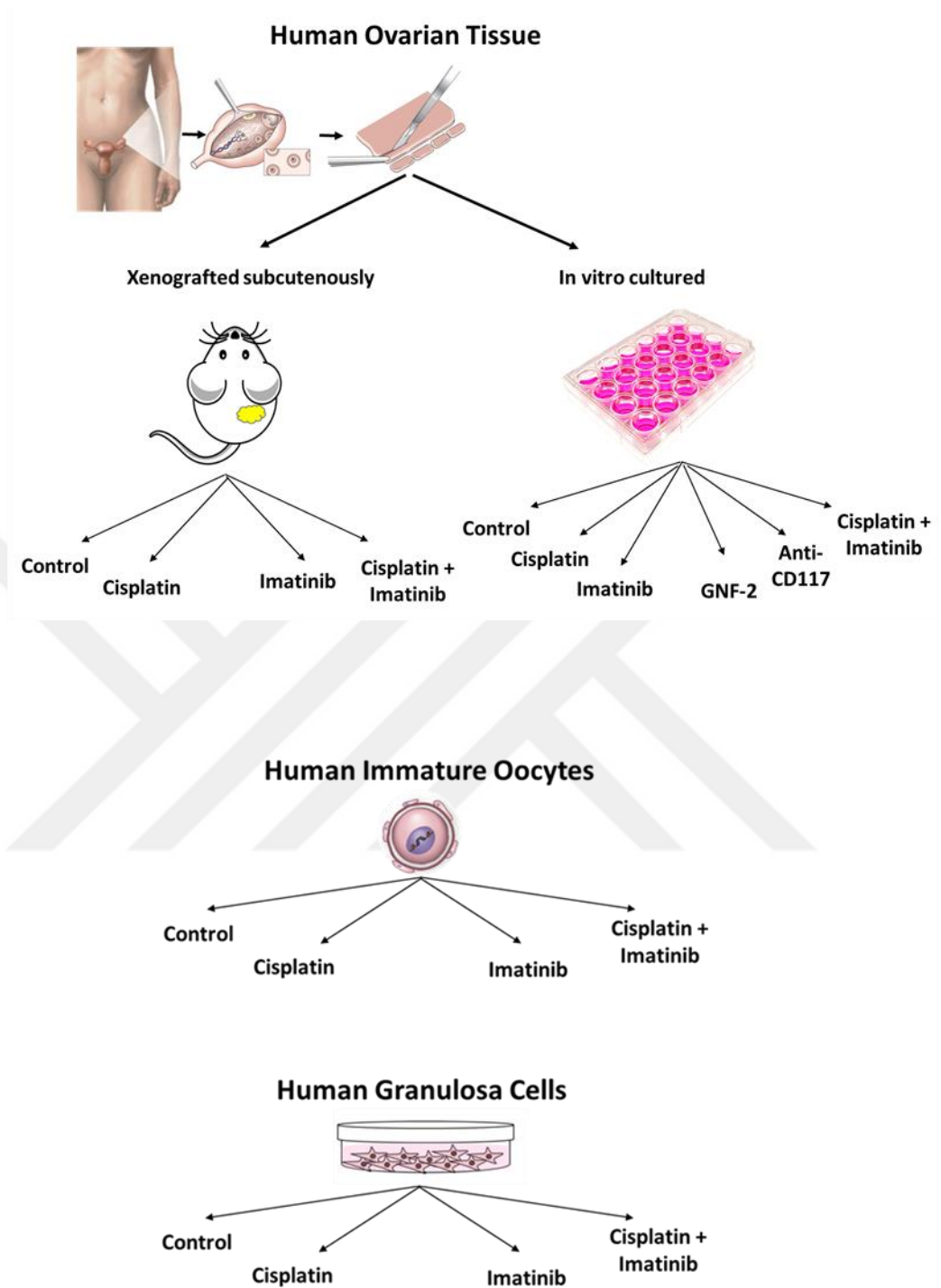
Figure 16: Overview of the experimental design.

CHAPTER 3

RESULTS

1. Human Ovarian Xenografts in Nude Mice

1.1. Assessment of Follicle Reserve and Steroidogenic Activity after Cisplatin Treatment

Treatment of the animals with a single intraperitoneal injection of cisplatin (5 mg/kg) 6 weeks after xenografting of human ovarian samples resulted in a significant decrease in the number of healthy primordial follicles in xenografted human ovarian tissues along with a reciprocal increase in the number of atretic primordial follicles at 24 hours post-injection compared to control animals receiving vehicle drug DMSO injections. The administration of imatinib (7.5 mg/kg) prior to (2 hours) cisplatin did not appear to confer any protective effect against cisplatin-induced follicle loss because the number of primordial follicles was comparable between the xenografts exposed to cisplatin vs. cisplatin+imatinib (Figure 17-A and 17-B). Interestingly, the magnitude of the gonadotoxicity after imatinib appeared to be similar to cisplatin when a comparison was made based on the degree of follicle loss and the reduction in AMH levels. Notably, bizarre shaped primordial follicles lacking oocytes and unclassifiable small follicles possessing atretic oocytes without granulosa cells were much more frequently observed in the samples exposed to imatinib in comparison to control xenografts and those exposed to cisplatin (33% vs. %1 vs. 8% $p<0.01$, respectively) (Figure 18). We were not able to assess the effect of cisplatin and imatinib on the secondary follicles (namely, primary, pre-antral and antral stage follicles) as they constitute approximately 10% of total follicle pool in the human ovary, precluding us from making a quantitative analysis.

These in-vivo findings provided histomorphological evidence for possible gonadotoxic effects of imatinib on the human ovary and prompted us to analyze ovarian effects of this drug more thoroughly using the following in vitro and in vitro experiments.

	PF (Healthy)	PF (Atretic)	AMH
Control	1.65±0.25	0.43±0.1	2.54±0.2
Cisplatin	0.45±0.2	1.88±0.3	1.68±0.2
Imatinib	0.58±0.2	1.75±0.25	1.88±0.2
Cisplatin + Imatinib	0.35±0.15	1.94±0.3	1.45±0.2

*: p<0.001 compared to control
**: p<0.01 compared to control

p>0.05
Cisplatin vs Imatinib
Cisplatin+Imatinib vs Imatinib
Cisplatin+Imatinib vs Cisplatin
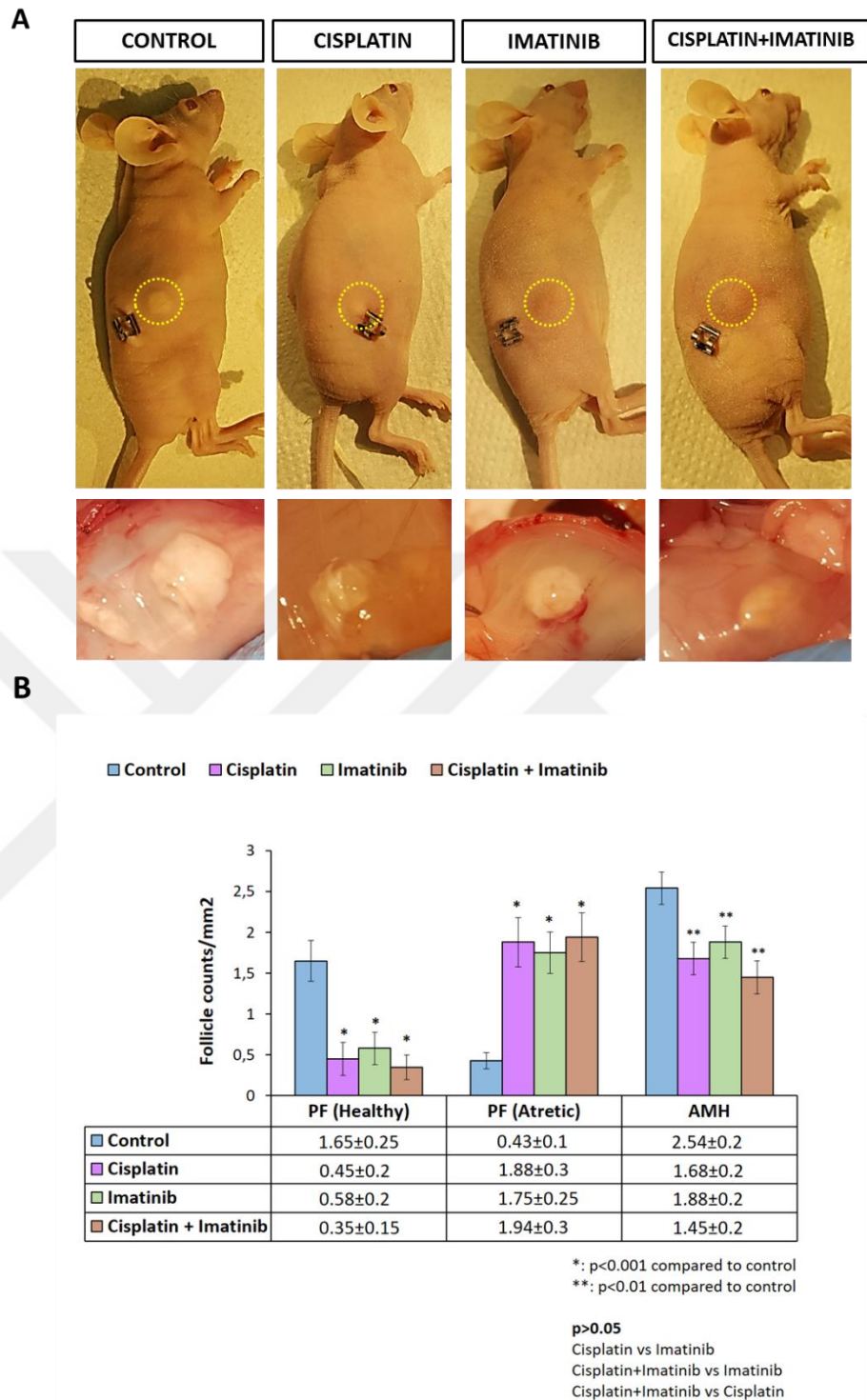
Figure 17: Human ovarian xenografting in nude mice. **(A)** Human ovarian tissues xenografted subcutaneously. **(B)** Intraperitoneal administration of a single dose of cisplatin 6 weeks after transplantation resulted in a drastic decrease in the number of primordial follicles along with a reciprocal increase in the number of atretic primordials in the xenografts at 24 hours post-exposure.

The administration of imatinib 2 hours prior to cisplatin did not prevent follicle loss. The reductions in the primordial follicle numbers were comparable among the animals treated with cisplatin, imatinib or both. Serum AMH levels were significantly decreased in the animals treated with cisplatin, imatinib or both compared to control animals.
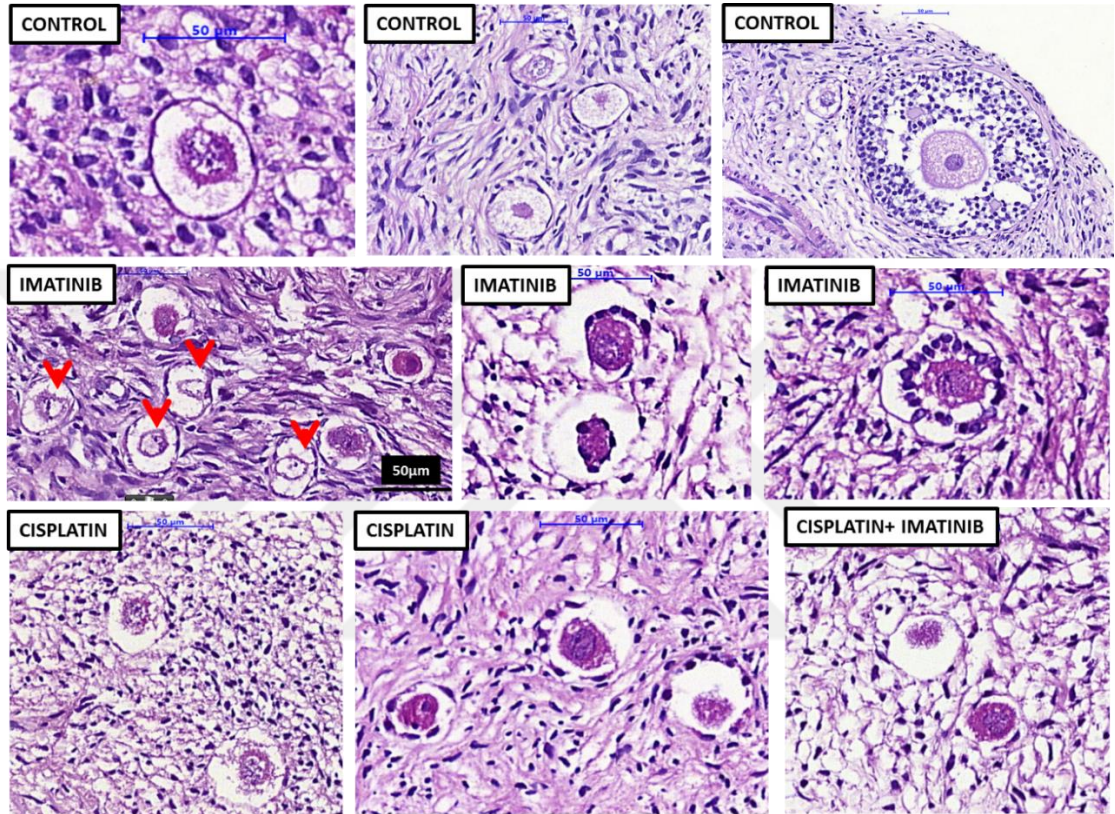
Figure 18: Histological examination of xenografted human ovarian tissue. Primordials and small follicles lacking an oocyte and empty zona oocytes without granulosa cells were more abundantly observed in the xenografts exposed to imatinib (Hematoxylin-eosin staining, red arrows).

1.2. Histological Assessment of The Animals' Own Ovaries

Histological examination of the animals' own ovaries revealed similar findings to what we obtained in the ovarian xenografts. The number of primordial follicles was significantly reduced in the mouse ovaries treated with cisplatin. Imatinib treatment with cisplatin did not prevent cisplatin-induced follicle loss. Furthermore, primordial follicle number was substantially reduced and there

were multiple small follicles lacking oocytes in the animals receiving imatinib alone without cisplatin. On the other hand, the number of pre-antral and antral follicles were comparable among the control animals and those treated with cisplatin, imatinib or both (Figure 19).
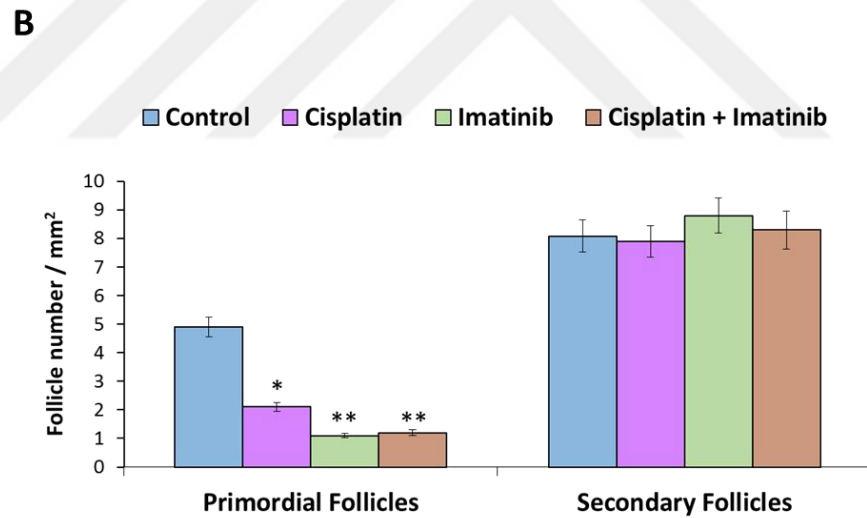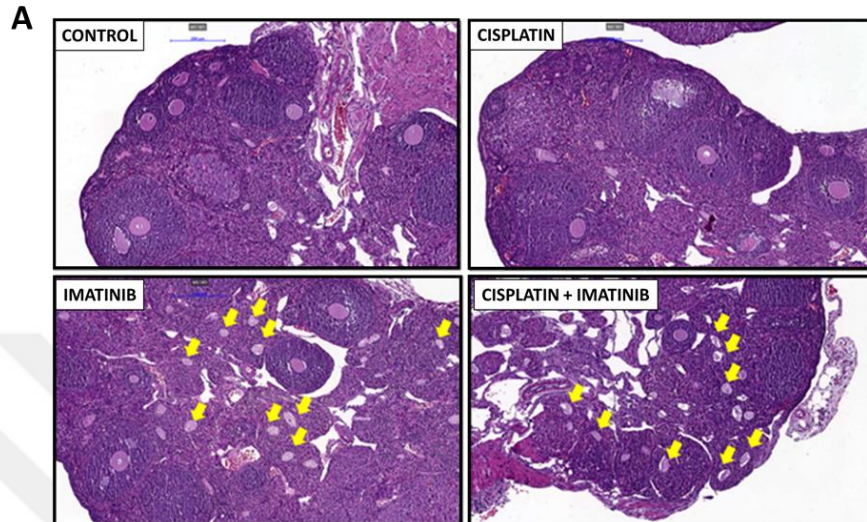
*: p<0.01
**: p<0.001 for comparison with control

Figure 19: Histological examination of animals' own ovarian tissue. **(A)** Similar to the grafted tissues, there were multiple small follicles lacking oocytes (yellow arrows) in the animals' own ovaries exposed to imatinib. **(B)** The number of primordial follicles was significantly reduced in the animals treated with cisplatin. Imatinib treatment with cisplatin did not prevent cisplatin-induced follicle loss.

2. In Vitro Model of Human Ovarian Tissue

2.1. In Vitro Treatment of Ovarian Cortical Samples with Cisplatin, Imatinib or Both

Treatment of ovarian cortical pieces in culture with cisplatin for 24 hours resulted in significant reductions in the number of healthy primordial follicles and in vitro estradiol and AMH production of the samples along with a reciprocal increase in the number of atretic follicles. Imatinib treatment prior to or concurrent with cisplatin neither ameliorated cisplatin-induced follicle loss nor improved in vitro hormone productions of the samples compared to those treated with cisplatin alone (Figure 20). When a comparison was made based on the healthy and atretic fractions of the primordial follicles and E_2 and AMH levels, imatinib and cisplatin appeared to exert a similar degree of cytotoxicity on the ovarian tissue samples under in vitro conditions. Furthermore, in vitro imatinib treatment resulted in the morphological abnormalities in the follicles in the ovarian tissue samples that were similar to those observed in the ovarian xenografts of the animals treated with imatinib. Namely, bizarre shaped primordial follicles, follicles lacking granulosa cell layer and/or oocytes and empty zona oocytes were more commonly observed in the samples treated with imatinib compared to control and cisplatin-treated ones (42% vs. 2% vs. 7%, $p < 0.01$) (Figure 21).

Exposure of human ovarian tissue to cisplatin at 20 μM concentration for short (30 minutes) and long (24 hours) terms induced SAPK/JNK and TAp63 pathways and triggered apoptosis as evidenced by an increase in the protein expression of the cleaved form of caspase-3 in immunoblotting. However, TAp63 activation after cisplatin was not associated with any notable change in the protein level of c-Abl (Figure 22).

	PF (Healthy)	PF (Atretic)	AMH	E2
☐ Control	1.86±0.2	0.36±0.1	2.1±0.2	1.48±0.2
☐ Ima	0.53±0.1	1.94±0.3	0.45±0.2	0.65±0.3
☐ Cis	0.43±0.2	1.96±0.2	0.36±0.2	0.59±0.2
☐ Cis + Ima	0.35±0.1	2.1±0.4	0.25±0.1	0.42±0.2
☐ Anti-CD117	0.83±0.2	1.42±0.3	1.1±0.3	0.87±0.2
☐ GNF-2	1.35±0.2	0.6±0.1	1.6±0.1	1.38±0.2
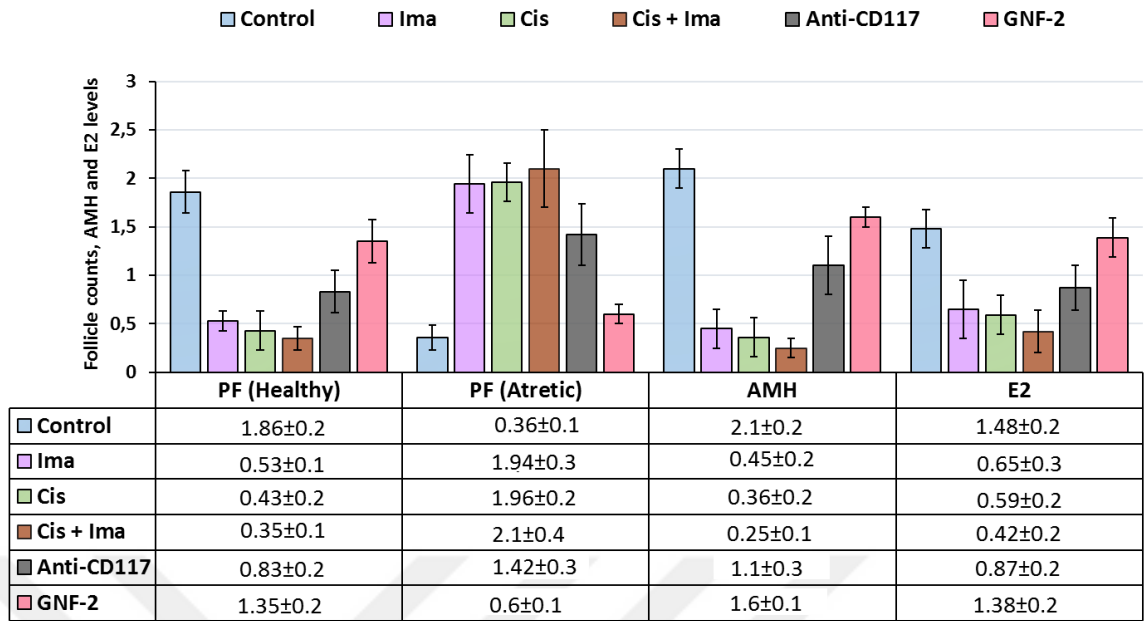
PF: Primordial follicle count/mm^2 ,
AMH: Antimullerian hormone (ng/mL),
E2: Estradiol (x10^3 pg/mL),
Cis: Cisplatin (20µM),

Anti-CD117: c-kit blocking ab (3.2pg/mL),
GNF-2 (14µM),
Imatinib (10µM)

PRIMORDIAL FOLLICLE COUNT

p<0.001
Control vs. Imatinib
Control vs. Cis
Control vs. Cis+Imatinib
p<0.01
Control vs. anti-CD117
p<0.05
Anti-CD117 vs. Imatinib
Anti-CD117 vs. Cis
Anti-CD117 vs. Cis+Imatinib
p>0.05
Control vs. GNF-2

AMH & ESTRADIOL

p<0.01
Control vs. Imatinib
Control vs. Cis
Control vs. Cis+Imatinib
Control vs. anti-CD117
p<0.05
Anti-CD117 vs. Imatinib
Anti-CD117 vs. Cis
Anti-CD117 vs. Cis+Imatinib
p>0.05
Control vs. GNF-2

Figure 20: Follicle counts and hormone production comparison in ovarian tissue culture model. In-vitro treatment of ovarian cortical pieces with cisplatin for 24 hours resulted in significant reductions in the number of primordial follicles and in vitro E$_2$ and AMH production of the samples along with an increase in the number of atretic follicles. The reduction in follicle counts and hormone productions were comparable among the samples exposed to cisplatin, imatinib or both. Follicle atresia at such a degree was also observed in the samples exposed to c-kit blocking agent anti-CD177 but not in those treated with another c-Abl inhibitor GNF-2, which does not possess c-kit blocking action.
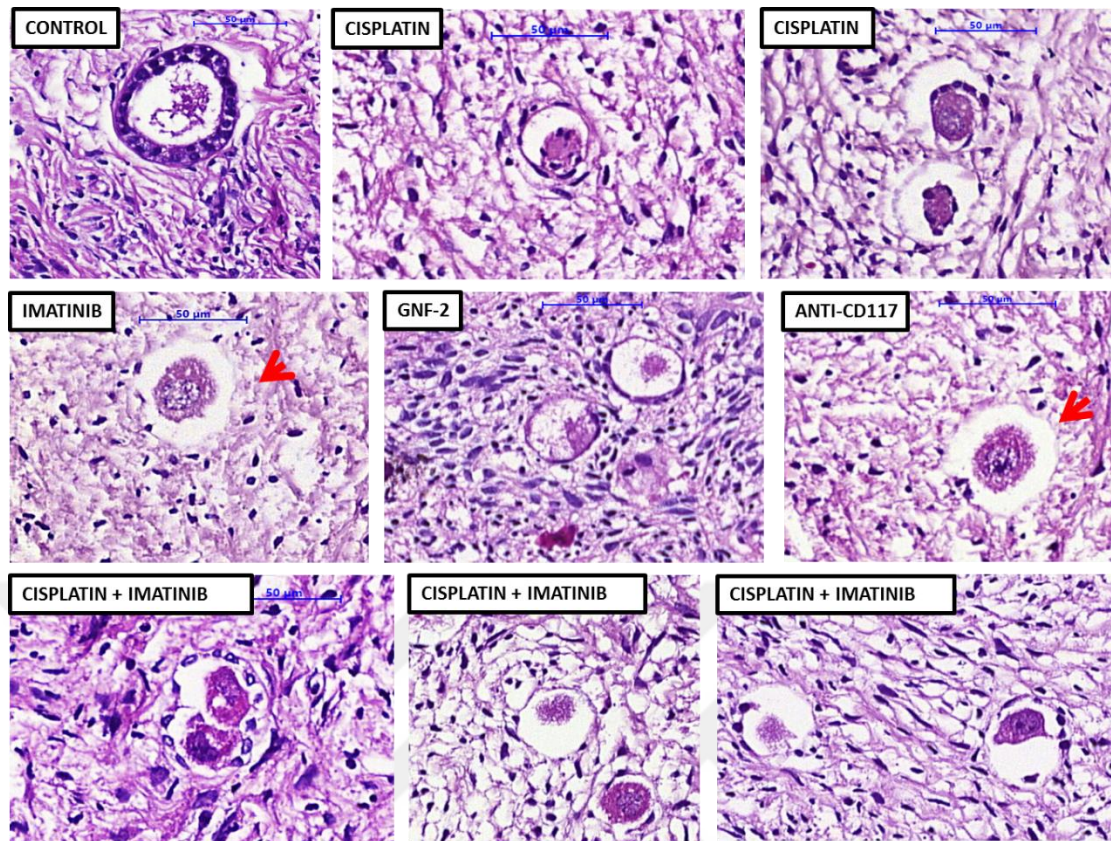
Figure 21: Histological examination of in vitro cultured human ovarian tissue. Bizarrely shaped follicles and small follicles lacking an oocyte were more commonly observed in the samples treated with imatinib and anti-CD177 but not in the control and cisplatin-treated ones (red arrows).
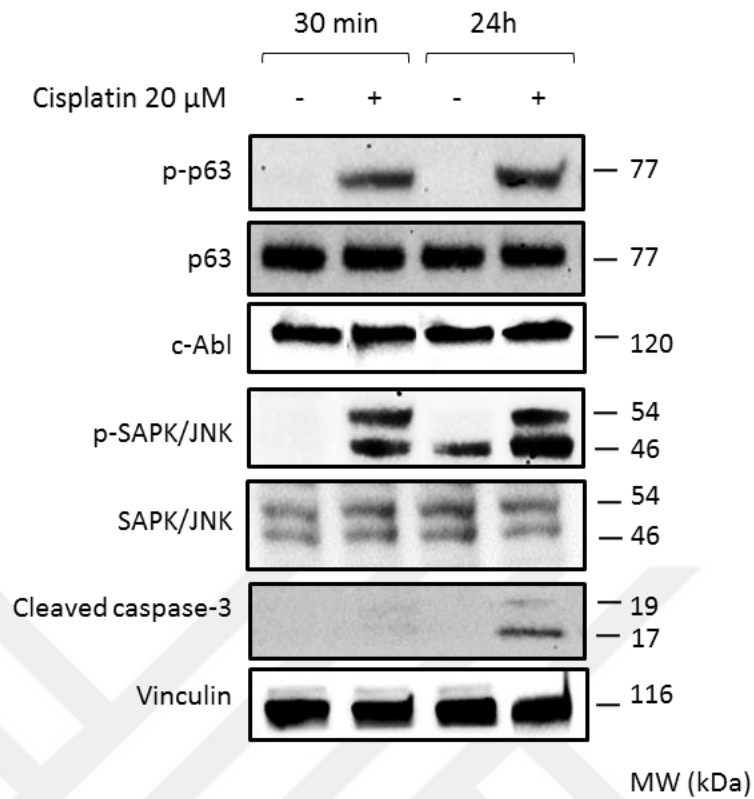
Figure 22: Western blot analysis of human ovarian tissue exposed to cisplatin at 20 μM concentration for short (30 minutes) and long (24 hours) terms. In the short term as well as long term, 20 μM cisplatin-induced phosphorylation of SAPK/JNK and TAp63 pathways and triggered caspase-3 cleavage in immunoblotting. However, TAp63 activation after cisplatin was not associated with any notable change in the protein level of c-Abl.

In another set of experiments, we repeated ovarian tissue culture tests with imatinib used at three different concentrations and found that follicle atresia was increased and steroidogenic activity of the samples was decreased with increasing the concentration of the drug, suggesting that ovarian toxicity of imatinib is dose-dependent (Figure 23).

A

	PF (Healthy)	PF (Atretic)	AMH	E2
☐ Control	2.3 ± 0.2	0.2 ± 0.1	2.6 ± 0.2	1.8 ± 0.2
☐ Imatinib (2.5µM)	1.7 ± 0.2	0.8 ± 0.2	1.3 ± 0.2	0.9 ± 0.3
☐ Imatinib (5µM)	1.3 ± 0.1	1.2 ± 0.1	0.7 ± 0.2	0.7 ± 0.1
☐ Imatinib (10µM)	0.6 ± 0.1	1.6 ± 0.1	0.4 ± 0.1	0.6 ± 0.1

PRIMORDIAL FOLLICLE COUNT
$p<0.001$
Control vs. Imatinib 5µM
Control vs. Imatinib 10µM
$p<0.01$
Control vs. Imatinib 2.5µM

AMH & E2
$p<0.001$
Control vs. Imatinib 2.5µM
Control vs. Imatinib 5µM
Control vs. Imatinib 10µM

PF: Primordial follicle count/mm^2 ,
AMH: Antimullerian hormone (ng/mL),
E2: Estradiol (x10^3 pg/mL),

Figure 23: Primordial follicle counts, E$_2$ and AMH measurements after treatment with different imatinib concentrations. In vitro treatment of human ovarian cortical pieces with imatinib at three different concentrations for 24 hours caused a dose-dependent decrease in primordial follicle number and their steroidogenic activity.

3. Cisplatin-Induced Apoptosis and TAp63 in Immature Oocytes

3.1. Viability Analysis After In Vitro Exposure to Cisplatin, Imatinib or Both

The abundance of small follicles lacking oocytes in the ovarian samples exposed to imatinib led us to investigate the effect of this drug on individual oocytes obtained from IVF patients. We observed that exposure of the oocytes to imatinib for 12 hours tremendously increased the rate of atresia to 82%. During the same incubation period, only 2% of the control oocytes exposed to DMSO as vehicle drug underwent atresia ($p<0.001$). Cisplatin exposure caused a similar degree of oocyte atresia (88%) and imatinib treatment 2 hours before cisplatin did not rescue the oocytes from apoptosis (92%, $p>0.05$) (Figure 24).
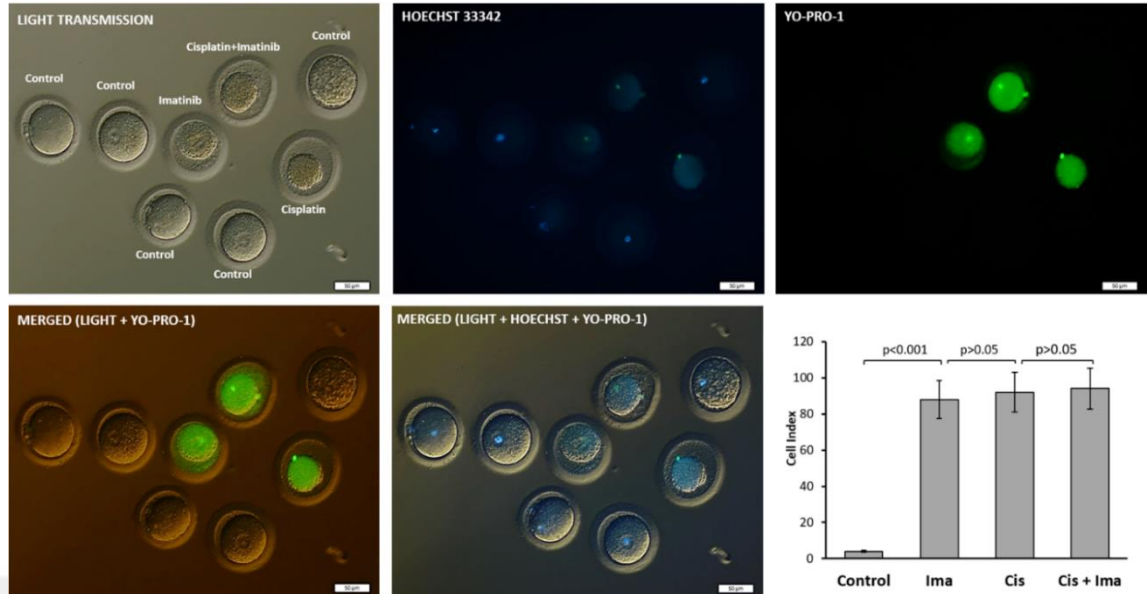
Figure 24: Viability after in vitro exposure of isolated oocytes to cisplatin, imatinib or both. While only 2% of the control oocytes underwent atresia after 12 hours incubation period, the rate of apoptosis was significantly increased to 82, 88 and 92% after treatment with imatinib, cisplatin and cisplatin with imatinib, respectively (p<0.001). Imatinib treatment before with cisplatin did not rescue the oocytes from atresia. (Scale bar: 50 μm)

Based on the in vivo and in vitro findings that we obtained so far we hypothesized that the observed toxic effects of imatinib on human ovary might be related to its inhibitory actions on c-kit, which is another tyrosine kinase crucial for the survival of ovarian follicles [94]. For this purpose, we repeated ovarian tissue culture experiments with GNF-2, another c-Abl tyrosine kinase inhibitor lacking c-kit blocking action, and with anti-CD117, which is a pure c-kit blocking drug. We found that while there were no significant differences between control and GNF-2 treated samples in terms of follicle counts and in vitro E_2 and AMH productions, treatment with anti-CD117 was associated with significant reduction in the primordial follicle count and in vitro hormone productions of the samples compared to control and GNF-2 treated pieces (Figure 20). When a comparison was made between the ovarian samples exposed to imatinib vs. anti-CD117 it appeared that imatinib was associated

with a greater reduction in primordial follicle number, E_2, and AMH levels, suggesting that the detrimental effects of imatinib on the follicles includes but is not limited to its inhibitory actions on c-kit. These results also show that anti-CD117 had a moderate and GNF-2 had the least ovarian toxicity. It is also worthwhile to note that bizarre shaped primordial and unclassifiable small follicles possessing atretic oocytes without granulosa cells were much more abundantly observed in the samples exposed to imatinib (45% of the atretic follicles) and anti-CD177 (37%) compared to those treated with GNF-2 (2%) or cisplatin (6.3%) (Figure 21).

3.2. TAp63 Activation and DNA Damage Response after Cisplatin-Induced DNA Damage in Isolated Oocytes

In order to address the question as to whether genomic damage induced by cisplatin activates c-Abl along with TAp63 pathway in the human ovary, we utilized isolated oocytes. Incubation of the oocytes with cisplatin for 5 minutes induced double-strand DNA damage and activated TAp63 as shown by increased expressions of γ-H2AX phosphorylated at Ser139 and phospho-p63 Ser395 on immunofluorescence staining. But there was no signal of c-Abl detected before or after cisplatin treatment (Figure 25).
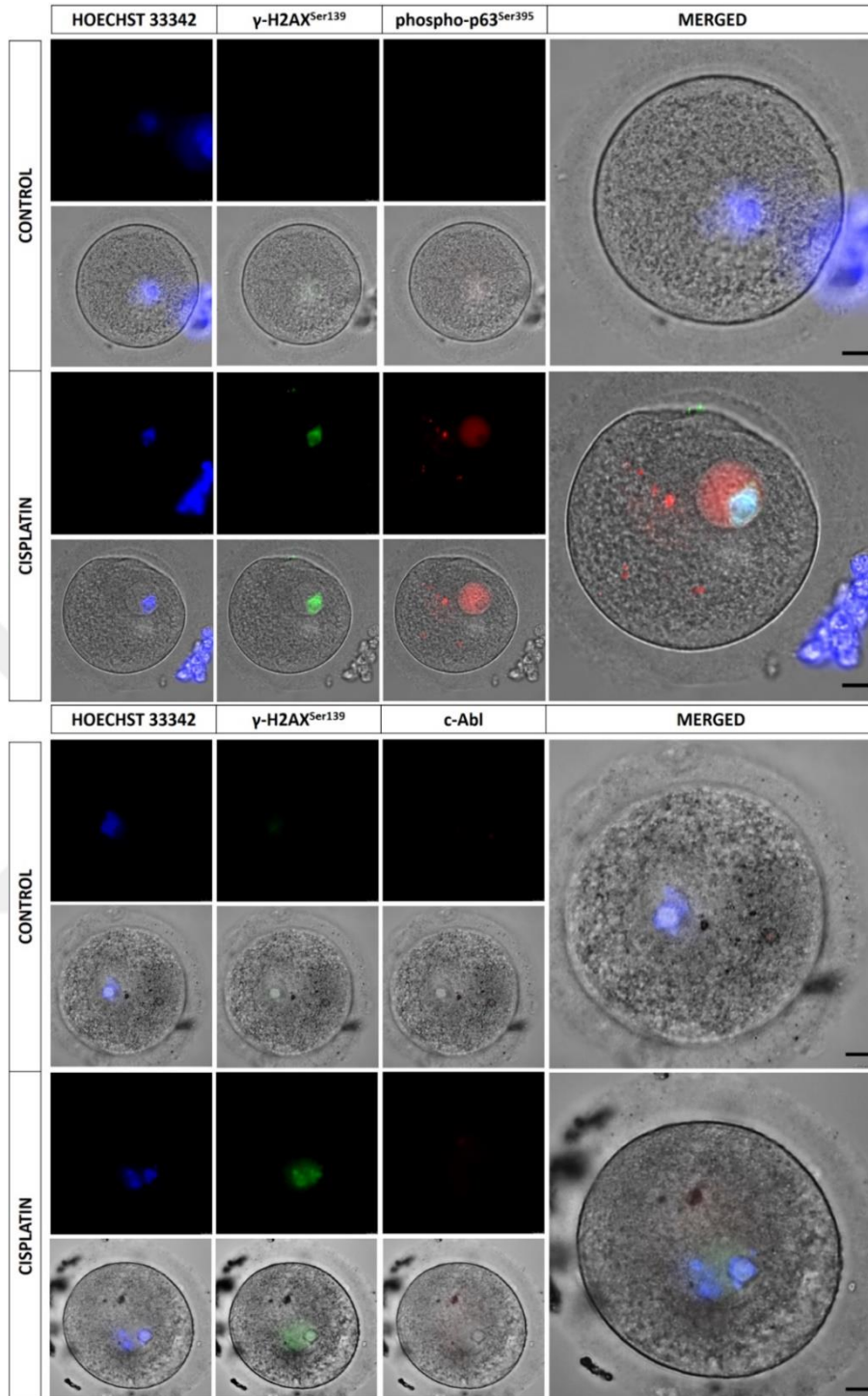
Figure 25: The expression of TAp63 and c-Abl in human oocytes before and after exposure to cisplatin in vitro. Exposure of the oocytes to cisplatin (20 µM) for 5 minutes increased the expression of γ-H2AX phosphorylation [Ser139] and phospho-TAp63[Ser395] compared to control oocytes. However, there was no signal of c-Abl detected in the oocytes after cisplatin exposure despite the

marked expression of γ-H2AX phosphorylation [Ser139] as an evidence for the occurrence of double-strand DNA breaks after cisplatin. (Scale bar: 10 μm)

4. Cisplatin-Induced Apoptosis and TAp63 in Granulosa Cells

4.1. Monitorization of DNA Damage Response in Granulosa Cells Exposed to Cisplatin

Histone H2AX phosphorylated on Ser139 forms γ-H2AX, in response to DNA double-strand breaks generated by exogenous genotoxic agents. Phosphorylation can extend up to several thousand nucleosomes from the actual site of the DSB and may mark the surrounding chromatin for recruitment of proteins required for DNA damage signaling and repair. Extensive phosphorylation may also serve to intensify the damage signal or facilitate to repair of persistent lesions. HGrC1 cells exposed to cisplatin monitored up to 4 hours for γ-H2AX[Ser139] levels and foci appeared as early as 5 minutes post-exposure and became more pronounced at 30 minutes, 2 and 4 hours after exposure in immunofluorescence analysis (Figure 26).
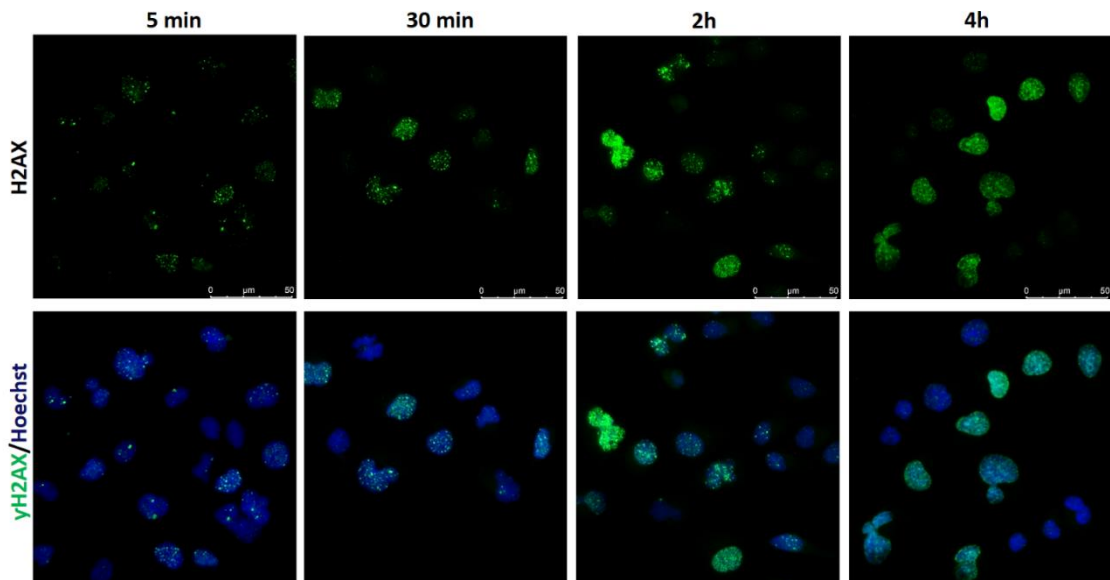
Figure 26: In-vitro exposure of HGrC1 cells to cisplatin caused double-strand DNA breaks as shown by increased expression of γ-H2AX[Ser139] as early as 5

minutes post-exposure. The intensity of the signal (the number of foci) was increased when the duration of cisplatin exposure was extended up to 4 hours in immunofluorescence staining. (Scale bar: 50 μm)

4.2. Characterization of DNA Damage Response Elements and TAp63 pathway after Cisplatin-Induced DNA Damage

In immunoblot analysis, exposure of HGrC1 cells to cisplatin at two different concentrations for 4 hours induced genomic damage, activated cell cycle checkpoint sensors, SAPK/JNK and TAp63 pathways, and triggered apoptosis as evidenced by a dose-dependent increase in the expression of the phosphorylated forms of γ-H2AX^{Ser139}, Chk-1^{Ser345} and Chk-2^{Thr68}, SAPK/JNK$^{Thr183/Tyr185}$, p63^{Ser395}, and cleaved forms of PARP and caspase-3. However, TAp63 activation after cisplatin was not associated with an increase in the protein level of c-Abl (Figure 27). At 24 hours post-exposure, nuclear fragmentation and apoptosis of the cells became evident in immunofluorescence analysis (Figure 28).
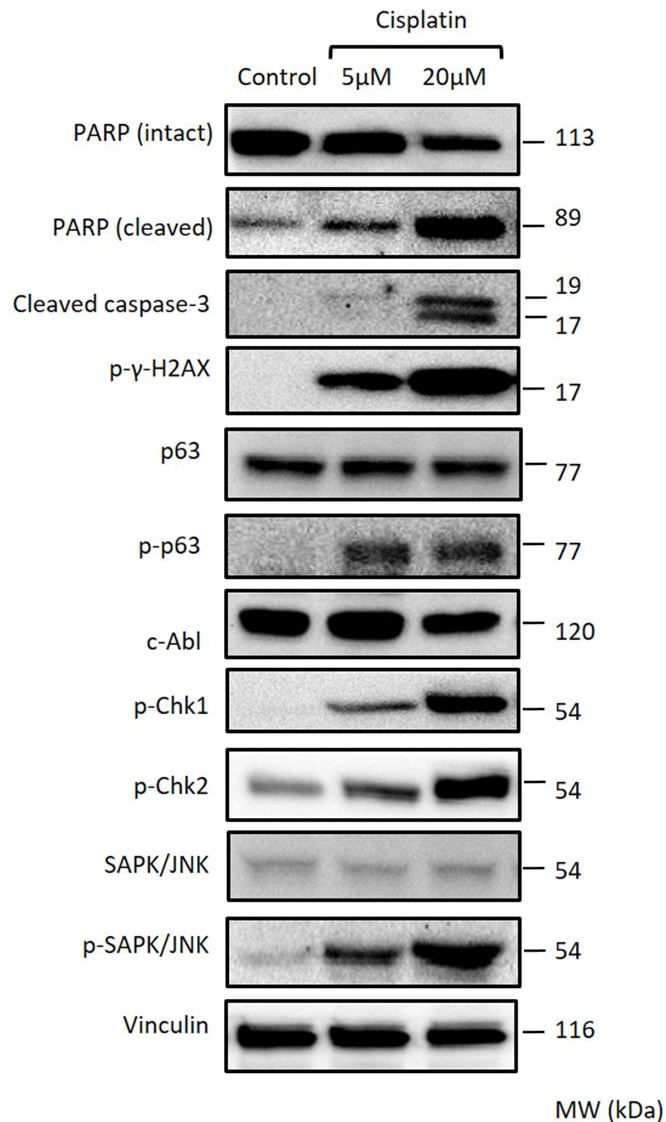
Figure 27: Protein profiler of DNA damage response and checkpoint analysis of granulosa cells exposed to cisplatin. Exposure of HGrC1 cells to cisplatin at 5 and 20 µM concentrations for 4 hours induced genomic damage, activated cell cycle checkpoint sensors, SAPK/JNK and TAp63 pathways, and triggered apoptosis as evidenced by a dose-dependent increase in the protein expression of the γ-H2AX phosphorylation [Ser139], phosphorylated forms of Chk-1 and Chk-2, SAPK/JNK[Thr183/Tyr185], p63[Ser395], and cleaved forms of PARP and caspase-3 respectively in immunoblotting. But, TAp63 activation after cisplatin was not associated with any notable change in the protein level of c-Abl.
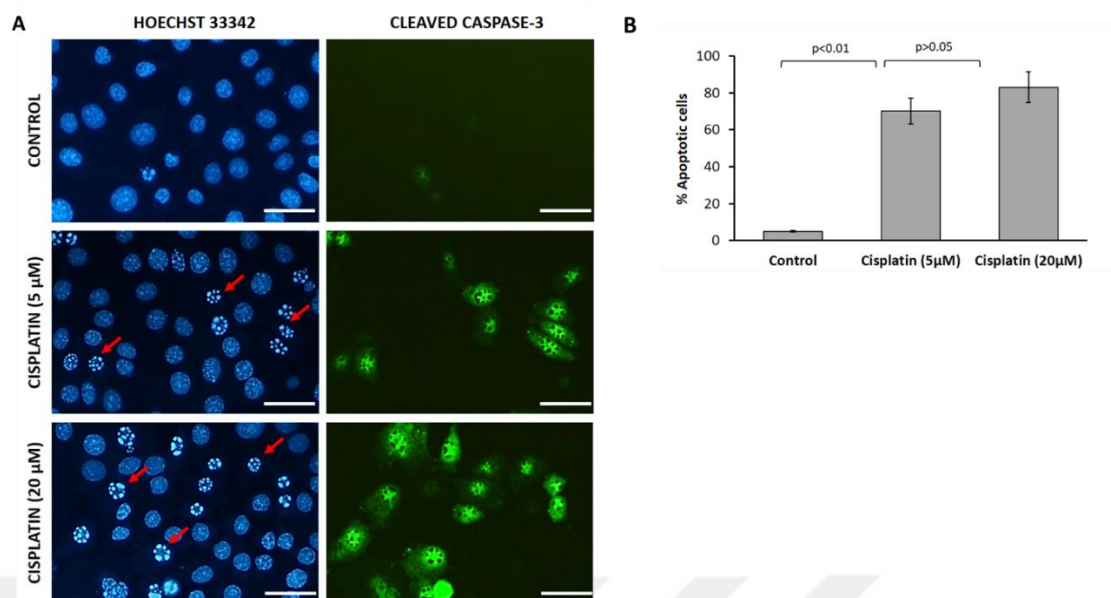
Figure 28: Analysis of apoptosis and nuclear fragmentation. **(A)** Apoptotic signal and nuclear fragmentation became evident at 24 hours post-exposure in immunofluorescence analysis confirming apoptosis-inducing effects of cisplatin at these concentrations. **(B)** Percentage of apoptotic cells increased dose-dependently up to 73% and 82%, respectively. (Scale bar: 50 μm)

4.3. Imatinib Co-administrated with Cisplatin Does Not Prevent Activation of DNA Damage Response Elements and TAp63-mediated Apoptosis

Afterward describing cisplatin-induced DNA damage response of HGrC1 cells in previous experiments, the effects of pretreatment with imatinib before cisplatin was analyzed. Administration of imatinib alone or 2 hours before cisplatin slightly decreased the expression of c-Abl but did not cause any notable decrease in the expression of the phosphorylated forms of γ-H2AX, Chk-1/Chk-1, SAPK/JNK, and TAp63 compared to those treated with cisplatin alone in the immunoblotting analysis (Figure 29).

Viability of HGrC1 cells was assessed with intra-vital YO-PRO-1 on immunofluorescence, it appeared that cisplatin treatment resulted in a significant reduction in the number of viable cells compared to control samples

while imatinib treatment did not prevent cisplatin-induced death of the cells (Figure 30).
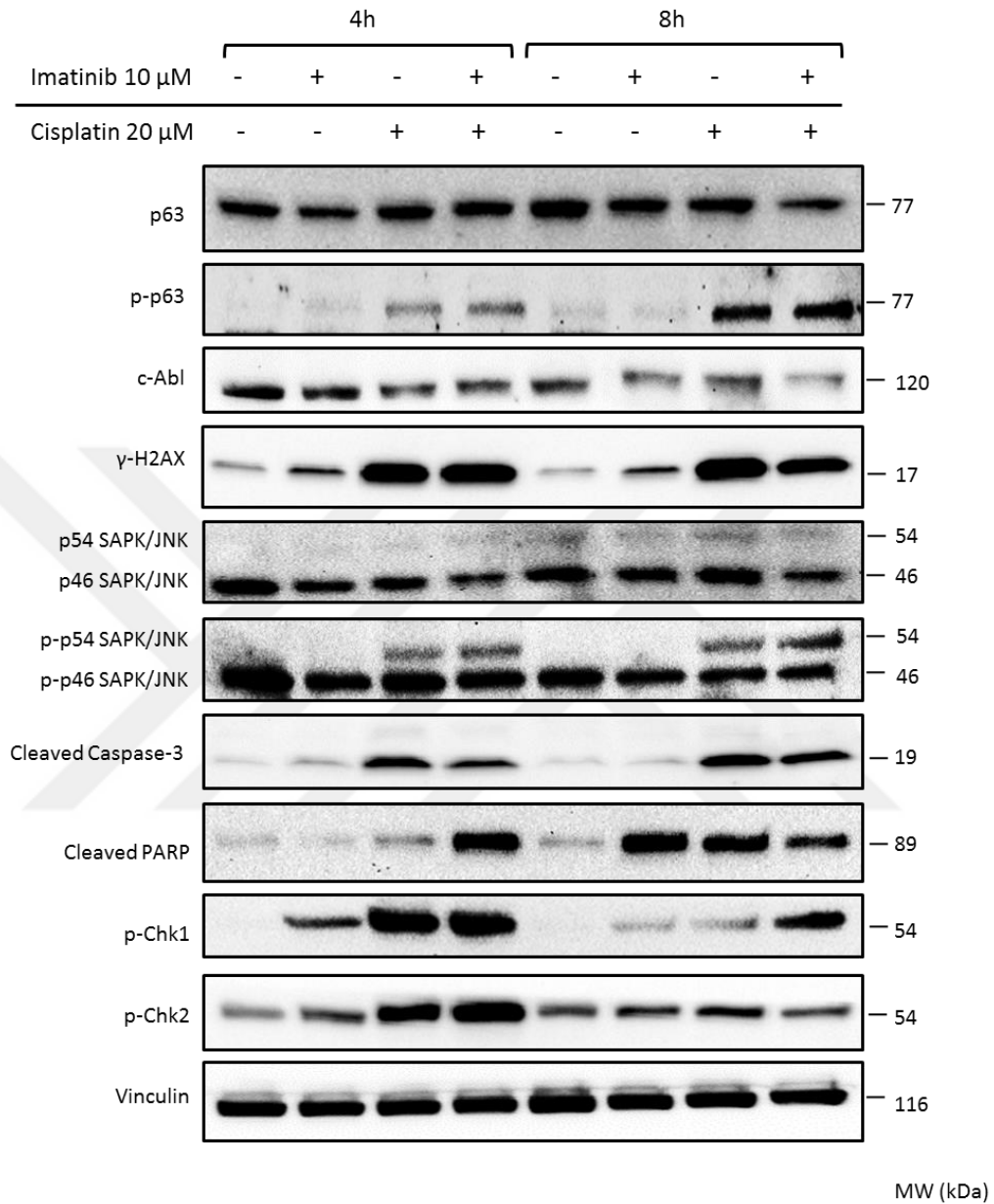
Figure 29: The protein levels of DNA damage, cell cycle checkpoint and apoptosis markers in HGrC1 cells exposed to cisplatin, imatinib or both. Administration of imatinib 2 hours before cisplatin did not cause any notable change in the expression of c-Abl, and phosphorylated forms of γ-H2AX, Chk-1/Chk-1, SAPK/JNK, and p63 compared to those treated with cisplatin alone in an immunoblotting analysis at 4 and 8 hours post-exposure.
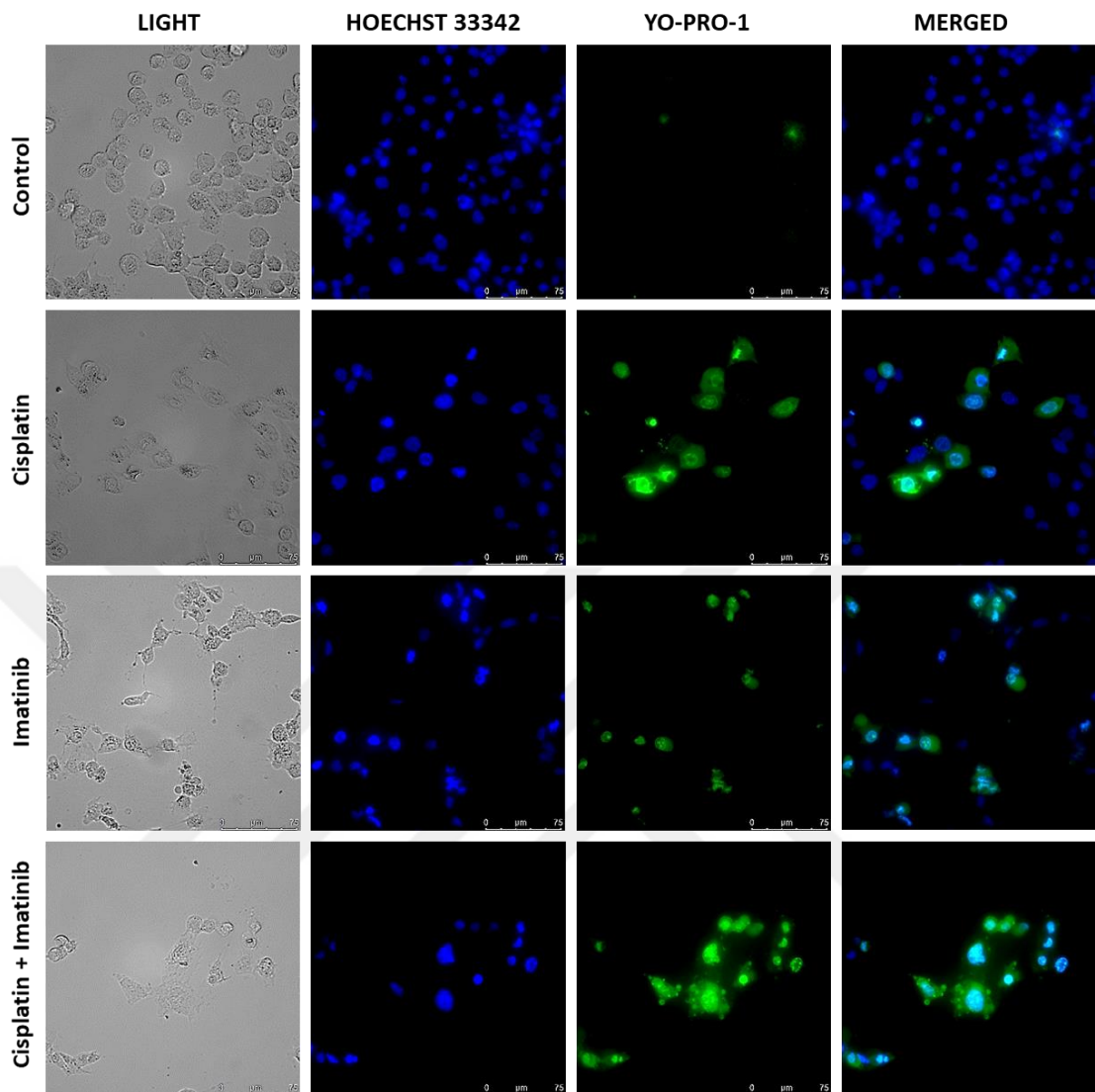
Figure 30: Viability of HGrC1 cells exposed to cisplatin, imatinib or both. When cell viability was assessed with intra-vital YO-PRO-1 on immunofluorescence, it appeared that cisplatin treatment resulted in a significant reduction in the number of viable cells compared to control samples while imatinib treatment did not prevent cisplatin-induced death of the cells. (Scale bar: 50 µm)

4.4. TAp63 Activation Unaccompanied by c-Abl is not Specific to A Particular Chemotherapy Drug or Granulosa Cells Type

In order to eliminate the idea that observed effects may only be specific to the chemotherapy drug cisplatin or HGrC1 cell line, the same set of

experiments were performed with another drug, 4-OOH CY and other two types of granulosa cells. Similar results were obtained when the experiments on HGrC1 cells were repeated with 4-OOH CY, in vitro active metabolite of cyclophosphamide, similar results were obtained suggesting that absence of c-Abl up-regulation after TAp63 activation after genomic damage is not specific to cisplatin (Figure 31).

Furthermore, the same set of experiments were applied with other two types of granulosa cells; another human granulosa cell line COV434 and primary non-mitotic human luteal granulosa cells. Results were comparable in all types of granulosa cells, signifying that the absence of c-Abl up-regulation after TAp63 activation after genomic damage is neither specific to a particular type of granulosa cells nor chemotherapy drug. Furthermore, additional to Ser395 phosphorylation of TAp63, Ser160/162 residue was also investigated. Results show that cisplatin exposure is associated with increased expression of TAp63 phosphorylated at both Ser395 and Ser160/162 residues but does not require c-Abl up-regulation (Figure 32).
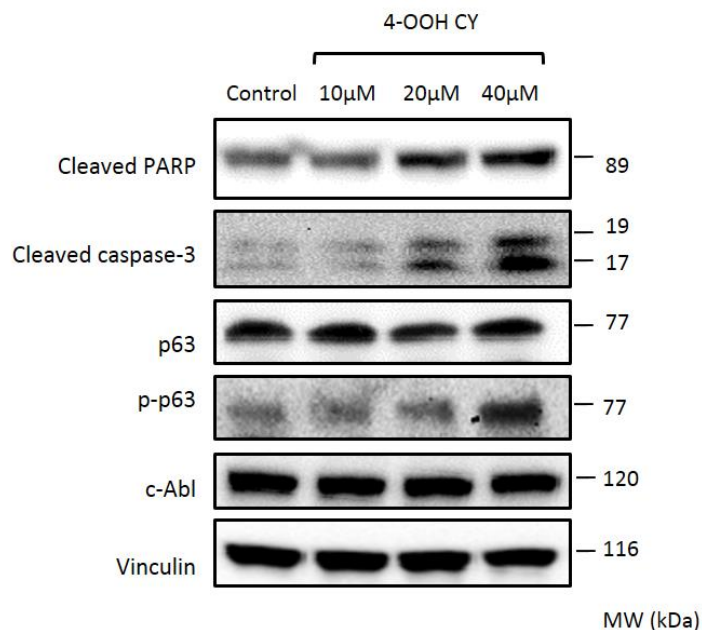
Figure 31: Treatment of the granulosa cells with 4-OOH CY at three different concentrations activated TAp63 pathway and apoptotic machinery as shown by increased expression of cleaved forms of PARP and caspase-3 without any notable change in the expression of c-Abl in immunoblotting.
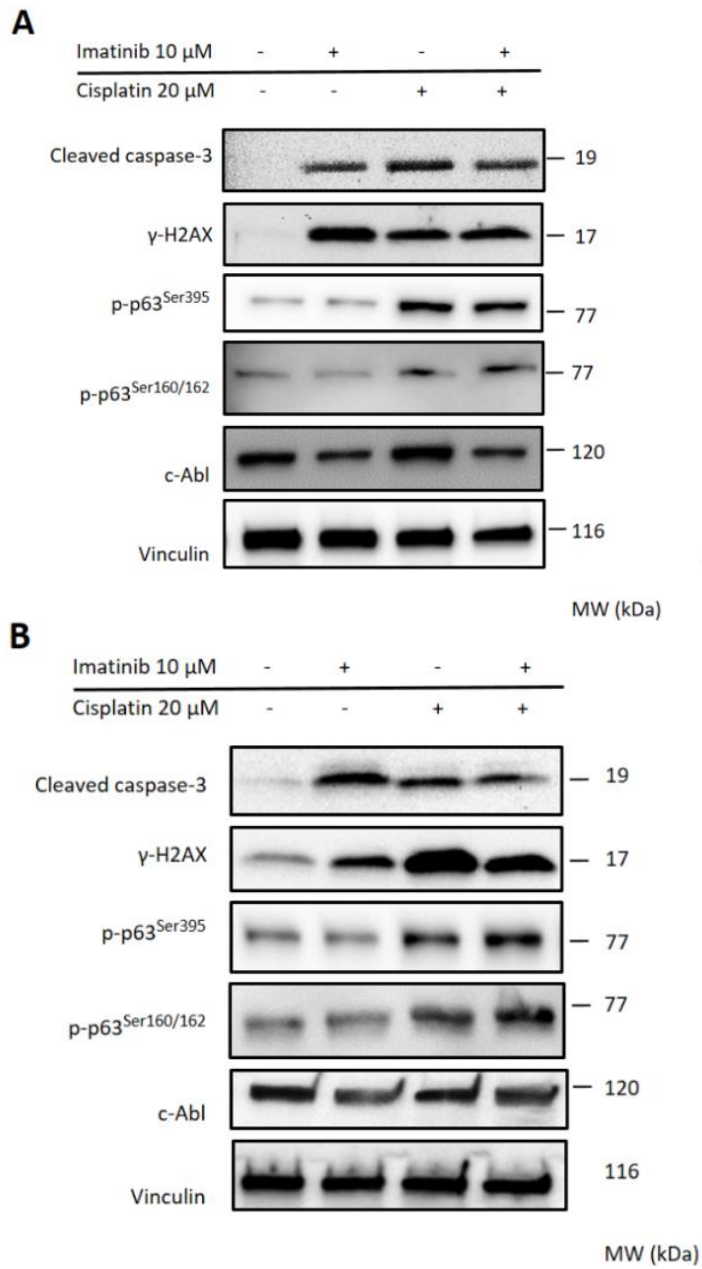
Figure 32: Treatment of COV434 **(A)** and human luteal granulosa cell **(B)** with cisplatin increased the expression of phosphorylated forms of γ-H2AX ^{Ser139}, both p63^{Ser395} and p63$^{Ser160/162}$ and cleaved caspase-3 without any increase in the expression of c-Abl. Imatinib treatment alone was associated with increased the expression of γ-H2AX phosphorylation^{Ser139} and cleaved caspase-3 and decreased c-Abl expression without any increase in phosphorylated forms of p63 on both Ser395 and Ser160/162.

4.5. qRT-PCR Profiler Assay for Gene Expression of Caspase-3, NOXA, and PUMA Before and After Cisplatin Exposure

We carried out a qRT-PCR profiler assay to see the mRNA expression of NOXA and PUMA before and after cisplatin as these pro-apoptotic proteins function as downstream transcriptional targets of TAp63 to mediate primordial follicle oocyte apoptosis at least in mice [78]. While there is an almost 2-fold increase in NOXA expression in the ovarian cortical samples, HGrC1 and COV434 cell lines exposed to cisplatin for 24 hours PUMA expression did not change. By contrast, in the luteal granulosa cells, PUMA was increased by 4.5-fold but NOXA was significantly down-regulated after the same duration of exposure to cisplatin, suggesting that granulosa cell apoptosis upon exposure to cisplatin downstream TAp63 is differentially regulated depending upon the type of granulosa cells in human (Figure 33).
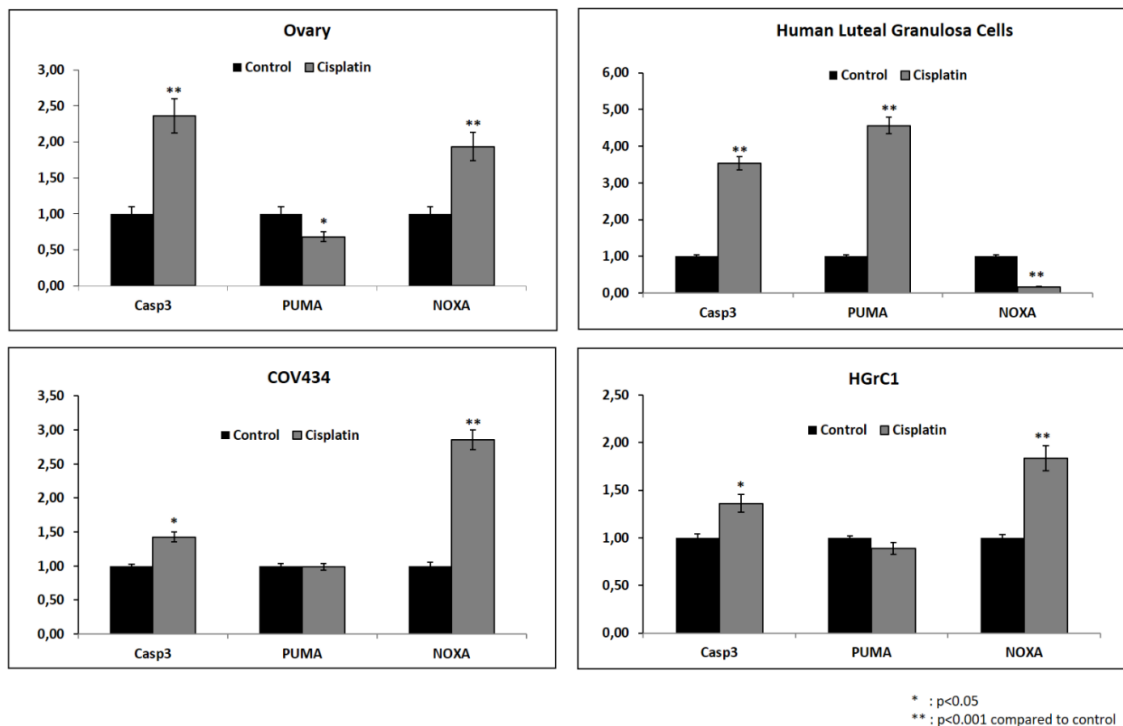
Figure 33: Gene expression results show that even though granulosa cell apoptosis is TAp63 activation dependent, downstream targets of TAp63 is differentially regulated depending upon the type of granulosa cells in human. (Asterix: for comparison to control)

4.6. Assessment of the Effects of Imatinib on the Proliferation and Viability of Human Granulosa Cells

In view of the fact that we observed imatinib treatment alone increased the expression of γ-H2AX^{Ser139} in the granulosa cells at 4 and 8 hours after exposure in immunoblotting (Figure 29). This effect of imatinib was shown previously on the different types of malignant cells on culture including leukemia and gastrointestinal stromal tumor cells in the prediction of response to therapy [76, 77]. Therefore, in another set of the experiment, the granulosa cells were treated with imatinib at different concentrations and extended culture period up to 24 hours to analyze the long-term effect of imatinib exposure on granulosa cell viability and proliferation. Imatinib treatment caused dose-dependent growth arrest and induced apoptosis of the mitotic granulosa cell line HGrC1 (Figure 34-A and 34-B). Decreased viability and apoptosis of the cells after exposure to imatinib was also confirmed with YO-PRO-1 vitality assay on immunofluorescence staining and increased expression of cleaved forms of caspase-3 and PARP on the immunoblotting analysis (Figure 35-A and 35-B). We also conducted a conventional CTG cytotoxicity assay on the mitotic HGrC1 and COV434 granulosa cells and obtained similar findings (Figure 36).
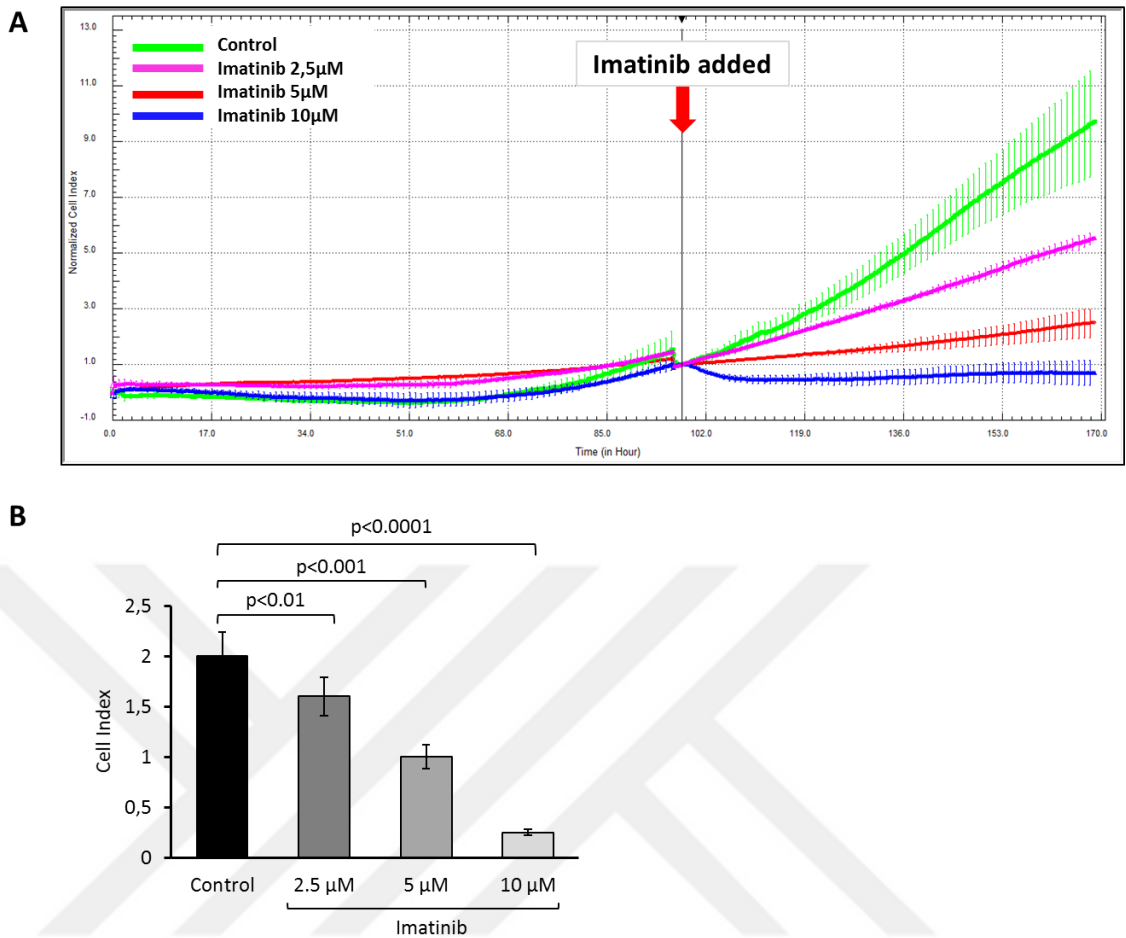
Figure 34: Exhaustive cytotoxicity analysis via the xCELLigence system. **(A)** Treatment of the cells with imatinib at the indicated concentrations caused dose-dependent growth arrest in the real-time growth curves of the cells on the xCELLigence system. **(B)** The mean cell index as a measure of viable cell mass declined with increasing concentrations of imatinib.
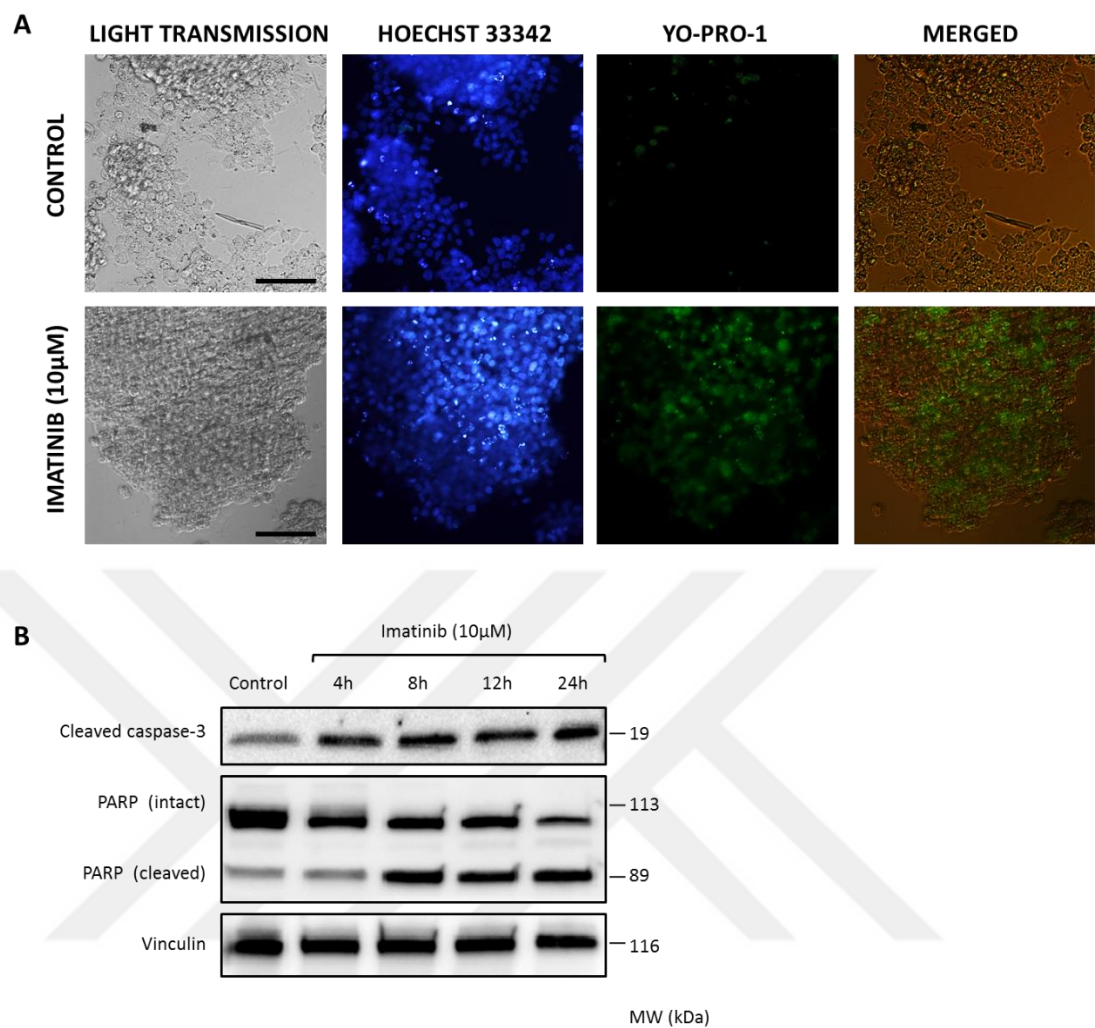
Figure 35: Analyses of cell viability and apoptosis after different doses of imatinib. **(A)** Cell death was confirmed with intravital YO-PRO1 staining in immunofluorescence microscopy and **(B)** by increased expression of cleaved forms of caspase-3 and PARP on immunoblotting. There were dose and exposure time-dependent decrease in the proliferation and increase in the apoptosis of the cells when they were treated with imatinib. (Scale bar: 50 μm)
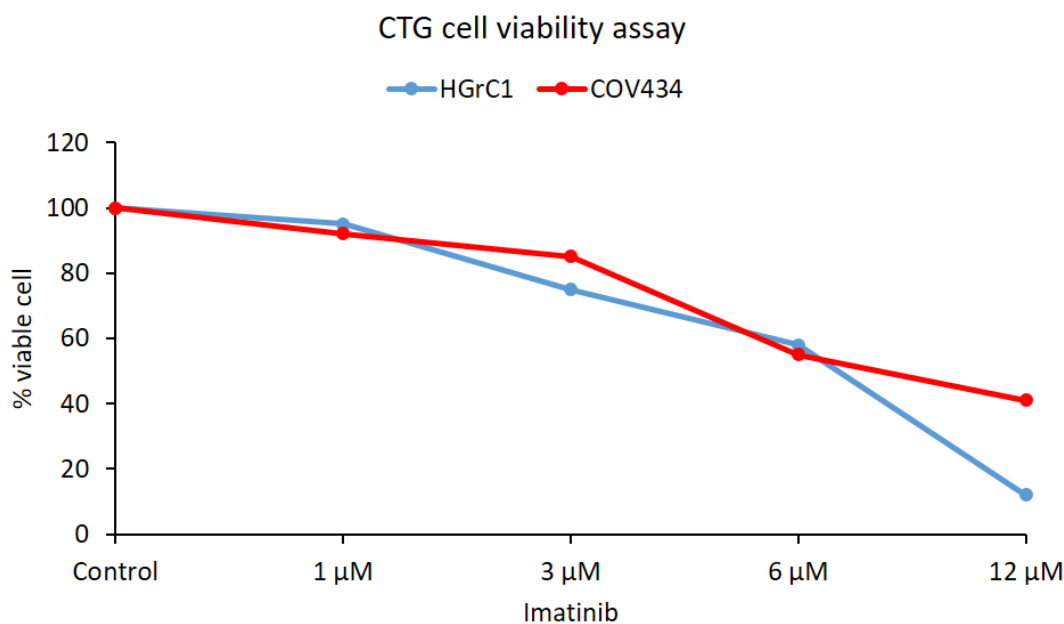
Figure 36: Cell viability assay showed that imatinib caused a dose-dependent decrease in the viability of HGrC1 and COV434 granulosa cells.

4.7. Comparison of the effects of Imatinib, GNF-2, and anti-CD117

The expression of c-Abl was gradually diminished on immunoblotting when the HGrC1 granulosa cells were treated with increasing concentrations of imatinib and GNF-2, confirming in-vitro functionality of these drugs (Figure 37). As the last part of the experiments, we analyzed how mitotic activity and viability of the granulosa cells change when they were exposed to imatinib, GNF-2, anti-CD177, and cisplatin with and without imatinib or GNF-2 by monitoring real-time growth curves of the cells on the xCELLigence platform and assessing their viability on immunofluorescence analysis. The greatest reduction in proliferation and viability was observed in the cells exposed to cisplatin followed by in order of decreasing cytotoxicity imatinib and anti-CDD17 and GNF-2. Indeed, the proliferation rate of the cells treated with GNF-2 was comparable to control. The co-administration of imatinib or GNF-2 with cisplatin did not rescue the cell from apoptosis (Figure 38).

When a comparison was made between imatinib vs. anti-CD117 it appeared that imatinib was associated with a greater reduction in proliferation suggesting that the destructive effects of imatinib on the granulosa cells include but is not limited to its inhibitory actions on c-kit. These results support the previous data obtained from human ovarian tissues and also show that anti-CD117 had a moderate and GNF-2 had the least ovarian toxicity in mitotic granulosa cells.

Cell death was confirmed with intravital YO-PRO1 staining in immunofluorescence microscopy. The greatest reduction in viability was observed in the cells exposed to cisplatin followed by in order of decreasing cytotoxicity imatinib and anti-CD117 and GNF-2 (Figure 39).
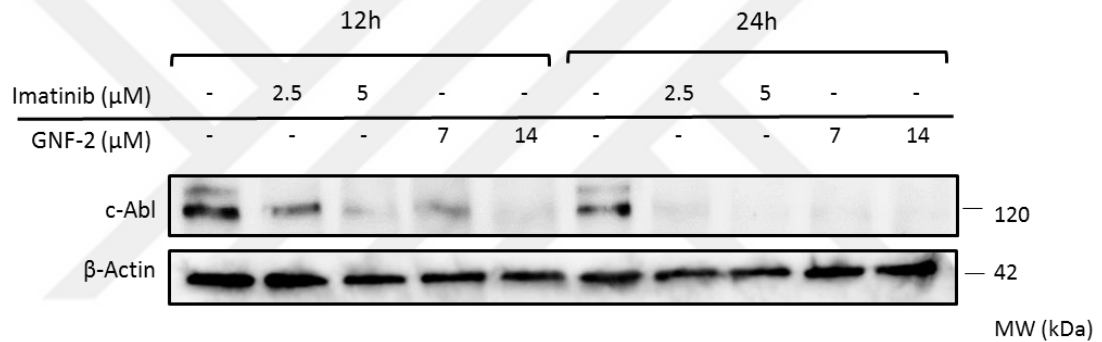
Figure 37: The expression of c-Abl was gradually diminished on immunoblotting when the HGrC1 granulosa cells were treated with increasing concentrations of imatinib or GNF-2, as a validation experiment showing in-vitro biological activity of these drugs.
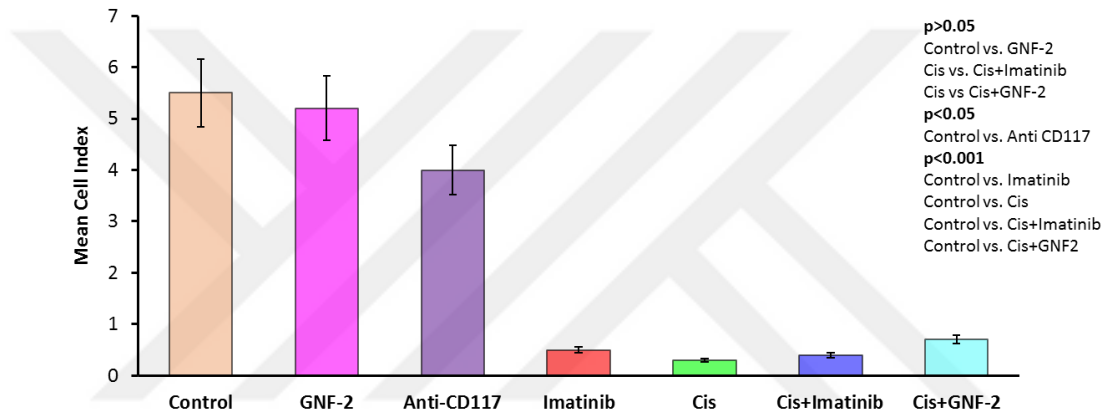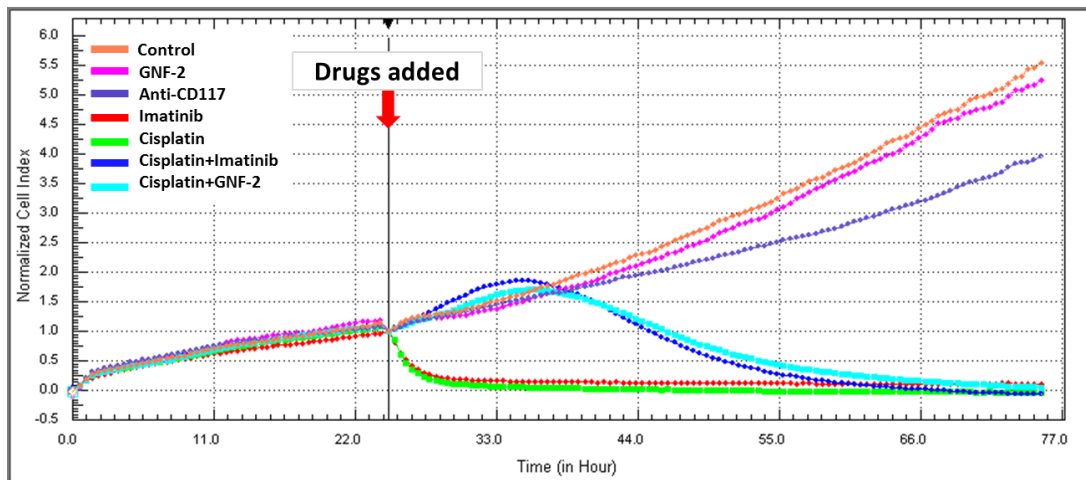
Figure 38: Real-time growth curves of the cells treated with imatinib, GNF-2, anti-CD117 and cisplatin in vitro. The greatest reduction in proliferation and viability was observed in the cells exposed to cisplatin followed by in order of decreasing cytotoxicity imatinib and anti-CDD17 and GNF-2. Indeed, the proliferation rate of the cells treated with GNF-2 was comparable to control. The co-administration of imatinib or GNF-2 with cisplatin did not rescue the cell from apoptosis.

Figure 39: Cell death was confirmed with intravital YO-PRO1 staining in immunofluorescence microscopy. The greatest reduction in viability was observed in the cells exposed to cisplatin followed by in order of decreasing cytotoxicity imatinib and anti-CD117 and GNF-2. (Scale bar: 75 µm)
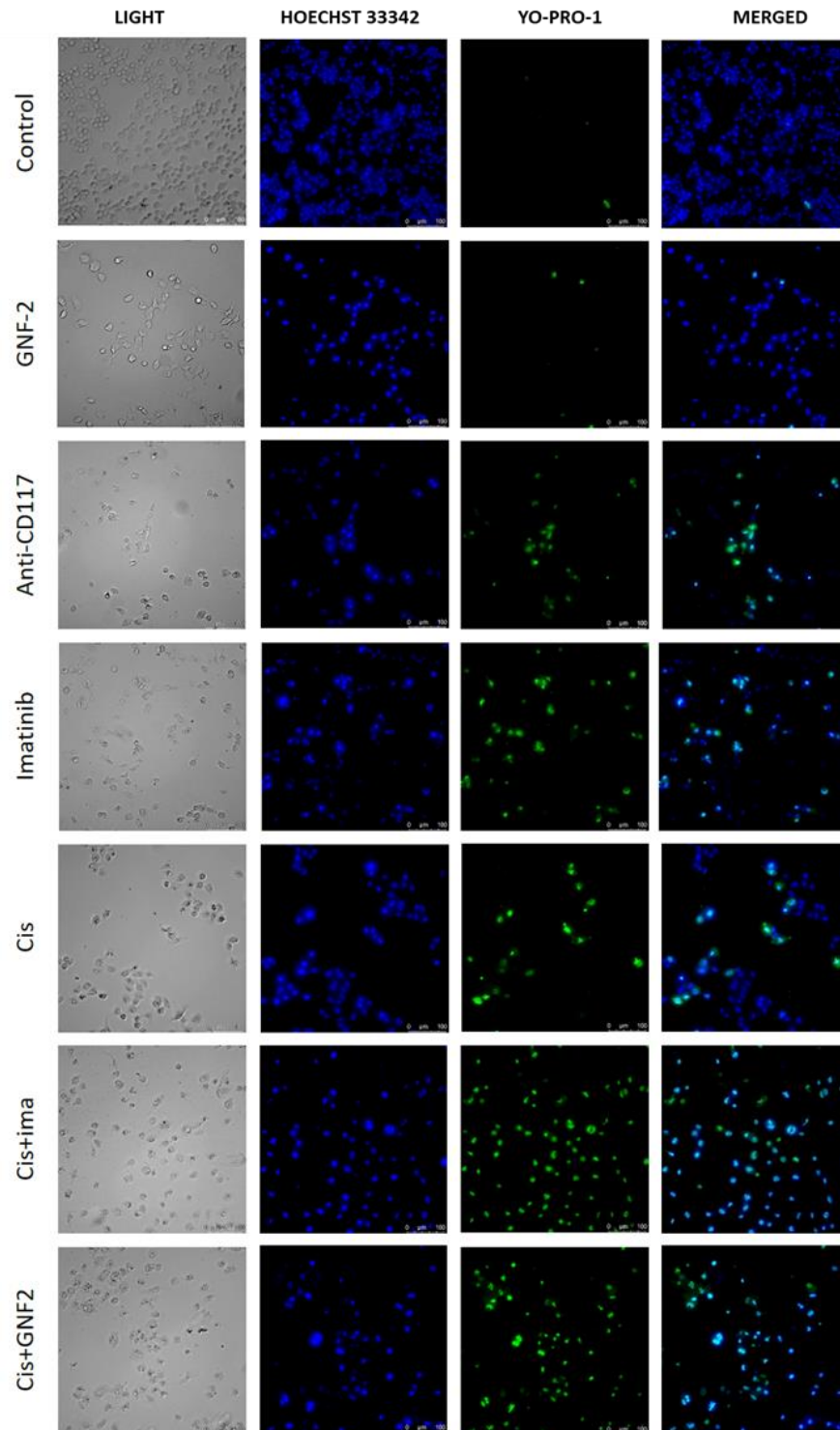
5. Limitations, Reasons for Caution

Our theoretical knowledge of TAp63-mediated oocyte apoptosis is mainly rooted in the studies conducted on mice. Its phosphorylation upon induction of double-strand breaks in the DNA, which triggers conformational change and results in the formation of an open active and tetrameric structure. All of these previous data were obtained in mouse oocytes and the results presented in this dissertation establish the first comprehensive molecular analysis in human. Therefore, it is yet unclear if the conformational change in TAp63 structure upon induction of DNA damage is crucial in human oocyte. Unfortunately, we did not focus to answer this question in this thesis, which could be the subject of another major project. Further investigations are needed to reveal the importance and essentiality of novel phosphorylation sites, Ser395 and Ser 160/162, that we described for the first time in this study.

6. Wider Implications of the Findings

Our findings could be important from the perspective of the biology of human ovary because we have for the first time identified TAp63-mediated oocyte and granulosa cell apoptosis in human upon induction of DNA damage. Moreover, these findings could be important from the perspective of fertility preservation strategies in human. Focusing on research to discover new pharmacological options to protect ovarian follicles against chemotherapy-induced death in the ovary should be a priority. Obviously, such an achievement may prevent premature menopause and prolong reproductive life span by preventing total exhaustion of follicle stockpile in the ovary exposed to gonadotoxic cancer drugs. These results can be implicated to develop new strategies to prevent TAp63-mediated apoptosis in oocytes and granulosa cells which will result in the impaired trigger of apoptosis and ultimately protect the healthy follicle pool from undergoing atresia in young women at reproductive age suffering cancer treatments. Moreover, provide for the first time a molecular evidence in human that imatinib might be gonadotoxic effects on the human ovary. These findings together with two separate cases of a severely compromised ovarian response to gonadotropin stimulation and premature

ovarian failure in patients who were receiving imatinib [82, 83] further heighten the concerns about its potential gonadotoxicity on the human ovary and urge caution in its use in young female patients.

CHAPTER 4
DISCUSSION

Infertility and premature ovarian failure are reproductive sequels of exposure to cytotoxic chemotherapy regimens in young females with cancer. They cause follicle death by inducing genomic damage in the oocyte and somatic cells of dormant primordials and growing follicles [12-14]. Premature ovarian failure is also associated with other adverse health-related consequences, including osteoporosis, hot flashes, sleep disturbance, and sexual dysfunction, which can negatively impact on short- and long-term quality of life. Ovarian tissue banking cannot fully restore ovarian function after transplantation and reverse menopause [95, 96]. Furthermore, this strategy is considered still experimental, therefore should be performed under An institutional review board approval and guidance [56]. Even though oocyte or embryo freezing prior to chemotherapy can help women achieve pregnancy and live birth after chemotherapy-induced premature ovarian failure, these strategies cannot reverse menopause. Therefore, focusing on research to discover new pharmacological options to protect ovarian follicles against chemotherapy-induced death in the ovary should be a priority. Obviously, such an achievement may prevent premature menopause and prolong reproductive life span by preventing total exhaustion of follicle stockpile in the ovary exposed to gonadotoxic cancer drugs.

Up to now, several pharmacological agents and compounds were tested at in vitro and in vivo animal studies to explore their protective effects against chemotherapy-induced follicle damage/loss in the ovary. Imatinib is such a drug that inhibits oncogenic tyrosine kinases c-Abl and c-kit used in the treatment of chronic leukemias and gastrointestinal stromal tumors respectively [76, 77]. Since the initial report that showed the protective effect of this drug on chemotherapy-induced follicle loss in mouse ovary several other studies were conducted with inconsistent results [66, 70, 78-81].

Lack of human data on this controversial issue became our motivation in conducting this translational study and we have obtained several important findings as follows.

The major outcome of this study is that DNA damage induced by chemotherapy drug cisplatin is associated with increased expression of TAp63 phosphorylated at Ser395 and Ser160/162 residues but does not require c-Abl up-regulation in xenografted and in vitro cultured human ovarian cortical samples, isolated oocytes, luteal and mitotic granulosa cells. To the best of our knowledge, it is a novel finding in the human ovary as no previous studies documented such an association between TAp63 phosphorylation at these residues and DNA damage induced by chemotherapy exposure.

The full-length TAp63 contains several Ser-Pro motifs (serine residues followed by a proline) that are expected to be phosphorylated during mitosis as potential substrates for CDKs. These can be listed as serines at positions 160, 162, 395 and 455. While Ser160-162 phosphorylation has been previously linked to cell cycle control and proliferation [97], phosphorylation of Ser395 has not yet been associated with any function. Therefore, our study is the first to define Ser395 as a site for TAp53 activation in response to DNA damage. Interestingly, whilst both Ser160 and 162 sites are conserved between p53, p63, and p73; Ser395 is not conserved, perhaps underlining some of the unique functions exhibited by this protein.

TAp63 is a member of the Trp53 family (Trp53, Trp63, and Trp73), which is predominantly expressed by the oocytes of the primordial follicles [98] and essential for oocyte death after genotoxic stress [65]. As an oocyte-specific homolog of p53 TAp63 is expressed in meiotically arrested oocytes and act as a post-pachytene checkpoint to eliminate the oocytes which have sustained DNA damage [81]. It is phosphorylated upon induction of double-strand breaks in the DNA, which triggers conformational change and results in the formation of an open active and tetrameric structure. As transcription targets of TAp63 pro-apoptotic BH3 only proteins PUMA and NOXA coordinate DNA damage-induced, TAp63-mediated primordial follicle oocyte apoptosis in mice [78]. These data were obtained in mouse oocytes and no data is available in human oocytes. Therefore, it is unclear if there is a conformational change in TAp63 upon induction of DNA damage in human oocyte.

In human fetal ovary, no staining for p63 was observed in the oogonia and during early prophase, I, using ovaries obtained at between 7 and 15 weeks of gestation. Strong staining of late pachytene- and diplotene-stage oocytes were detected in ovaries obtained at 24 and 26 weeks of gestation [98]. No data is available regarding its expression pattern in the adult human ovary. In this study, we have shown that TAp63 is expressed not only by oocytes but also by granulosa cells in human. In response to DNA damage induced by different chemotherapy drugs such as cisplatin and active in vitro metabolite of cyclophosphamide 4 hydro-peroxy cyclophosphamide TAp63 is phosphorylated at Ser395 and Ser160/162 residues in human oocytes and granulosa cells without any increase in c-Abl expression. This finding, in fact, may explain why imatinib does not confer any protection against follicle loss induced by cisplatin. Another important point to emphasize that there might be some other mechanisms after chemotherapy exposure that contribute to the depletion of follicle reserve in addition to direct toxic effects of chemotherapy drugs on the oocyte and granulosa cells. One of them is vascular damage that more commonly occurs after administration of particular chemotherapy drugs such as cyclophosphamide and cisplatin accelerates follicle loss and aging process of the ovary [89, 99]. The second mechanism is the so-called burn out phenomenon. It was hypothesized that cyclophosphamide exposure activates phosphatidylinositol 3-kinase signaling pathway, which in turn causes premature activation of primordial follicles and hence ''burn out'' or early depletion of follicle pool [100]. It was also suggested as a third possible mechanism, at least in the mouse ovary that chemotherapy drugs may induce different mechanisms of follicle loss [101]. Taken together these findings suggest that there could be a multitude of distinct pathogenetic mechanisms underlying chemotherapy-induced gonadotoxicity and ovarian failure.

A further consequence is that imatinib mesylate did not confer any protection against cisplatin-induced follicle loss in human ovary samples, different types of granulosa cells and oocytes in vitro experiments and in vivo human ovarian xenograft model. The administration of imatinib prior to cisplatin did not appear to confer any protective effect against cisplatin-induced follicle

loss because the number of primordial follicles was comparable between the xenografts exposed to cisplatin vs. cisplatin+imatinib. Moreover, imatinib did not show any protective effects in animals' own ovaries.

Interestingly, the magnitude of the gonadotoxicity after imatinib treatment appeared to be similar to cisplatin when a comparison was made based on the degree of follicle loss and the reduction in AMH levels. Particularly, bizarre shaped primordial follicles lacking oocytes and unclassifiable small follicles possessing atretic oocytes without granulosa cells led us to investigate its molecular actions.

Further analysis revealed that imatinib itself exerted cytotoxic effects on human ovary based on the reduction of follicle pool and steroidogenic activity of ovarian samples. There were specific structural abnormalities in the follicles that were much more frequently observed in the ovarian samples exposed to imatinib and c-kit blocking drug anti-CD117 but not in those incubated with cisplatin or GNF-2, another c-Abl inhibitor devoid of c-kit blocking action, suggesting that ovarian toxicity of imatinib is mainly related to its inhibitory actions on c-kit which is a crucial survival factor for human follicles. These results support the findings of Kerr et al in the mouse ovary [78] and provide for the first time a molecular evidence in human that imatinib might be gonadotoxic effects on the human ovary and does not confer any protection against cisplatin-induced follicle death in human. Also, our findings together with two separate cases of a severely compromised ovarian response to gonadotropin stimulation and premature ovarian failure in patients who were receiving imatinib [82, 83] further heighten the concerns about its potential gonadotoxicity on the human ovary and urge caution in its use in young female patients.

CONCLUSION

In conclusion, imatinib mesylate itself may show cytotoxic effects on the human ovary and does not appear to confer any protection against follicle loss induced by cisplatin in the human ovary. Dissection of the molecular mechanisms underlying TAp63-triggered oocyte apoptosis is of paramount importance not only for a better understanding of pathologic forms of oocyte death but also for developing new pharmacological strategies to preserve ovarian reserve during cancer therapy in the human ovary.

BIBLIOGRAPHY

1.   Morgan, S., et al., *How do chemotherapeutic agents damage the ovary?* Hum Reprod Update, 2012. **18**(5): p. 525-35.

2.   Bleyer, W.A., *The U.S. pediatric cancer clinical trials programmes: international implications and the way forward.* Eur J Cancer, 1997. **33**(9): p. 1439-47.

3.   Nieman, C.L., et al., *Fertility preservation and adolescent cancer patients: lessons from adult survivors of childhood cancer and their parents.* Cancer Treat Res, 2007. **138**: p. 201-17.

4.   SEER Program (National Cancer Institute (U.S.)), et al., *SEER cancer statistics review*, in *NIH publication*. 1993, U.S. Dept. of Health and Human Services, Public Health Service, National Institutes of Health, National Cancer Institute: Bethesda, Md. p. v.

5.   Miller, K.D., et al., *Cancer treatment and survivorship statistics, 2016.* CA Cancer J Clin, 2016. **66**(4): p. 271-89.

6.   Ferlay, J., et al., *Cancer incidence and mortality worldwide: sources, methods and major patterns in GLOBOCAN 2012.* Int J Cancer, 2015. **136**(5): p. E359-86.

7.   Siegel, R.L., K.D. Miller, and A. Jemal, *Cancer statistics, 2016.* CA Cancer J Clin, 2016. **66**(1): p. 7-30.

8.   Ward, E., et al., *Childhood and adolescent cancer statistics, 2014.* CA Cancer J Clin, 2014. **64**(2): p. 83-103.

9.   Oktem, O. and B. Urman, *Options of fertility preservation in female cancer patients.* Obstet Gynecol Surv, 2010. **65**(8): p. 531-42.

10.   Oktem, O. and K. Oktay, *Preservation of menstrual function in adolescent and young females.* Ann N Y Acad Sci, 2008. **1135**: p. 237-43.

11.   Bedoschi, G., P.A. Navarro, and K. Oktay, *Chemotherapy-induced damage to ovary: mechanisms and clinical impact.* Future Oncol, 2016. **12**(20): p. 2333-44.

12. Oktem, O. and K. Oktay, *A novel ovarian xenografting model to characterize the impact of chemotherapy agents on human primordial follicle reserve.* Cancer Res, 2007. **67**(21): p. 10159-62.

13. Oktem, O. and K. Oktay, *Quantitative assessment of the impact of chemotherapy on ovarian follicle reserve and stromal function.* Cancer, 2007. **110**(10): p. 2222-9.

14. Plowchalk, D.R. and D.R. Mattison, *Phosphoramide mustard is responsible for the ovarian toxicity of cyclophosphamide.* Toxicol Appl Pharmacol, 1991. **107**(3): p. 472-81.

15. Oktem, O., et al., *Ovarian and Uterine Functions in Female Survivors of Childhood Cancers.* Oncologist, 2018. **23**(2): p. 214-224.

16. Schover, L.R., *Premature ovarian failure and its consequences: vasomotor symptoms, sexuality, and fertility.* J Clin Oncol, 2008. **26**(5): p. 753-8.

17. Faubion, S.S., et al., *Long-term health consequences of premature or early menopause and considerations for management.* Climacteric, 2015. **18**(4): p. 483-91.

18. Shuster, L.T., et al., *Premature menopause or early menopause: long-term health consequences.* Maturitas, 2010. **65**(2): p. 161-6.

19. Duncan, F.E., B.F. Kimler, and S.M. Briley, *Combating radiation therapy-induced damage to the ovarian environment.* Future Oncol, 2016. **12**(14): p. 1687-90.

20. Wo, J.Y. and A.N. Viswanathan, *Impact of radiotherapy on fertility, pregnancy, and neonatal outcomes in female cancer patients.* Int J Radiat Oncol Biol Phys, 2009. **73**(5): p. 1304-12.

21. Partridge, A.H., et al., *Web-based survey of fertility issues in young women with breast cancer.* J Clin Oncol, 2004. **22**(20): p. 4174-83.

22. Bines, J., D.M. Oleske, and M.A. Cobleigh, *Ovarian function in premenopausal women treated with adjuvant chemotherapy for breast cancer.* J Clin Oncol, 1996. **14**(5): p. 1718-29.

23. Ben-Aharon, I. and R. Shalgi, *What lies behind chemotherapy-induced ovarian toxicity?* Reproduction, 2012. **144**(2): p. 153-63.

24. Louis, J., L.R. Limarzi, and W.R. Best, *Treatment of chronic granulocytic leukemia with myleran.* AMA Arch Intern Med, 1956. **97**(3): p. 299-308.

25. Yuksel, A., et al., *The magnitude of gonadotoxicity of chemotherapy drugs on ovarian follicles and granulosa cells varies depending upon the category of the drugs and the type of granulosa cells.* Hum Reprod, 2015. **30**(12): p. 2926-35.

26. Sreerama, L., *Alkylating Agents*, in *Encyclopedia of Cancer*, M. Schwab, Editor. 2011, Springer Berlin Heidelberg: Berlin, Heidelberg. p. 132-136.

27. Parulekar, W.R., et al., *Incidence and prognostic impact of amenorrhea during adjuvant therapy in high-risk premenopausal breast cancer: analysis of a National Cancer Institute of Canada Clinical Trials Group Study--NCIC CTG MA.5.* J Clin Oncol, 2005. **23**(25): p. 6002-8.

28. Jarrell, J., et al., *Ovarian toxicity of cyclophosphamide alone and in combination with ovarian irradiation in the rat.* Cancer Res, 1987. **47**(9): p. 2340-3.

29. Meirow, D., et al., *Toxicity of chemotherapy and radiation on female reproduction.* Clin Obstet Gynecol, 2010. **53**(4): p. 727-39.

30. Poklar, N., et al., *Influence of cisplatin intrastrand crosslinking on the conformation, thermal stability, and energetics of a 20-mer DNA duplex.* Proc Natl Acad Sci U S A, 1996. **93**(15): p. 7606-11.

31. Rudd, G.N., J.A. Hartley, and R.L. Souhami, *Persistence of cisplatin-induced DNA interstrand crosslinking in peripheral blood mononuclear cells from elderly and young individuals.* Cancer Chemother Pharmacol, 1995. **35**(4): p. 323-6.

32. Blommaert, F.A. and C.P. Saris, *Detection of platinum-DNA adducts by 32P-postlabelling.* Nucleic Acids Res, 1995. **23**(8): p. 1300-6.

33. Wang, D. and S.J. Lippard, *Cellular processing of platinum anticancer drugs.* Nat Rev Drug Discov, 2005. **4**(4): p. 307-20.

34. Rocha, C.R.R., et al., *DNA repair pathways and cisplatin resistance: an intimate relationship.* Clinics (Sao Paulo), 2018. **73**(suppl 1): p. e478s.

35. Soleimani, R., et al., *Mechanisms of chemotherapy-induced human ovarian aging: double strand DNA breaks and microvascular compromise.* Aging (Albany NY), 2011. **3**(8): p. 782-93.

36. Smith, M.L. and M.A. Kumar, *The "Two faces" of Tumor Suppressor p53-revisited.* Mol Cell Pharmacol, 2010. **2**(3): p. 117-119.

37. Letourneau, J.M., et al., *Acute ovarian failure underestimates age-specific reproductive impairment for young women undergoing chemotherapy for cancer.* Cancer, 2012. **118**(7): p. 1933-9.

38. Xiao, S., et al., *Doxorubicin Has Dose-Dependent Toxicity on Mouse Ovarian Follicle Development, Hormone Secretion, and Oocyte Maturation.* Toxicol Sci, 2017. **157**(2): p. 320-329.

39. Berliere, M., et al., *Incidence of reversible amenorrhea in women with breast cancer undergoing adjuvant anthracycline-based chemotherapy with or without docetaxel.* BMC Cancer, 2008. **8**: p. 56.

40. Davis, A.L., M. Klitus, and D.M. Mintzer, *Chemotherapy-induced amenorrhea from adjuvant breast cancer treatment: the effect of the addition of taxanes.* Clin Breast Cancer, 2005. **6**(5): p. 421-4.

41. Reh, A., O. Oktem, and K. Oktay, *Impact of breast cancer chemotherapy on ovarian reserve: a prospective observational analysis by menstrual history and ovarian reserve markers.* Fertil Steril, 2008. **90**(5): p. 1635-9.

42. Fornier, M.N., et al., *Incidence of chemotherapy-induced, long-term amenorrhea in patients with breast carcinoma age 40 years and younger after adjuvant anthracycline and taxane.* Cancer, 2005. **104**(8): p. 1575-9.

43. Han, H.S., et al., *Analysis of chemotherapy-induced amenorrhea rates by three different anthracycline and taxane containing regimens for early breast cancer.* Breast Cancer Res Treat, 2009. **115**(2): p. 335-42.

44. Marci, R., et al., *Radiations and female fertility.* Reprod Biol Endocrinol, 2018. **16**(1): p. 112.

45. Roudebush, W.E., W.J. Kivens, and J.M. Mattke, *Biomarkers of Ovarian Reserve.* Biomark Insights, 2008. **3**: p. 259-268.

46. Roness, H., et al., *Ovarian follicle burnout: a universal phenomenon?* Cell Cycle, 2013. **12**(20): p. 3245-6.

47. Nguyen, Q.N., et al., *Loss of PUMA protects the ovarian reserve during DNA-damaging chemotherapy and preserves fertility.* Cell Death Dis, 2018. **9**(6): p. 618.

48. Chang, H.J. and C.S. Suh, *Fertility preservation for women with malignancies: current developments of cryopreservation.* J Gynecol Oncol, 2008. **19**(2): p. 99-107.

49. Mahajan, N., *Fertility preservation in female cancer patients: An overview.* J Hum Reprod Sci, 2015. **8**(1): p. 3-13.

50. Fadini, R., et al., *Human oocyte cryopreservation: comparison between slow and ultrarapid methods.* Reprod Biomed Online, 2009. **19**(2): p. 171-80.

51. Batuhan, O. and A.H. Safaa, *Techniques for ovarian tissue, whole ovary, oocyte and embryo cryopreservation.* J Reprod Infertil, 2010. **11**(1): p. 3-15.

52. Domingo, J. and J.A. Garcia-Velasco, *Oocyte cryopreservation for fertility preservation in women with cancer.* Curr Opin Endocrinol Diabetes Obes, 2016. **23**(6): p. 465-469.

53. Igarashi, H., T. Takahashi, and S. Nagase, *Oocyte aging underlies female reproductive aging: biological mechanisms and therapeutic strategies.* Reprod Med Biol, 2015. **14**(4): p. 159-169.

54. Argyle, C.E., J.C. Harper, and M.C. Davies, *Oocyte cryopreservation: where are we now?* Human Reproduction Update, 2016. **22**(4): p. 440-449.

55. Donnez, J. and M.M. Dolmans, *Ovarian cortex transplantation: 60 reported live births brings the success and worldwide expansion of the technique towards routine clinical practice.* J Assist Reprod Genet, 2015. **32**(8): p. 1167-70.

56. Practice Committee of American Society for Reproductive, M., *Ovarian tissue cryopreservation: a committee opinion.* Fertil Steril, 2014. **101**(5): p. 1237-43.

57.   Sonmezer, M. and K. Oktay, *Assisted reproduction and fertility preservation techniques in cancer patients.* Curr Opin Endocrinol Diabetes Obes, 2008. **15**(6): p. 514-22.

58.   Oktay, K. and O. Oktem, *Ovarian cryopreservation and transplantation for fertility preservation for medical indications: report of an ongoing experience.* Fertil Steril, 2010. **93**(3): p. 762-8.

59.   Levine, A.J. and M. Oren, *The first 30 years of p53: growing ever more complex.* Nat Rev Cancer, 2009. **9**(10): p. 749-58.

60.   Khoury, M.P. and J.C. Bourdon, *The isoforms of the p53 protein.* Cold Spring Harb Perspect Biol, 2010. **2**(3): p. a000927.

61.   Amelio, I., et al., *p63 the guardian of human reproduction.* Cell Cycle, 2012. **11**(24): p. 4545-51.

62.   Marcel, V., et al., *Biological functions of p53 isoforms through evolution: lessons from animal and cellular models.* Cell Death Differ, 2011. **18**(12): p. 1815-24.

63.   Murray-Zmijewski, F., D.P. Lane, and J.C. Bourdon, *p53/p63/p73 isoforms: an orchestra of isoforms to harmonise cell differentiation and response to stress.* Cell Death Differ, 2006. **13**(6): p. 962-72.

64.   De Laurenzi, V., et al., *Two new p73 splice variants, gamma and delta, with different transcriptional activity.* J Exp Med, 1998. **188**(9): p. 1763-8.

65.   Suh, E.K., et al., *p63 protects the female germ line during meiotic arrest.* Nature, 2006. **444**(7119): p. 624-8.

66.   Kim, S.Y., et al., *Rescue of platinum-damaged oocytes from programmed cell death through inactivation of the p53 family signaling network.* Cell Death Differ, 2013. **20**(8): p. 987-97.

67.   Deutsch, G.B., et al., *DNA damage in oocytes induces a switch of the quality control factor TAp63alpha from dimer to tetramer.* Cell, 2011. **144**(4): p. 566-76.

68.   Coutandin, D., et al., *Quality control in oocytes by p63 is based on a spring-loaded activation mechanism on the molecular and cellular level.* Elife, 2016. **5**.

69.   Krauskopf, K., et al., *Regulation of the Activity in the p53 Family Depends on the Organization of the Transactivation Domain.* Structure, 2018. **26**(8): p. 1091-1100 e4.

70.   Gonfloni, S., et al., *Inhibition of the c-Abl-TAp63 pathway protects mouse oocytes from chemotherapy-induced death.* Nat Med, 2009. **15**(10): p. 1179-85.

71.   Shaul, Y. and M. Ben-Yehoyada, *Role of c-Abl in the DNA damage stress response.* Cell Res, 2005. **15**(1): p. 33-5.

72.   Shaul, Y., *c-Abl: activation and nuclear targets.* Cell Death Differ, 2000. **7**(1): p. 10-6.

73.   Shiloh, Y., *ATM and related protein kinases: safeguarding genome integrity.* Nat Rev Cancer, 2003. **3**(3): p. 155-68.

74.   Kharbanda, S., et al., *Functional role for the c-Abl protein tyrosine kinase in the cellular response to genotoxic stress.* Biochim Biophys Acta, 1997. **1333**(2): p. O1-7.

75.   Wang, J.Y.J., *The Capable ABL: What Is Its Biological Function?* Molecular and Cellular Biology, 2014. **34**(7): p. 1188-1197.

76.   Croom, K.F. and C.M. Perry, *Imatinib mesylate: in the treatment of gastrointestinal stromal tumours.* Drugs, 2003. **63**(5): p. 513-22; discussion 523-4.

77.   Deininger, M., E. Buchdunger, and B.J. Druker, *The development of imatinib as a therapeutic agent for chronic myeloid leukemia.* Blood, 2005. **105**(7): p. 2640-53.

78.   Kerr, J.B., et al., *Cisplatin-induced primordial follicle oocyte killing and loss of fertility are not prevented by imatinib.* Nat Med, 2012. **18**(8): p. 1170-2; author reply 1172-4.

79.   Carlsson, I.B., et al., *Kit ligand and c-Kit are expressed during early human ovarian follicular development and their interaction is required for the survival of follicles in long-term culture.* Reproduction, 2006. **131**(4): p. 641-9.

80.   Morgan, S., et al., *Cisplatin and doxorubicin induce distinct mechanisms of ovarian follicle loss; imatinib provides selective protection only against cisplatin.* PLoS One, 2013. **8**(7): p. e70117.

81.   Tuppi, M., et al., *Oocyte DNA damage quality control requires consecutive interplay of CHK2 and CK1 to activate p63.* Nat Struct Mol Biol, 2018. **25**(3): p. 261-269.

82.   Zamah, A.M., et al., *Will imatinib compromise reproductive capacity?* Oncologist, 2011. **16**(10): p. 1422-7.

83.   Christopoulos, C., V. Dimakopoulou, and E. Rotas, *Primary ovarian insufficiency associated with imatinib therapy.* N Engl J Med, 2008. **358**(10): p. 1079-80.

84.   Teicher, B.A., et al., *Antitumor efficacy and pharmacokinetic analysis of 4-hydroperoxycyclophosphamide in comparison with cyclophosphamide +/- hepatic enzyme effectors.* Cancer Chemother Pharmacol, 1996. **38**(6): p. 553-60.

85.   Casale, F., et al., *Plasma concentrations of 5-fluorouracil and its metabolites in colon cancer patients.* Pharmacol Res, 2004. **50**(2): p. 173-9.

86.   Bonetti, A., et al., *Inductively coupled plasma mass spectroscopy quantitation of platinum-DNA adducts in peripheral blood leukocytes of patients receiving cisplatin- or carboplatin-based chemotherapy.* Clin Cancer Res, 1996. **2**(11): p. 1829-35.

87.   Mittal, B., et al., *Cytochrome P450 in Cancer Susceptibility and Treatment.* Adv Clin Chem, 2015. **71**: p. 77-139.

88.   Chu, E., *Cancer Chemotherapy*, in *Basic & Clinical Pharmacology, 14e*, B.G. Katzung, Editor. 2017, McGraw-Hill Education: New York, NY.

89.   Bildik, G., et al., *GnRH agonist leuprolide acetate does not confer any protection against ovarian damage induced by chemotherapy and radiation in vitro.* Hum Reprod, 2015. **30**(12): p. 2912-25.

90.   Lobb, D.K. and E.V. Younglai, *A simplified method for preparing IVF granulosa cells for culture.* J Assist Reprod Genet, 2006. **23**(2): p. 93-5.

91.   Bayasula, et al., *Establishment of a human nonluteinized granulosa cell line that transitions from the gonadotropin-independent to the gonadotropin-dependent status.* Endocrinology, 2012. **153**(6): p. 2851-60.

92.   Zhang, H., et al., *Characterization of an immortalized human granulosa cell line (COV434).* Mol Hum Reprod, 2000. **6**(2): p. 146-53.

93.   Bird, C. and S. Kirstein, *Real-time, label-free monitoring of cellular invasion and migration with the xCELLigence system.* Nature Methods, 2009. **6**: p. 622.

94.   Welt, C.K., *Primary ovarian insufficiency: a more accurate term for premature ovarian failure.* Clin Endocrinol (Oxf), 2008. **68**(4): p. 499-509.

95.   Greve, T., et al., *Evaluation of the ovarian reserve in women transplanted with frozen and thawed ovarian cortical tissue.* Fertil Steril, 2012. **97**(6): p. 1394-8 e1.

96.   Janse, F., et al., *Limited value of ovarian function markers following orthotopic transplantation of ovarian tissue after gonadotoxic treatment.* J Clin Endocrinol Metab, 2011. **96**(4): p. 1136-44.

97.   Suzuki, D., et al., *The carboxy-terminus of p63 links cell cycle control and the proliferative potential of epidermal progenitor cells.* Development, 2015. **142**(2): p. 282-90.

98.   Livera, G., et al., *p63 null mutation protects mouse oocytes from radio-induced apoptosis.* Reproduction, 2008. **135**(1): p. 3-12.

99.   Meirow, D., et al., *Cortical fibrosis and blood-vessels damage in human ovaries exposed to chemotherapy. Potential mechanisms of ovarian injury.* Hum Reprod, 2007. **22**(6): p. 1626-33.

100.   Kalich-Philosoph, L., et al., *Cyclophosphamide triggers follicle activation and "burnout"; AS101 prevents follicle loss and preserves fertility.* Sci Transl Med, 2013. **5**(185): p. 185ra62.

101.   Himelstein-Braw, R., H. Peters, and M. Faber, *Morphological study of the ovaries of leukaemic children.* Br J Cancer, 1978. **38**(1): p. 82-7.

Rumelifeneri Yolu Sarıyer 34450 İstanbul **T:** 0212 338 10 00 **F:** 0212 338 12 05 **www.ku.edu.tr**

KOÇ ÜNİVERSİTESİ

ETİK KURUL KARARI

Toplantı Tarihi:	31.08.2015
Karar No:	2015.204.IRB2.074
Sorumlu Araştırıcı:	Özgür Öktem
Araştırma Başlığı:	İnsan over ve testis dokusunda kemoterapiye ve radyasyona bağlı hasarı önlemede c-abl-Tap63 kinaz inhibitörü olan imatinib mesilatın rolü
Başlangıç tarihi:	03.09.2015
Etik Kurul izninin süresi:	1 yıl

Koç Üniversitesi Etik Kurulu'na değerlendirilmek üzere başvuruda bulunduğunuz yukarıda künyesi yazılı projenizin başvuru dosyası ve ilgili belgeleri, Üniversitemiz "Biyomedikal Araştırmalar Etik Kurulu" tarafından araştırmanın gerekçe, amaç, yaklaşım ve yöntemleri dikkate alınarak incelenmiştir.

Üniversite Senatosunun 5 Nisan 2012 tarih ve 04 sayılı oturumunda kabul edilen "Etik Kurullar Yönergesi" uyarınca yapılan inceleme sonucunda çalışmanın gerçekleştirilmesinde etik ve bilimsel sakınca bulunmadığına karar verilmiştir. Araştırmaya yukarıda verilen başlangıç tarihi itibariyle başlayabilirsiniz.
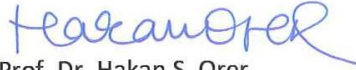
Notlar:
- Araştırma başlangıç tarihinin gecikmesi durumunda Etik Kurul'a başvurularak tarihlerin değiştirilmesi gereklidir.
- Etik Kurul incelemesi ve onayı olmadan bu araştırmada kullanılan prosedürler, formlar ya da protokollerde herhangi bir değişiklik yapılamaz.
- Araştırmanın gerçekleştirileceği birimlerin yöneticilerinden de ayrıca izin alınması gerekli olabilir.

Saygılarımla,

Hakan S. Orer
Başkan

Rumelifeneri Yolu Sarıyer 34450 İstanbul **T:** 0212 338 10 00 **F:** 0212 338 12 05 **www.ku.edu.tr**

**KOÇ
ÜNİVERSİTESİ**

ETİK KURUL KARARI

Tarih: 31.08.2015

Karar No: 2015.204.IRB2.074

Proje Başlığı: İnsan over ve testis dokusunda kemoterapiye ve radyasyona bağlı hasarı önlemede c-abl-Tap63 kinaz inhibitörü olan imatinib mesilatın rolü

Sorumlu Araştırıcı: Özgür Öktem

Koç Üniversitesi Biyomedikal Araştırmalar Etik Kurulu tarafından yapılan inceleme sonucunda çalışmanın gerçekleştirilmesinde etik ve bilimsel açıdan sakınca bulunmadığına karar verilmiştir.

ADI	SOYADI	KURUM	KATILIM Var - Yok		İMZA
Hakan S.	Orer	KÜ Tıp Fakültesi	☑	☐	Hakanörer
Özgür	Öktem	KÜ Tıp Fakültesi	☐	☐	
Tuğba	Gürsoy	KÜ Tıp Fakültesi	☐	☐	
Aygül	Akyüz	KÜ Hemşirelik YO	☐	☐	
Baler	Bilgin	KÜ İktisadi ve İdari Bilimler Fakültesi	☑	☐	
Funda	Şar	KÜ Fen Fakültesi	☑	☐	
Demircan	Canadinç	KÜ Mühendislik Fakültesi	☐	☐	
Zeynep	Cemalcılar	KÜ İnsani Bilimler Edebiyat Fakültesi	☑	☐	
Nadiye Pınar	Ay	Marmara Üniversitesi Tıp Fakültesi	☐	☐	
Aslı	Ortakmaç	Kanser Savaşçıları Derneği	☑	☐	
Umut Nazif	Çelik	Koç Holding	☑	☐	

KÜ Biyomedikal Araştırmalar Etik Kurulu

KOÇ ÜNİVERSİTESİ

HAYVAN DENEYLERİ YEREL ETİK KURUL KARARI

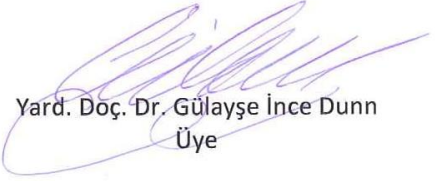|	
Toplantı tarihi:	**02/09/2015**
Toplantı sayısı:	**2015/05**
Dosya kayıt numarası:	**2015-** 19
Etik Kurul karar sayısı:	**2015-20**
Hayvan türü ve sayıları:	**Fare, 80**

Doç. Dr. Özgür Öktem'in yürütücüsü olduğu **" İnsan Over ve Testis Dokusunda Kemoterapi ve Radyasyona Bağlı Hasarı Önlemede c-Abl-TAp63 Kinaz İnhibitörü İmatinib Mesilat'ın Rolü "** konulu araştırma deney protokolü Etik Kurul tarafından görüşülmüş, yapılan değerlendirme sonucu çalışma Koç Üniversitesi Hayvan Deneyleri Yerel Etik Kurulu Yönergesine uygun bulunarak onaylanmasına karar verilmiştir.

Prof. Dr. Hakan S. Orer
Başkan

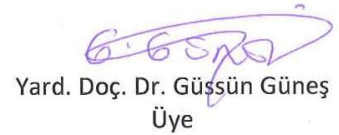Dr. Ali Cihan Taşkın
Başkan Vekili

KÜ-HADYEK
TOPLANTIYA KATILMADI
Doç. Dr. Fuat Balcı
Üye

Yard. Doç. Dr. Gülayşe İnce Dunn
Üye

Doç. Dr. Aslı Çarkoğlu
Üye

Yard. Doç. Dr. Güssün Güneş
Üye

KÜ-HADYEK
TOPLANTIYA KATILMADI
Doç. Dr. Seda Kızılel
Üye

Not: Dr. Ali Cihan Taşkın değerlendirmeye katılmamıştır.

VITA

Gamze Bildik Elcik was born in Adana, Turkey in 1991. She received a Bachelor of Science degree with a major in Molecular Biology and Genetics from Istanbul University in 2013. From 2014 to 2016, she attended Reproductive Biology Master Program at Graduate School of Health Sciences in Koç University. She continued to her doctoral studies in Cellular and Molecular Medicine Program at Graduate School of Health Sciences in Koç University where she has worked as a research and teaching assistant.